1984

The synthesis and characterization of tetranuclear molybdenum iodide clusters

Steven Mark Stensvad
Iowa State University

Stensvad, Steven Mark

THE SYNTHESIS AND CHARACTERIZATION OF TETRANUCLEAR MOLYBDENUM-IODIDE CLUSTERS

Iowa State University PH.D. 1984

The synthesis and characterization of tetranuclear molybdenum iodide clusters

by

Steven Mark Stensvad

A Dissertation Submitted to the
Graduate Faculty in Partial Fulfillment of the
Requirements for the Degree of
DOCTOR OF PHILOSOPHY

Department: Chemistry
Major: Inorganic Chemistry

Approved:

Signature was redacted for privacy.

In Charge of Major Work

Signature was redacted for privacy.

For the Major Department

Signature was redacted for privacy.

For the Graduate College

Iowa State University
Ames, Iowa

1984

TABLE OF CONTENTS

	Page
INTRODUCTION	1
Trinuclear Structures	1
Tetranuclear Structures	5
Pentanuclear Structures	9
Hexanuclear Structures	10
Summary	11
EXPERIMENTAL	13
Chemicals	13
Analytical Methods	13
Physical Methods	14
X-Ray Diffraction Measurements	18
Reactions	20
Reaction A - Preparation of $(R_4N)Mo(CO)_5I$ and $(R_4N)Mo(CO)_4I_3$ (where R = n-C_4H_9 or n-C_3H_7)	20
Reaction B - Preparation of $(TBA)_2Mo_4I_{11}$ from $(TBA)Mo(CO)_4I_3$	22
Reaction C - Modified preparation of $(TBA)_2Mo_4I_{11}$	22
Reaction D - Preparation of $(TPA)_2Mo_4I_{11}$	23
Reaction E - Thermolysis of $(TBA)Mo(CO)_4I_3$ under vacuum	23
Reaction F - Thermolysis of $(TBA)Mo(CO)_4I_3$ in refluxing benzene	24
Reaction G - Thermolysis of $(TBA)Mo(CO)_4I_3$ in refluxing o-dichlorobenzene	24

Page

Reaction H - Zinc reduction of $(TBA)_2Mo_4I_{11}$ in acetonitrile 25

Reaction I - Zinc reduction of $(TBA)_2Mo_4I_{11}$ in refluxing acetonitrile 25

Reaction J - Thermolysis of $(TBA)Mo(CO)_4I_3$ in the presence of hydrogen 26

Reaction K - Thermolysis of $(TPA)Mo(CO)_4I_3$ in the presence of nitrogen 26

Reaction L - Thermolysis of $(TPA)Mo(CO)_4I_3$ in the presence of hydrogen 28

Reaction M - Reaction of $(TBA)_2Mo_4I_{11}$ with I_2 28

Reaction N - Reaction of $Mo_4I_9(CH_3CN)_4$ with (TBA)I 29

SYNTHESES AND CHARACTERIZATIONS OF $(TBA)_2Mo_4I_{11}$ AND $(TPA)_2Mo_4I_{11}$ 30

Syntheses 30

Spectra of $(TBA)_2Mo_4I_{11}$ and $(TPA)_2Mo_4I_{11}$ 32

Cyclic Voltammetry 33

Magnetic Properties 36

Photoelectron Spectroscopy (PES) 40

X-Ray Crystal Structure Determination 45

Bonding 58

RESULTS FOR RELATED COMPOUNDS 67

Syntheses of $Mo_4I_{11}^{2.5-}$ and "$Mo_4I_{10}^{2-}$" Salts 67

Related Reactions 73

Magnetic Properties 76

Cyclic Voltammetry 81

Spectra of the "$Mo_4I_{10}^{2-}$" Salts and $Mo_4I_9(CH_3CN)_4$ 84

Thermogravimetric Analysis 87

Page

Photoelectron Spectroscopy (PES) 88

Mass Spectroscopy 91

SUMMARY 93

BIBLIOGRAPHY 97

APPENDIX 100

LIST OF TABLES

		Page
Table 1.	Trinuclear structures and their bonding	4
Table 2.	Tetranuclear structures and their bonding	7
Table 3.	Selected hexanuclear structures and their bonding	12
Table 4.	Summary of structural types	12
Table 5.	Far-infrared spectra of $(TBA)_2Mo_4I_{11}$ and $(TPA)_2Mo_4I_{11}$	32
Table 6.	EPR spectra for $(TBA)_2Mo_4I_{11}$ and $(TPA)_2Mo_4I_{11}$	40
Table 7.	PES results for (TBA) and (TPA) salts of $Mo_4I_{11}^{2-}$	42
Table 8.	Bond distances in $Mo_4I_{11}^{2-}$ (Å)	48
Table 9.	Selected least-squares planes and interplane angles for $Mo_4I_{11}^{2-}$	56
Table 10.	Selected bond angles in $Mo_4I_{11}^{2-}$ (degrees)	59
Table 11.	EPR spectra of the $Mo_4I_{11}^{2-}$, "$Mo_4I_{10}^{2-}$", and $Mo_4I_9(CH_3CN)_4$ compounds	79
Table 12.	Far-infrared spectra of the "$Mo_4I_{10}^{2-}$" salts	85
Table 13.	PES spectra for $Mo_4I_9(CH_3CN)_4$, and (TBA) and (TPA) salts of "$Mo_4I_{10}^{2-}$"	90
Table 14.	Analysis of the percent $CDHCl_2$ in the sample as determined by mass spectroscopy	92
Table 15.	X-ray powder pattern d-spacings and relative intensities	101
Table 16.	Final atomic positional and isotropic thermal parameters for $(TBA)_2Mo_4I_{11}$	102
Table 17.	Selected I-I nonbonding distances in the $Mo_4I_{11}^{2-}$ anion	104
Table 18.	A qualitative molecular orbital scheme for $Mo_4I_{11}^{2-}$	105

Page

Table 19. Bond distances in the $(TBA)_2Mo_4I_{11}$ cations 106

Table 20. Selected bond angles in the $(TBA)_2Mo_4I_{11}$ cations 107

Table 21. Atomic temperature factors for $(TBA)_2Mo_4I_{11}$ 108

LIST OF FIGURES

		Page
Figure 1.	Known trinuclear molybdenum clusters	2
Figure 2.	Known molybdenum tetranuclear clusters	6
Figure 3.	Cell for electrochemistry experiments	16
Figure 4.	Schlenk reaction vessel with gas collection gauge	21
Figure 5.	Reaction vessel with gas bubbler	27
Figure 6.	Stationary Pt electrode voltammograms: (A) 1.9 x 10^{-3} M (TBA)I and (B) 5.8 x 10^{-4} M $(TBA)_2Mo_4I_{11}$; scan rate was 1 V/sec	34
Figure 7.	χ_m vs. 1/T plot for $(TBA)_2Mo_4I_{11}$	37
Figure 8.	EPR spectrum of $(TBA)_2Mo_4I_{11}$	39
Figure 9.	Calculated iodine spectrum of $(TPA)_2Mo_4I_{11}$, two components	43
Figure 10.	Calculated iodine spectrum of $(TPA)_2Mo_4I_{11}$, three components	44
Figure 11.	ORTEP view of the $(Mo_4I_7)I_4^{2-}$ anion	47
Figure 12.	Structures of fragments generated from $(M_6X_8)X_6^{2-}$: (A) $(Mo_6Cl_8)Cl_6^{2-}$, (B) $(Mo_5Cl_8)Cl_5^{2-}$, (C) $[Mo_4(O\text{-}i\text{-}Pr)_8]Cl_4$, (D) $[Mo_4(O\text{-}i\text{-}Pr)_8]Br_4$, and (E) $(Mo_4I_7)I_4^{2-}$	51
Figure 13.	The atomic orbital coordinate system at each metal atom	61
Figure 14.	The "metallic" MO diagram of the $Mo_4I_{11}^{2-}$ anion. (The numbers give percentage Mo character of each MO.)	63
Figure 15.	The total cluster MO energy (E_{tot}) and metal MO energy as a function of dihedral angle	65
Figure 16.	χ_m vs. 1/T plot for $(TPA)_4Mo_8I_{20}X$	77

Page

Figure 17. EPR spectra of (TBA) salts: (A) $Mo_4I_{11}^{2-}$, (B) "$Mo_4I_{10}^{2-}$" made by Reaction I, and (C) "$Mo_4I_{10}^{2-}$" made by Reaction J 80

Figure 18. Spinning Pt electrode voltammograms: (A) 6.2 x 10^{-4} M $(TBA)_2Mo_4I_{11}$ and (B) 3.0 x 10^{-4} M "$(TBA)_2Mo_4I_{10}$" and 6.0 x 10^{-4} M (TBA)I; the scan rate was 0.200 V/sec and the electrode rotation rate was 600 RPM 82

Figure 19. The infrared spectrum of $Mo_4I_9(CH_3CN)_4$ from 2000 to 2500 cm^{-1} 86

INTRODUCTION

The objective of this research has been to devise new and improved methods for construction of cluster compounds, especially those of molybdenum and tungsten. In a systematic synthesis of a particular metal cluster, it would be beneficial to understand what factors favor one structure over another. To put this in perspective, this discussion will start with a brief review of the known molybdenum and tungsten cluster types.

Trinuclear Structures

The number of trinuclear molybdenum and tungsten cluster compounds is small. The five known structures are shown in Fig. 1. One is a linear chain, and the other four structures all contain metal triangles, but differ in the number and arrangement of their ligands.

The only compound believed to have a linear arrangement of metal atoms is $(TBA)_3Mo_3Cl_{12}$, $(TBA) = (n\text{-}C_4H_9)_4N)^+$. It is thought to have a confacial trioctahedral structure [1]. Its precursor, $Mo_2Cl_9^{2-}$, has a confacial bioctahedral structure. The electronic and infrared spectra of the $Mo_3Cl_{12}^{3-}$ anion agree with the assigned linear structure. Although no additional experimental work has verified it, a rough molecular orbital scheme predicts the trinuclear cluster has three of each type of metal-metal orbitals: bonding, nonbonding and antibonding. The middle metal atom is eight-coordinate and the end metal atoms are seven-coordinate.

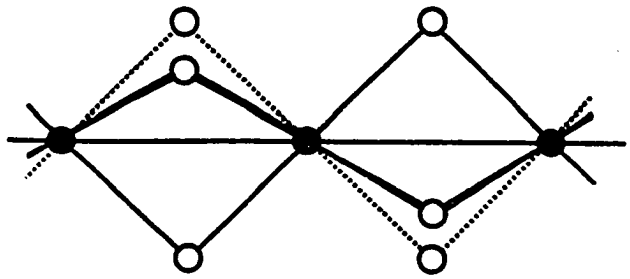

1) M_3X_{12}

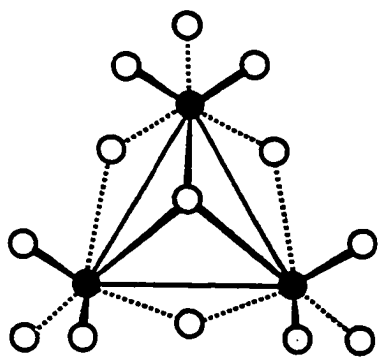

2) M_3X_{13}

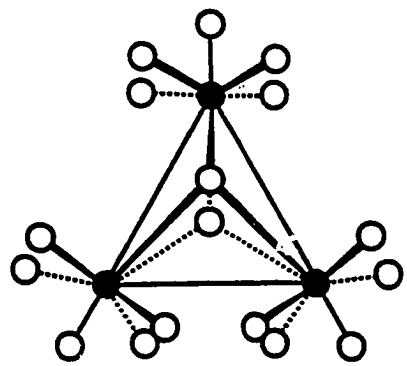

3) M_3X_{17}

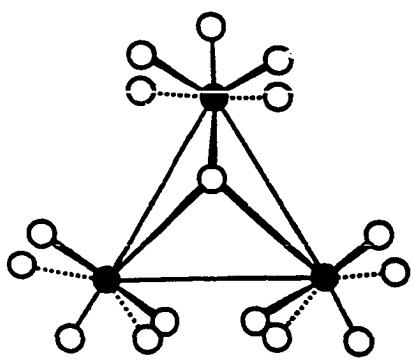

4) M_3X_{16}

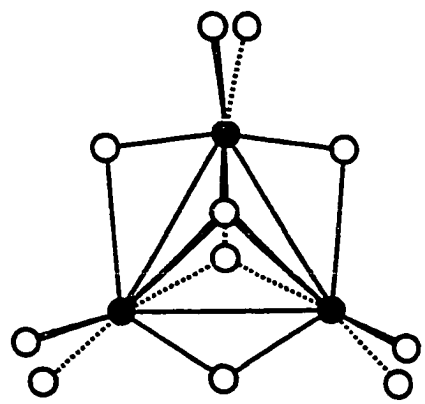

5) M_3X_{11}

Figure 1. Known trinuclear molybdenum clusters

The most common trigonal cluster type is the M_3X_{13} structure. The basic frame is the M_3X_4 unit in which one atom caps the metal triangle, bridging all three metal atoms, and the other three atoms each lie below an edge of the metal triangle and bridge two metal atoms. Each metal atom is eight-coordinate (including the metal-metal bonds). Using a set of three d-orbitals not involved in M-X σ bonds from each metal atom, a rough molecular orbital scheme has been derived by Cotton for C_{3v} clusters of this type [2]. This MO scheme predicts three strongly bonding orbitals (a_1 + e), five strongly antibonding orbitals (2e + a_2) and one orbital (a_1) with either weakly bonding or antibonding character. Examples of both six and eight metal-based cluster electrons (MCE) are listed in Table 1. McCarley has suggested that donation of the electron density from π ligand orbitals on the edge bridging ligands raises the energy of the second a_1 orbital from bonding to antibonding [3].

The frame of the M_3X_{17} structure is a metal triangle capped above and below by triply bridging atoms, forming a M_3X_2 unit. Each triangle edge is also bridged above and below by acetate ligands. Together with a terminal ligand, the oxygen atoms of the edge bridging acetate ligands have a square pyramid arrangement around each metal atom. The set of two orbitals on each metal atom not involved in M-X bonds interact to form three bonding and three antibonding orbitals. Therefore, each metal atom is nine-coordinate, with seven M-X bonds and two M-M bonds.

The next trigonal structure, the M_3X_{16} structure, has a M_3X basic frame. It differs from the M_3X_{17} structure in that only one face of

Table 1. Trinuclear structures and their bonding

	Structure Type	MCE	Avg. d(M-M), Å	Ref.
$Mo_3Cl_{12}^{3-}$	1	9	-[a]	1
$Mo_3O_4(C_2O_4)_3(H_2O)_3^{2-}$	2	6	2.486(1)	4
$Mo_3OCl_3(O_2CCH_3)_3(H_2O)_3^{2+}$	2	8	2.550(2)	5
$W_3O_4F_9^{5-}$	2	6	2.515(1)	6
$Mo_3(CCH_3)_2(O_2CCH_3)_6(H_2O)_3^{2+}$	3	4	2.883(1)	7
$Mo_3(CCH_3)_2(O_2CCH_3)_6(H_2O)_3^{+}$	3	5	2.815(7)	7
$Mo_3O_2(O_2CCH_3)_6(H_2O)_3^{2+}$	3	6	2.757(1)	7
$W_3O_2(O_2CCH_3)_6(H_2O)_3^{2+}$	3	6	2.745(1)	8
$W_3O(O_2CCH_3)_6(H_2O)_3^{2+}$	4	8	2.710(4)	9
$Mo_3O(OCH_2C(CH_3)_3)_{10}$	5	6	2.529(9)	10

[a]Structural assignment based on electronic and infrared spectra, not x-ray data.

the metal triangle is capped by an atom. The arrangement of the edge bridging and terminal ligands remains the same. Now, each metal atom has three orbitals not involved in M-X bonds. A Fenske-Hall molecular orbital calculation showed that a fourth weakly M-M bonding orbital is formed [9]. Each metal atom is then eight-coordinate, with two M-M bonds and six M-X bonds. Also, there are four M-M bonding orbitals delocalized over three M-M bonds.

The final trinuclear structure has a M_3X_5 basic frame. The M_3X_{11} structure has ligand atoms bridging each face and each edge of the metal triangle. In contrast to prior structures, the edge bridging atoms now lie in the metal plane. In addition to bonding within the basic frame, each metal is bonded to two terminal ligands, making the metal atoms eight-coordinate. The only known compound with this structure has six MCE.

Tetranuclear Structures

There are four tetranuclear cluster structures: a tetrahedron, a butterfly (or open tetrahedron), a planar butterfly (rhomboidal), and a rectangle. The last three structures may be derived from the tetrahedron by stretching or compressing edges and opening up the dihedral angle between triangular faces as seen in Fig. 2. Compounds of each cluster type are given in Table 2.

The word tetrahedron signifies a cluster with four metal atoms, each bonded to its three neighbors and all six metal-metal bonds are of approximately equal length. The only known group VI metal tetrahedral clusters have a cubane structure with interpenetrating tetrahedrons of

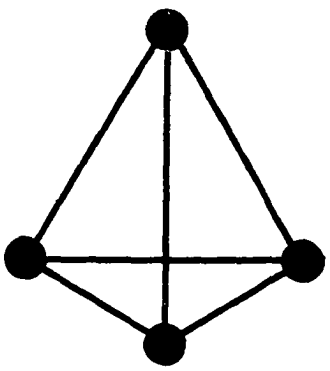

1) Tetrahedron (T_d)

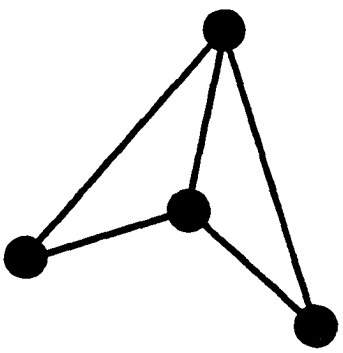

2) Butterfly (C_{2v})

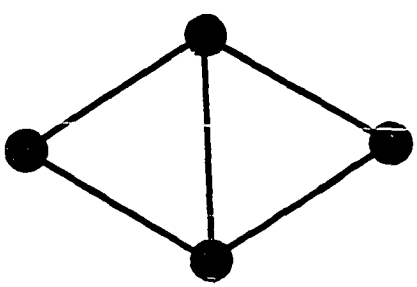

3) Planar Butterfly (C_{2h})

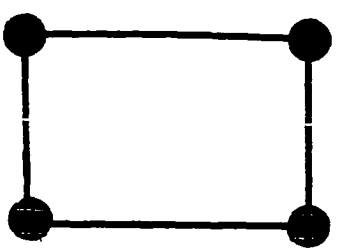

4) Rectangle (C_{2h})

Figure 2. Known molybdenum tetranuclear clusters

Table 2. Tetranuclear structures and their bonding

	Structure Type	MCE	Avg. d(Mo-Mo), Å	Ref.
$GaMo_4S_4S_{12/3}$	1	11	2.823[a]	11
$Mo_4S_4Br_{12/3}$	1	12	2.798[a]	12
$Mo_4Br_4[OCH(CH_3)_2]_8$	2	12	2.508(1)	13
$(TBA)_2Mo_4I_{11}$	2	15	2.567(5)[b]	14
$Ba_{1.14}(Mo_4O_8^{2-})(Mo_4O_8^{0.28-})$[c]	3	10[c] 8.28[c]	2.593(2) 2.668(2)	15
$W_4(OC_2H_5)_{16}$	3	8	2.785(2)	16
$Mo_4Cl_4[OCH(CH_3)_2]_8$	4	12	2.378(1)	13
$Mo_4Cl_8[P(C_2H_5)_3]_4$	4	16	2.211(3), 2.901(2)	17

[a]Estimated standard deviations not given.

[b]The average d(Mo-Mo) with the 3.035(5) Å nonbonding distance included is 2.645(5) Å.

[c]Contains two clusters of the same type, but different MCE.

molybdenum and sulfur. $GaMo_4S_4S_{12/3}$ and $Mo_4S_4Br_{12/3}$ are solid state examples [11,12]. In both compounds, each metal is nine-coordinate and forms bonds with its three neighboring metal atoms.

The butterfly structure results when the dihedral angle between two triangular faces in a tetrahedron opens up. One or more of the edges of the tetrahedron are stretched, transforming the metal frame into two triangles sharing a common base (hinge). The dihedral angle may assume values anywhere from 70.5° (found in the regular tetrahedron) to 180° (found in the planar butterfly structure). As the dihedral angle increases, the length of the sixth edge increases until there is no longer any bonding between the atoms on the outer tips of the triangles.

The third structure is the planar butterfly, well-known as the cluster unit in the compound $CsNb_4Cl_{11}$. The metal atoms are coplanar, forming two isosceles triangles sharing a common base. There is a face bridging atom above and two edge bridging atoms below the metal plane for one metal triangle, and the ligand arrangement in the other triangle is related by inversion to that of the first. Including the terminal ligands, both hinge metal atoms are nine coordinate (with three metal-metal bonds and six metal-ligand bonds) while each outer tip metal atom is eight-coordinate (with two metal-metal bonds and six metal-ligand bonds). Because only eight valence orbitals are required to form the six metal-ligand and two metal-metal bonds, each outer metal atom may have a localized nonbonding orbital. The only known molybdenum compound with this structure, $Ba_{1.14}Mo_8O_{16}$, contains both a regular and a

distorted form of this cluster type. The regular form has 10 MCE while the distorted form has 8.28 MCE (average) as indicated in the formula $Ba_{1.14}(Mo_4O_8^{2-})(Mo_4O_8^{0.28-})$ [15].

The final structure, having a rectangular cluster, is obtained conceptually by stretching the interior metal-metal bond in the planar butterfly structure. The word rectangle denotes that the metal atoms are planar with 90° angles between them and the cluster has possibly two sets of bond lengths. Two modifications with this basic structure have been found. An example of the first type, $Mo_4Cl_4[OCH(CH_3)_2]_8$, has a square metal frame and is synthesized from two triply bonded molybdenum dimers [13]. The cluster has six delocalized metal-metal bonding orbitals and each metal atom is seven-coordinate. The second type, such as for $Mo_4Cl_8[P(C_2H_5)_3]_4$, has a rectangular metal frame and has eight localized metal-metal bonding orbitals [17]. The alternating triple bond, single bond arrangement in the cluster is obtained by utilizing the four d-orbitals which previously formed the delta bonds within the separated dimers to form two single bonds between the two dimers. Even though the coordination number for each metal is only six, the cluster is stabilized by the high degree of metal-metal bonding and the steric effects of the large phosphine ligands.

Pentanuclear Structures

Although several pentanuclear metal clusters can be envisioned, only the $Mo_5Cl_{13}^{2-}$ structure is germane to this discussion [18]. The arrangement of the metal and ligand atoms in the $Mo_5Cl_{13}^{2-}$ cluster can be best described as a fragment of the octahedral $(Mo_6Cl_8)Cl_6^{2-}$ cluster,

with one metal atom and its associated terminal ligand removed. The remaining metal atoms form a square pyramid with the apex atom nine-coordinate (four metal-metal and five metal-ligand bonds) and the four basal atoms eight-coordinate (three metal-metal and five metal-ligand bonds). If each edge of the square pyramid has a bond order of unity as indicated by the average Mo-Mo bond length of 2.582(3) Å in $Mo_5Cl_{13}^{2-}$, compared to 2.61(1) Å in Mo_6Cl_{12} [19], the cluster has eight bonding orbitals. Since the cluster has nineteen MCE, the remaining three electrons must occupy essentially nonbonding orbitals located on the basal metal atoms.

Hexanuclear Structures

There are two main types of hexanuclear metal clusters. Both contain an octahedron of metal atoms, but differ in the number and arrangement of their bridging ligands. The number of metal cluster electrons appears to determine which structure is preferred.

In the more electron deficient clusters, the $M_6X_{12}^{n+}$ structure (Type 1) with the edge bridged octahedron is preferred. A rough MO treatment of the $M_6X_{12}^{n+}$ in O_h symmetry predicts the cluster will have only eight metal-metal bonding orbitals [20]. Each metal atom is nine-coordinate and the maximum bond order per metal-metal bond is 2/3, which means the metal-metal bonding is delocalized. The only known group VI compound with this structure is $(W_6Cl_{12})Cl_6$ [21]. It has eighteen MCE, two more than are necessary to fill all the bonding orbitals. The additional two electrons probably reside in antibonding orbitals and destabilize the cluster.

The second octahedral cluster type is $M_6X_8^{n+}$, where the ligands triply bridge each face of the metal octahedron. The structure can also be viewed as a cube formed by the eight ligand atoms with metal atoms lying in the center of each face of the cube. Molecular orbital theory predicts twelve metal-metal bonding orbitals for this structure [20]. Without changing the metal atoms' coordination number, the change in bridging ligand arrangement (compared to $M_6X_{12}^{n+}$) has increased the number of metal-metal bonds by four and the maximum bond order per metal-metal bond to one. Several examples of group VI metal compounds with the $M_6X_8^{n+}$ structure are listed in Table 3. The number of MCE for these compounds varies from twenty to twenty-four (the maximum number of bonding electrons predicted by MO theory).

Summary

A review of molybdenum and tungsten cluster compounds reveals a variety of structures. Two common features of all the structures are the prevalence of halide or chalcogenide bridging ligands and a metal oxidation state between 2+ and 3+. Even though there may be more than one structural type for a given number of metal atoms, as listed in Table 4, the number of metal-metal bonding orbitals and the number of MCE increase stepwise with cluster size.

Next, the synthesis and characterization of $(TBA)_2Mo_4I_{11}$ and its related compounds will be discussed. The $Mo_4I_{11}^{2-}$ anion is interesting because of its structure, a closed butterfly structure, and its simple synthesis.

Table 3. Selected hexanuclear structures and their bonding

	Structure Type	MCE	Avg. d(M-M), Å	Ref.
$(W_6Cl_{12})Cl_6$	1	18	2.92[a]	21
Mo_6S_8	2	20	2.780[a]	22
$PbMo_6S_8$	2	22	2.702[a]	23
$(Mo_6Cl_8)Cl_{4/2}Cl_2$	2	24	2.61(1)	19
$(W_6Br_8)Br_4(Br_4)_{2/2}$	2	22	2.64(2)	24

[a]Estimated standard deviations not given.

Table 4. Summary of structural types

Number of Metal Atoms	Number of Bonding Orbitals	Range of MCE
3	3[a], 4	4-9
4	5, 6, 8	8-16
5	8[a]	19
6	8, 12	14-24

[a]Does not include metal-metal nonbonding orbitals.

EXPERIMENTAL

Chemicals

Molybdenum hexacarbonyl was purchased from Pressure Chemical Company and used as received. Tetrapropylammonium (TPA) and tetrabutylammonium (TBA) iodide salts were purchased from Eastman Chemical Company and used as received. Chlorobenzene was obtained from Fisher Scientific Company. It was dried by refluxing over calcium hydride and then distilled under a nitrogen atmosphere into a Schlenk storage flask for later use. Acetonitrile from Fisher Scientific Company was refluxed over phosphorus pentoxide and distilled under a nitrogen atmosphere into a Schlenk storage flask. Iodine was used as received from Fisher Scientific Company.

Analytical Methods

The gravimetric analysis of molybdenum was performed by direct ignition of samples to molybdenum trioxide. Samples of weight between 150 and 250 mg were tared into dried porcelain crucibles. After transferring a sample from a capped vial into the crucible, it was first wetted with acetone, then treated with about 10 ml of a 10% $[(C_2H_5)_4N]OH$ aqueous solution to initiate oxidation and slowly heated to dryness. Further oxidation was promoted by adding a few milliliters of dilute nitric acid and heating to dryness; the oxidation was completed by repeating the process with concentrated nitric acid. Next, the sample was slowly charred to prevent the organic materials from bursting into flame when placed in the muffle furnace at 500°C for

several hours. After being cooled in a desiccator, the crucibles were again tared and the percent molybdenum determined.

Samples for iodide analyses were tared from capped vials and then poured into 250 ml beakers containing approximately 600 mg of sodium hydroxide and 50 ml of water. The sample was wetted with acetone if necessary before increasing the total volume to 175 ml with water. A minimal volume of hydrogen peroxide was added to the boiling solution to decompose the sample. After the solution had turned clear and any excess peroxides were decomposed by boiling, the solution was allowed to cool. Dilute nitric acid was added until the pH became about 2.0 and then the solution was potentiometrically titrated with a standardized silver nitrate solution using an Ag/AgI working electrode.

The carbon-hydrogen and nitrogen analyses were done by the Ames Laboratory Analytical Service Group.

Physical Methods

Infrared spectra were obtained from Nujol mulls prepared in the dry box and painted on CsI windows. A Beckman Acculab-4 spectrophotometer covered the range from 4000 cm^{-1} to 200 cm^{-1}. An IBM IR-98 FT-IR spectrophotometer covered the range 220 cm^{-1} to 20 cm^{-1}.

Electronic spectra were recorded with a Cary 14 spectrophotometer. The quartz cell was specially adapted for filling on a vacuum line. Samples were loaded in the dry box and the solvents vacuum distilled into the cell.

The variable temperature susceptibility of $(TBA)_2Mo_4I_{11}$ was measured on a Faraday balance constructed by Converse [25]. Nickel

ammonium sulfate hexahydrate was used to standardize this system. The variable temperature susceptibility of $(TPA)_2Mo_4I_{10}$ was measured on a different Faraday balance system designed by Stierman [26]. The second balance was standardized using a palladium standard. Both samples were loaded into sealed Teflon containers in the dry box and then tared. No decomposition of samples was detected for either compound.

Powder diffraction patterns were obtained using a 114.59 mm Debye-Scherrer camera with Cu Kα radiation. The samples were contained in sealed 0.2 mm Lindemann capillary tubes.

Cyclic voltammetry was performed on samples using in tandem a Model 175 universal programmer and a Model 173 potentiostat, both by Princeton Applied Research. The data were recorded on a x-y recorder. The cell is shown in Fig. 3. The three electrode system had a saturated NaCl-calomel reference electrode connected to the working solution by a salt bridge containing $(TBA)(BF_4)$, a spinning platinum disk working electrode, and a platinum wire counter electrode. The solvent was spectrograde acetonitrile and the supporting electrolyte was $(TBA)(BF_4)$. Solutions were deoxygenated by bubbling nitrogen gas through the solution for at least ten minutes; nitrogen flow over the solution was continued while measurements were in progress.

Mass spectra of "$(TPA)_2Mo_4I_{10}$" were obtained on a MS902 mass spectrometer by AEI Scientific Apparatus. The "$(TPA)_2Mo_4I_{10}$" was loaded in the dry box and the $CDCl_3$ was vacuum distilled into a flask adapted for use on a vacuum line. Later, the flask was connected directly to the mass spectrometer.

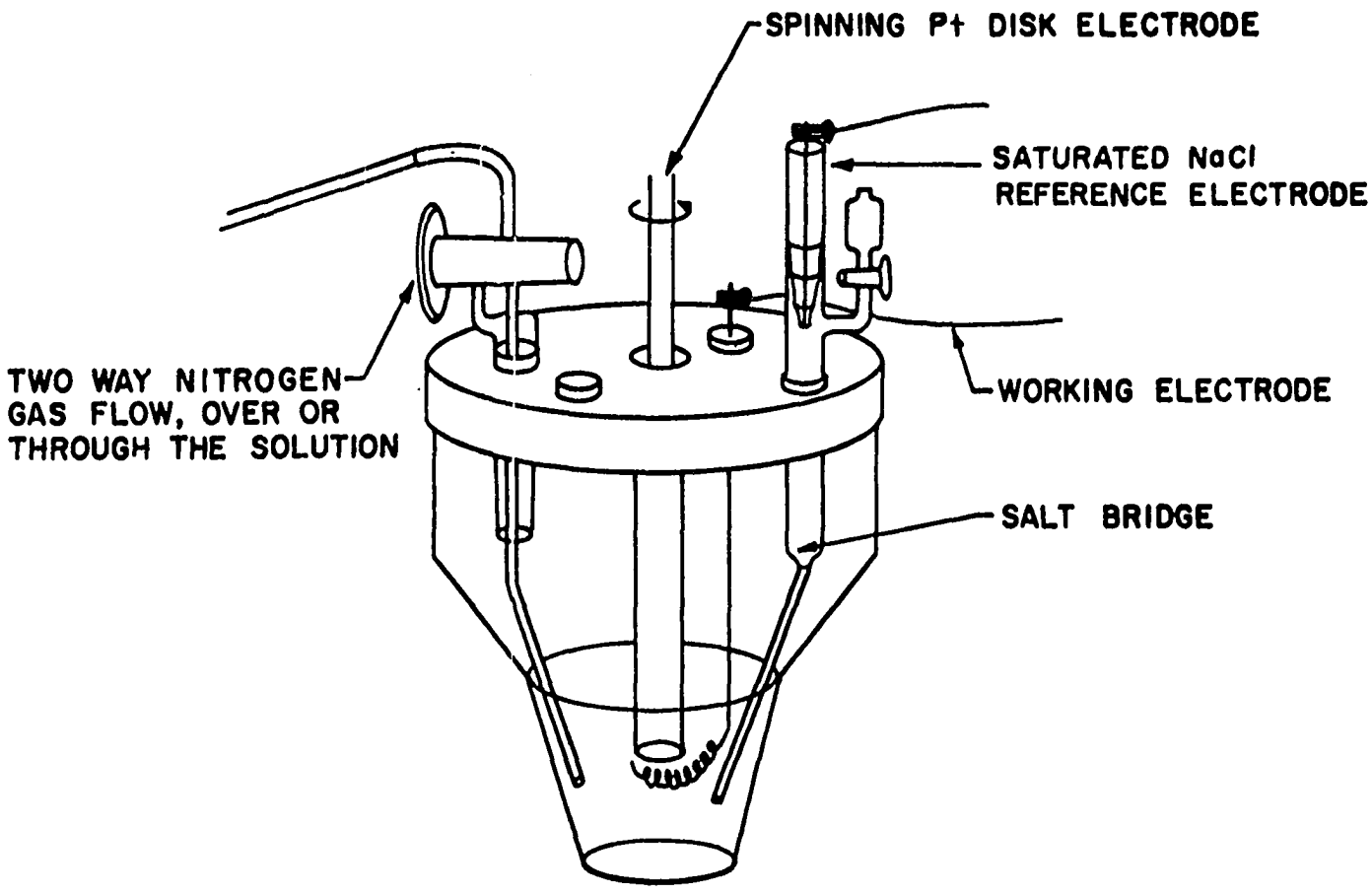

Figure 3. Cell for electrochemistry experiments

The thermogravimetric analysis of $Mo_4I_9(CH_3CN)_4$ was done by the 3M Central Research Laboratories-Analytical Research Group. A freshly made sample of $Mo_4I_9(CH_3CN)_4$, which had been sealed in the dry box to prevent decomposition, was submitted for analysis. The instrument used was a Perkin-Elmer TGS-1. The sample was maintained under a nitrogen atmosphere, and was heated at the rate of 2.5°C per minute.

Photoelectron spectra were obtained on a ES200B electron spectrometer by AEI Scientific Apparatus. Sealed samples were introduced into the dry box attached to the instrument prior to opening. Spectra were recorded using Al Kα radiation, 1486.6 eV. Commonly, spectra were obtained using the instrument with the narrowest slit opening and the electron flood gun on to prevent charging, but for some compounds, monochromatic Mg Kα radiation was used. Binding energies of peaks were referenced to a carbon 1s peak binding energy of 285.0 eV.

The spectra were resolved into component peaks using a nonlinear least-squares computer program developed by M. H. Luly [27]. The program also provided for smoothing the raw data, adjusting the baseline, and correcting the data for inelastic electron scattering. Certain variables of the fitting function were fixed by using values from a standard compound. For this work with metal iodide clusters, CsI and (TBA)I were the standards for fitting iodine $3d_{3/2,5/2}$ spectra. Each peak was treated as a combination of Gaussian and Cauchy shape functions and the following parameters were determined: fraction Gaussian (FG), full-width at half maximum (FWHM), relative height (or intensity), and binding energy at the peak maximum.

The iodine 3d peak is split into $3d_{3/2}$ and $3d_{5/2}$ components by spin-orbital coupling. For the photoelectron emission from each type of iodide ligand, the $3d_{3/2}$ and $3d_{5/2}$ components were assumed to have a constant energy difference and a fixed peak area ratio. These two peaks can thus be coupled together in the least squares fitting by fixing their separation energy and the ratio of their areas (area = FWHM x height). The following values were determined for the CsI standard: FG = 0.63, FWHM = 1.6 eV, spin-orbital separation energy = 11.6 eV, and the ratio of the $3d_{3/2}$ to $3d_{5/2}$ peak areas was 2 to 3. This procedure leaves the component height and the energy as the only variables, and there also was an option in the computer program to fix the ratio of component heights.

The optimum fit of the corrected data was judged on three factors: Chi-squared (χ^2), appearance, and known chemical information. χ^2 is the square of the sum of the differences between the calculated and the corrected counts for each value of the binding energy. When a good least-squares fit was obtained, the calculated and the corrected data curves would nearly coincide. And unless there is a partial occupancy for a particular type of iodide ligand, the peak area ratios were expected to be near integer values.

X-Ray Diffraction Measurements

The single crystal x-ray diffraction data for $(TBA)_2Mo_4I_{11}$ were collected with graphite-monochromated Mo Kα radiation, λ = 0.71069 Å. A crystal of dimension 0.1 x 0.2 x 0.3 mm was sealed in a 0.3 mm Lindemann capillary tube and placed on a gonimeter head. The crystal

was aligned on an automated four circle diffractometer designed and built for Ames Laboratory under the direction of Rohrbaugh and Jacobson [28]. From ω-oscillation photographs taken at ϕ = 0°, 30°, 60° and 90°, eleven independent reflections were selected. Their coordinates were input into an automatic indexing program [29], and the resulting reduced cell scalars indicated a possible C-centered monoclinic space group. But on close examination, small but significant deviations from expected values for a monoclinic system were observed for the α and γ angles and several selected intensity pairs which should be equivalent. Therefore, the unconventional space group $C\bar{1}$ in the triclinic system was selected. Data were first collected at 27°C. Subsequent refinement with this data set showed disorder in the butyl groups so the data were retaken at -75°C and only these results will be discussed [14]. The cell parameters at -75°C are a = 19.99(3), b = 12.49(3), c = 23.67(2) Å, α = 89.89(6), β = 105.80(5) and γ = 90.27(8)°.

Intensity data (8,767 reflections) with $2\theta \leq 50°$ were measured in the hkl, hk$\bar{l}$, h$\bar{k}$l, and h$\bar{k}\bar{l}$ octants using the ω-stepscan technique. Three standard peaks with $20° < 2\theta < 30°$ were checked every 75 reflections, and the crystal was automatically realigned as necessary. The subsequent data reduction and analysis of the structure factors were performed by the x-ray crystallography group under Dr. R. A. Jacobson.

Intensity data were corrected for polarization and Lorentz effects, and an absorption correction was made [30]. (The transmission factors ranged from 0.38 to 0.48.) The estimated error in each intensity was calculated by

$$O_I^2 = C_T + KC_B + (0.03\ C_T)^2 + (0.03\ C_B)^2 + (0.03\ C_I)^2 Ta^2 \quad (1)$$

where C_T, C_B, C_I, Ta, and K are the total count, the background count, the net count, the transmission factor, and the ratio of intensity to background count, respectively. The 0.03 is an estimate of nonstatistical errors. The finite difference method was used to calculate the estimated deviations in the structure factors [31a]. Equivalent data were averaged and yielded 6,791 reflections with Io > $3\sigma_I$ which were then used for structural solution and refinement.

Reactions

Reaction A - Preparation of $(R_4N)Mo(CO)_5I$ and $(R_4N)Mo(CO)_4I_3$ (where R = n-C_4H_9 or n-C_3H_7)

$Mo(CO)_6$ (2.640 g, 10.00 mmol) and (TBA)I (3.692 g, 10.00 mmol) or (TPA)I (3.133 g, 10.00 mmol) were loaded into a reaction flask containing a magnetic stirring bar (see Fig. 4). The flask was evacuated and purged with nitrogen gas before inserting 30 ml of chlorobenzene by syringe. The contents of the flask were then stirred and refluxed. The resulting gas evolution was allowed to continue until one mole of carbon monoxide per mole of iodide anion was lost, as required for the formation of $(R_4N)Mo(CO)_5I$ [31b]. The amber solution was then cooled to room temperature. At this point, the product was either used in a subsequent reaction (in situ) or precipitated as a yellow crystalline product by adding ether to the solution.

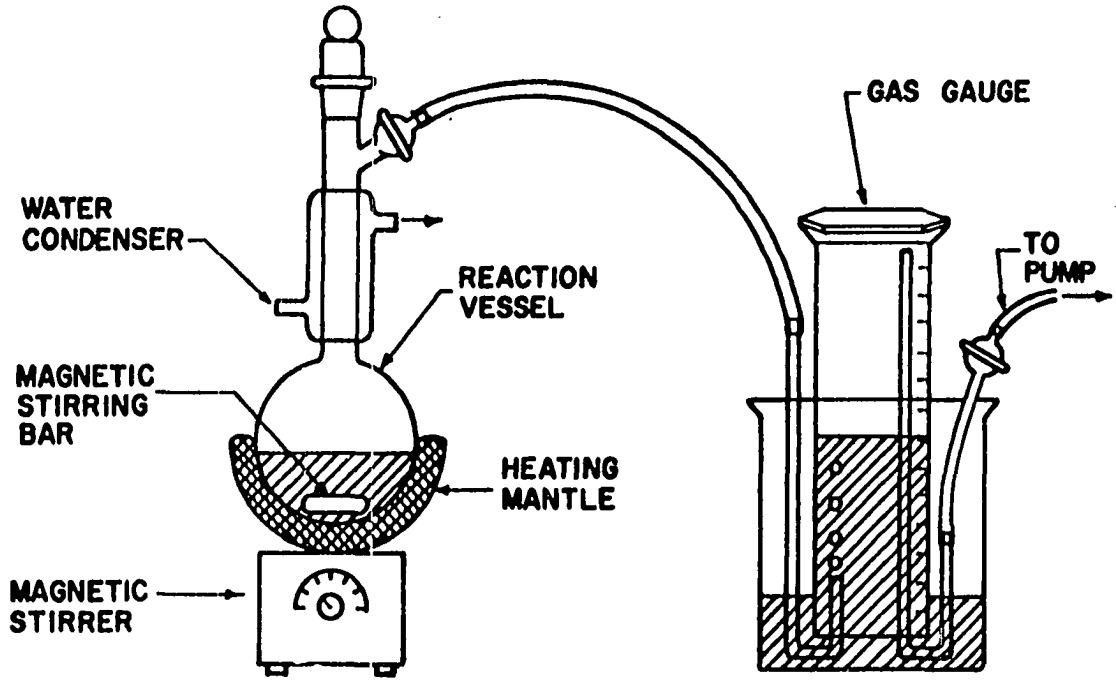

Figure 4. Schlenk reaction vessel with gas collection gauge

$(R_4N)Mo(CO)_4I_3$ was produced by adding I_2 (2.538 g, 10.00 mmol) to the previous solution [31b]. This second step proceeded quickly at room temperature with rapid gas evolution and was complete after a few minutes of stirring. The dark red-brown solution then contained $(R_4N)Mo(CO)_4I_3$. Just as in the previous step, the solution was either used directly for a further reaction (in situ) or the product was precipitated as a yellow-brown crystalline product by adding ether, then filtered and stored for later use.

Reaction B - Preparation of $(TBA)_2Mo_4I_{11}$ from $(TBA)Mo(CO)_4I_3$

In a typical reaction, I_2 (0.317 g, 1.25 mmol) was added to the $(TBA)Mo(CO)_4I_3$ solution (10.00 mmol in 30 ml of chlorobenzene) discussed at the end of reaction A. The flask was then flushed with nitrogen gas before being refluxed for two hours. The fine black powder which precipitated during the reaction was purified by extracting with solvent distilled from the reaction solution. The insoluble $(TBA)_2Mo_4I_{11}$ remaining on the frit was then dried under vacuum, and the yield based on molybdenum was 80%. The material was recrystallized by a slow extraction with acetonitrile. Anal. Calculated for $(TBA)_2Mo_4I_{11}$: Mo, 16.95; I, 61.64; C, 16.97; H, 3.20; N, 1.24. Found: Mo, 16.85; I, 61.58; C, 17.06; H, 3.22; N, 1.44; $\Sigma\%$ = 100.15; I/Mo = 2.76.

Reaction C - Modified preparation of $(TBA)_2Mo_4I_{11}$

The previous reaction procedure was modified to improve its yield. Using the procedure discussed in reaction A, a solution containing

$Mo(CO)_6$, $(TBA)Mo(CO)_4I_3$ and I_2, in a 2:6:3 ratio, was produced by first refluxing $Mo(CO)_6$ (2.640 g, 10.00 mmol) and (TBA)I (2.770 g, 7.50 mmol) in chlorobenzene, then I_2 (2.855 g, 11.25 mmol) was added and the solution was stirred until the carbon monoxide evolution ceased. The resulting mixture was finally refluxed for two hours which resulted in the precipitation of a fine black powder. The powder was purified and recrystallized using the same procedure described in reaction B. The yield based on molybdenum was now 90%. Anal. Calculated for $(TBA)_2Mo_4I_{11}$: Mo, 16.95; I, 61.64; I/Mo = 2.75. Found: Mo, 16.99; I, 61.54; I/Mo = 2.74.

Reaction D - Preparation of $(TPA)_2Mo_4I_{11}$

Using the same procedure as outlined in reaction B, I_2 (0.317 g, 1.25 mmol) was added to the $(TPA)Mo(CO)_4I_3$ solution (10.00 mmoles in 30 ml of chlorobenzene) which was then refluxed for four hours. A black powder containing both $(TPA)_2Mo_4I_{11}$ and (TPA)I precipitates during the course of the reaction. The $(TPA)_2Mo_4I_{11}$ was purified by extraction and recrystallization from acetonitrile. Anal. Calculated for $(TPA)_2Mo_4I_{11}$: Mo, 17.83; I, 64.85; C, 13.39; N, 1.31; H, 2.62. Found: Mo, 17.61; I, 63.86; C, 13.84; N, 1.49; H, 2.68; $\Sigma\%$ = 99.5; I/Mo = 2.74.

Reaction E - Thermolysis of $(TBA)Mo(CO)_4I_3$ under vacuum

$(TBA)Mo(CO)_4I_3$ (8.311 g, 10.00 mmol) was loaded into a Schlenk flask. After purging with nitrogen gas, the vessel was evacuated. The

vessel was then heated to 80°C and maintained under a dynamic vacuum for four hours. The resulting black solid lump was broken into pieces and extracted with chlorobenzene for a day, leaving a black powder on the frit. Anal. Found: Mo, 15.83; I, 57.75; I/Mo = 2.76. The remainder for material balance was assumed to be (TBA). The resulting (TBA)/Mo ratio was thus estimated to be 0.66.

Reaction F - Thermolysis of $(TBA)Mo(CO)_4I_3$ in refluxing benzene

$(TBA)Mo(CO)_4I_3$ (8.312 g, 10.00 mmol) was loaded into a reaction flask containing a magnetic stirring bar. After the vessel had been purged with nitrogen gas, 30 ml of benzene was syringed into the vessel and the benzene was refluxed for seven hours. The suspended $(TBA)Mo(CO)_4I_3$ was converted to a mixture of black and white solids. The black solid was purified by extracting with chlorobenzene for a day, leaving an insoluble black powder on the frit. Anal. Found: Mo, 16.14; I, 58.67; I/Mo = 2.75. The (TBA)/Mo ratio was estimated to be 0.62; this implied the formula was $(TBA)_5(Mo_4I_{11})_2$.

Reaction G - Thermolysis of $(TBA)Mo(CO)_4I_3$ in refluxing o-dichlorobenzene

$(TBA)Mo(CO)_4I_3$ (8.309 g, 10.00 mmol) was placed in a reaction flask containing a magnetic stirring bar. The flask was evacuated and then purged with nitrogen gas. About 40 ml of o-dichlorobenzene was syringed into the flask, dissolving the $(TBA)Mo(CO)_4I_3$ on stirring. The solution was brought to reflux, and the carbon monoxide appeared completely evolved within 15 minutes. At the same time, a few $Mo(CO)_6$

crystals formed inside the condenser section of the reaction flask. The solution was refluxed an additional 40 minutes and then cooled. The resulting black crystalline material was filtered, washed twice with chlorobenzene, and then dried under a vacuum. Anal. Calculated for $(TBA)_2Mo_4I_{11}$: Mo, 16.95; I, 61.64. Found: Mo, 16.78; I, 61.58; I/Mo = 2.77. The remainder for material balance was assumed to be (TBA), which would give a (TBA)/Mo ratio of 0.51. (The expected (TBA)/Mo ratio is 0.50.)

Reaction H - Zinc reduction of $(TBA)_2Mo_4I_{11}$ in acetonitrile

$(TBA)_2Mo_4I_{11}$ (6.288 g, 2.75 mmol), (TBA)I (1.016 g, 2.75 mmol), and zinc shot (0.131 g, 2.00 mmol) were loaded into a Schlenk flask along with a magnetic stirring bar. The flask was purged with nitrogen gas and then 30 ml of acetonitrile was syringed into the vessel. Finally, the flask was partially evacuated. The solution was stirred at room temperature for five days before it was filtered. The dark brown powder on the frit was extracted with fresh CH_3CN pumped dry and analyzed. Anal. Calculated for $(TBA)_5(Mo_4I_{11})_2$: Mo, 16.13; I, 58.66; C, 19.98; H, 3.77; N, 1.46; I/Mo = 2.75. Found: Mo, 16.15; I, 58.48; C, 19.41; H, 3.64; N, 1.38; $\Sigma\%$ = 99.1; I/Mo = 2.74.

Reaction I - Zinc reduction of $(TBA)_2Mo_4I_{11}$ in refluxing acetonitrile

$(TBA)_2Mo_4I_{11}$ (11.323 g, 5.00 mmol), (TBA)I (1.847 g, 5.00 mmol), zinc shot (0.787 g, 12.00 mmol), and 30 ml of acetonitrile were placed into a reaction flask as described in reaction F, and then the solution

was refluxed for twenty-four hours. The resulting solid material was filtered and then extracted with acetonitrile for two days. The very dark brown powder left on the frit was pumped dry. Anal. Calculated for "$(TBA)_2Mo_4I_{10}$": Mo, 17.95; I, 59.36; C, 17.98; H, 3.40; N, 1.31; I/Mo = 2.50. Found: Mo, 18.19; I, 59.55; C, 15.97; H, 2.98; N, 1.56; Σ% = 98.3; I/Mo = 2.48.

Reaction J - Thermolysis of $(TBA)Mo(CO)_4I_3$ in the presence of hydrogen

$(TBA)Mo(CO)_4I_3$ (8.310 g, 10.00 mmol) was loaded with a magnetic stirring bar into a reaction vessel fitted with a bubbler, see Fig. 5. After 70 ml of chlorobenzene was syringed into the vessel, the solution was saturated with hydrogen gas. The solution was then refluxed for eighteen hours with continuous hydrogen bubbling. The solvent was pumped off, and the resulting tar was broken with a minimal volume of acetonitrile, filtered, and extracted with fresh acetonitrile for two days. The remaining dark brown powder on the frit was then dried and analyzed as "$(TBA)_2Mo_4I_{10}$". Anal. Calculated: Mo, 17.95; I, 59.36; C, 17.98; H, 3.40; N, 1.31; I/Mo = 2.50. Found: Mo, 18.16; I, 59.46; C, 17.38; H, 3.29; N, 1.27; Σ% = 99.6; I/Mo = 2.48.

Reaction K - Thermolysis of $(TPA)Mo(CO)_4I_3$ in the presence of nitrogen

$(TPA)Mo(CO)_4I_3$ (7.751 g, 10.00 mmol) was dissolved in 70 ml of chlorobenzene in the same reaction vessel described in reaction H. After the solution was saturated with nitrogen gas, the solution was refluxed for sixteen hours with continuous nitrogen bubbling. The brown

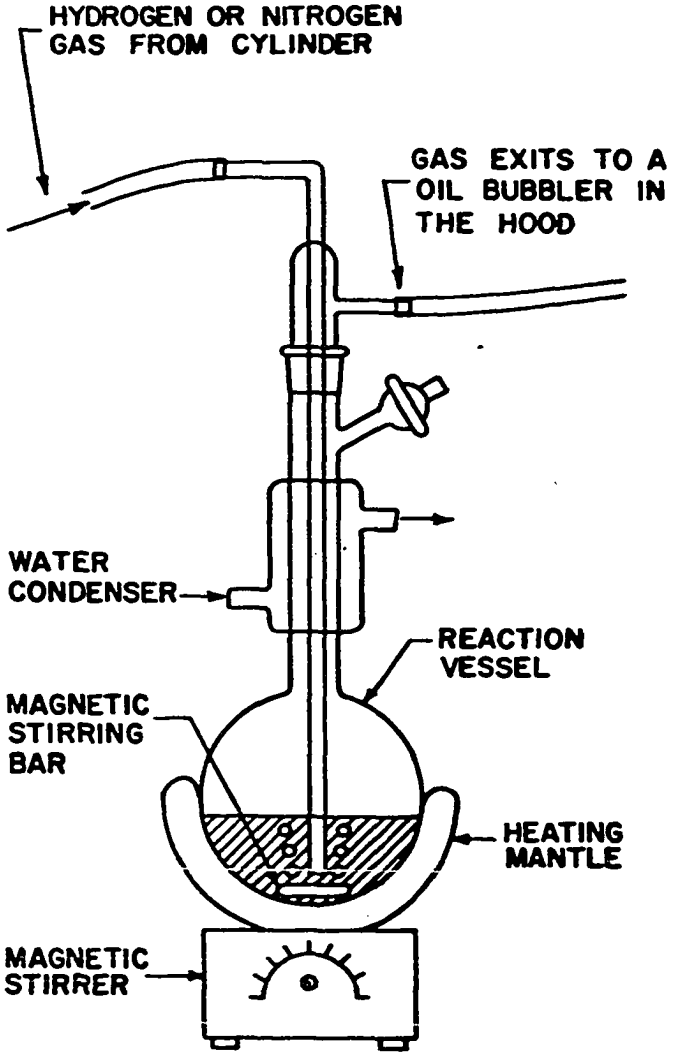

Figure 5. Reaction vessel with gas bubbler

powder which precipitates during the reaction was then filtered and extracted with chlorobenzene until the solution above the frit was clear. Finally, the powder was pumped dry and analyzed. The yield was 65% based on molybdenum. Anal. Calculated for "$(TPA)_2Mo_4I_{10}$": Mo, 18.95; I, 62.65; C, 14.23; H, 2.79; N, 1.38; I/Mo = 2.50. Found: Mo, 18.80; I, 62.63; C, 14.62; H, 2.89; N, 1.34; Σ% = 100.3; I/Mo = 2.52.

Reaction L - Thermolysis of $(TPA)Mo(CO)_4I_3$ in the presence of hydrogen

Reaction K was repeated with one change, hydrogen gas was bubbled through the solution containing $(TPA)Mo(CO)_4I_3$ (7.751 g, 10.00 mmol) in 70 ml of chlorobenzene, instead of nitrogen gas. The solution was refluxed for eighteen hours. The resulting brown powder was first extracted with chlorobenzene, and then further purified by extracting with acetonitrile. Just as when nitrogen was used as a purging gas, the product was "$(TPA)_2Mo_4I_{10}$", but the yield was higher, at 90%. Anal. Calculated: Mo, 18.95; I, 62.65; C, 14.23; H, 2.79; N, 1.38; I/Mo = 2.50. Found: Mo, 18.75; I, 61.78; C, 14.90; H, 2.86; N, 1.51; Σ% = 99.8; I/Mo = 2.49.

Reaction M - Reaction of $(TBA)_2Mo_4I_{11}$ with I_2

$(TBA)_2Mo_4I_{11}$ (7.926 g, 3.50 mmol) and I_2 (0.888 g, 3.50 mmol) were placed in a Schlenk flask containing a magnetic stirring bar, then the flask was evacuated and purged with nitrogen gas. About 30 ml of acetonitrile were syringed into the flask and the solution was then stirred at room temperature for two days. The product was then extracted

until the solvent above the frit was colorless. $Mo_4I_9(CH_3CN)_4$ was recovered on the frit as a fine brown powder in about an 85% yield. Anal. Calculated: Mo, 22.70; I, 67.52; C, 5.69; H, 0.72; N, 3.31; I/Mo = 2.25; N/Mo = 1.0. Found: Mo, 22.82; I, 67.52; C, 5.52; H, 0.73; N, 3.12; Σ% = 99.7; I/Mo = 2.24, N/Mo = 0.94.

Reaction N - Reaction of $Mo_4I_9(CH_3CN)_4$ with (TBA)I

$Mo_4I_9(CH_3CN)_4$ (3.026 g, 1.79 mmol) and (TBA)I (2.000 g, 5.41 mmol) were placed in a reaction vessel containing a magnetic stirring bar. After purging the vessel with nitrogen gas, 30 ml of chlorobenzene were syringed into the flask, and the solution was refluxed for eighteen hours. $(TBA)_2Mo_4I_{11}$ precipitates during the reaction as a black powder and is purified by extracting with chlorobenzene. Anal. Calculated for $(TBA)_2Mo_4I_{11}$: Mo, 16.95; I, 61.64; C, 16.97; H, 3.20; N, 1.24; I/Mo = 2.75. Found: Mo, 16.99; I, 61.54; C, 16.94; H, 3.16; N, 1.27; Σ% = 99.9; I/Mo = 2.74.

SYNTHESES AND CHARACTERIZATIONS OF $(TBA)_2Mo_4I_{11}$ AND $(TPA)_2Mo_4I_{11}$

The synthesis of metal-metal bonded cluster compounds by the thermolysis of group VI tetracarbonyltrihalometallate salts is a well documented procedure. The method was first successfully used by Delphin and Wentworth [32]. Based on the knowledge that the carbon monoxide ligands become more labile as the oxidation state of the metal increases, $Mo(CO)_4I_3^-$ salts are ideal starting materials. Also, their syntheses are straightforward, as discussed in the experimental section. In a refluxing noncoordinating solvent, the metal halocarbonyl species easily evolve carbon monoxide creating coordinately unsaturated metal species which condense to form metal-metal bonded clusters.

Syntheses

This project originated from work done by R. J. Hoxmeier and continued by J. L. Templeton. Hoxmeier conducted a quick synthetic survey of the possible thermolysis reactions with $(R_4N)^+M(CO)_4X_3^-$ salts (where R = C_2H_5, n-C_3H_7, n-C_4H_9, M = Mo, W and X = Br, I). The most interesting reaction to investigate further was the thermolysis of $(TBA)Mo(CO)_4I_3$ in refluxing chlorobenzene. A poorly characterized, black crystalline product was obtained. On recrystallization from 1,2-dichloroethane, crystals were obtained that were analyzed as $(TBA)_2Mo_4I_{10}Cl$ [33].

It was felt that the reaction could be modified by using iodine to oxidize the initial product instead of the chlorinated solvent. Stoichiometric quantities of $(TBA)Mo(CO)_4I_3$ and I_2, sufficient to form

$(TBA)_2Mo_4I_{11}$, were refluxed in chlorobenzene for eighteen hours. A brown solution was filtered off, leaving a black insoluble powder on the frit. Next, the powder was washed with fresh chlorobenzene and then dried under a dynamic vacuum. The reaction was successful; analysis of the powder provided an I/Mo ratio 2.75. An infrared spectrum of the material in the region 3000-600 cm^{-1} contained bands for only the (TBA) cation.

The reaction procedure has since been improved substantially. The most important improvement resulted from the adjustment of the free (TBA)I concentration in the reaction solution. In the original procedure, half of the TBA was recovered as $(TBA)_2Mo_4I_{11}$ and the other half remained in solution. Later, it was shown that (TBA)I reacts with $(TBA)_2Mo_4I_{11}$ in chlorobenzene in approximately a 4:1 ratio to form a poorly characterized, chlorobenzene-soluble by-product; the reaction was modified to limit excess (TBA)I. Now, only enough (TBA)I was added in the first step of the reaction to convert three-fourths of the $Mo(CO)_6$ to $(TBA)Mo(CO)_5I$. The same quantity of iodine was added in the second step as before, so after two steps one had a mixture of $Mo(CO)_6$, $(TBA)Mo(CO)_4I_3$, and I_2 in solution. After refluxing the solution for one to two hours, the reaction was complete. Any soluble by-products were then extracted away with chlorobenzene, leaving the fine black powder of $(TBA)_2Mo_4I_{11}$ in about 90% yield. Attempts to further limit the concentration of any free (TBA)I proved counter-productive. Since $(TBA)_2Mo_4I_{11}$ is reasonably soluble in acetonitrile, the product can be recrystallized by either extracting with acetonitrile or by slowly cooling a saturated solution.

The thermolysis of $(TPA)Mo(CO)_4I_3$ in refluxing chlorobenzene was then found to produce the analogous $(TPA)_2Mo_4I_{11}$ salt. $(TPA)_2Mo_4I_{11}$ and free (TPA)I both precipitate during the reaction, eliminating the chance of the previously mentioned side reaction. The soluble (TPA)I is separated from the less soluble $(TPA)_2Mo_4I_{11}$ by extraction with acetonitrile.

It is especially noteworthy that the synthetic approach outlined above was successful in producing a new molybdenum cluster species from a monomeric starting material under relatively mild conditions. The syntheses can be attained from the simple starting materials, $Mo(CO)_6$, $(R_4N)^+I^-$ and I_2 in the proper ratios in a one-pot reaction.

Spectra of $(TBA)_2Mo_4I_{11}$ and $(TPA)_2Mo_4I_{11}$

All bands observed in the infrared spectrum over the region 4000 to 600 cm^{-1} were assigned to the respective cations, (TBA) or (TPA). This verified that the compounds contained no residual carbon monoxide or coordinated solvent molecules. The bands observed in the far-infrared spectra over the range 220 to 20 cm^{-1} are listed in Table 5.

Table 5. Far-infrared spectra of $(TBA)_2Mo_4I_{11}$ and $(TPA)_2Mo_4I_{11}$

$(TBA)_2Mo_4I_{11}$	204(m), 191(s), 181(s), 169(s), 111(w), 104(m) cm^{-1}
$(TPA)_2Mo_4I_{11}$	203(w), 191(s), 183(s), 169(s), 107(m), 100(m) cm^{-1}

s = strong
m = medium
w = weak

The spectra of both salts are nearly the same with three strong Mo-I stretching bands at approximately 192, 182 and 169 cm^{-1} and a weaker Mo-I stretching band at 204 cm^{-1}. Each salt also exhibits two bands in the region 100 to 111 cm^{-1} which are unassigned.

The electronic spectrum of $(TBA)_2Mo_4I_{11}$ was obtained in both acetonitrile and in a nujol mull, whereas the spectrum of $(TPA)_2Mo_4I_{11}$ was obtained only in a nujol mull. In the mull spectrum of the (TBA) salt, band maxima were observed at 380, 510 and 625 nm; in acetonitrile, corresponding bands were found at 360, 490 and 640 (shoulder) nm. If the compound had been stored in the dry box for a long time, the band at 490 nm was shifted to approximately 530 nm. The values agreed with the findings of Glickman and Walton, who synthesized the same compound by reacting $Mo_2(O_2CCH_3)_4$ with HI in methanol [34]. The approximate absorption maxima of the (TPA) salt mull were similar at 380 (shoulder), 490 and 610 (shoulder) nm.

X-ray powder patterns of reaction products were routinely used for identification and comparison of products. The d-spacings were based on the 2θ values obtained with Cu Kα radiation. The d-spacings of both salts are listed in Table 15 (in the Appendix).

Cyclic Voltammetry

After it had been shown that $(TBA)_2Mo_4I_{11}$ could be chemically reduced with zinc metal in acetonitrile, it was decided to investigate the reduction further by electrochemical means. This study was hampered by the low solubility of $(TBA)_2Mo_4I_{11}$ in acetonitrile, viz. less than

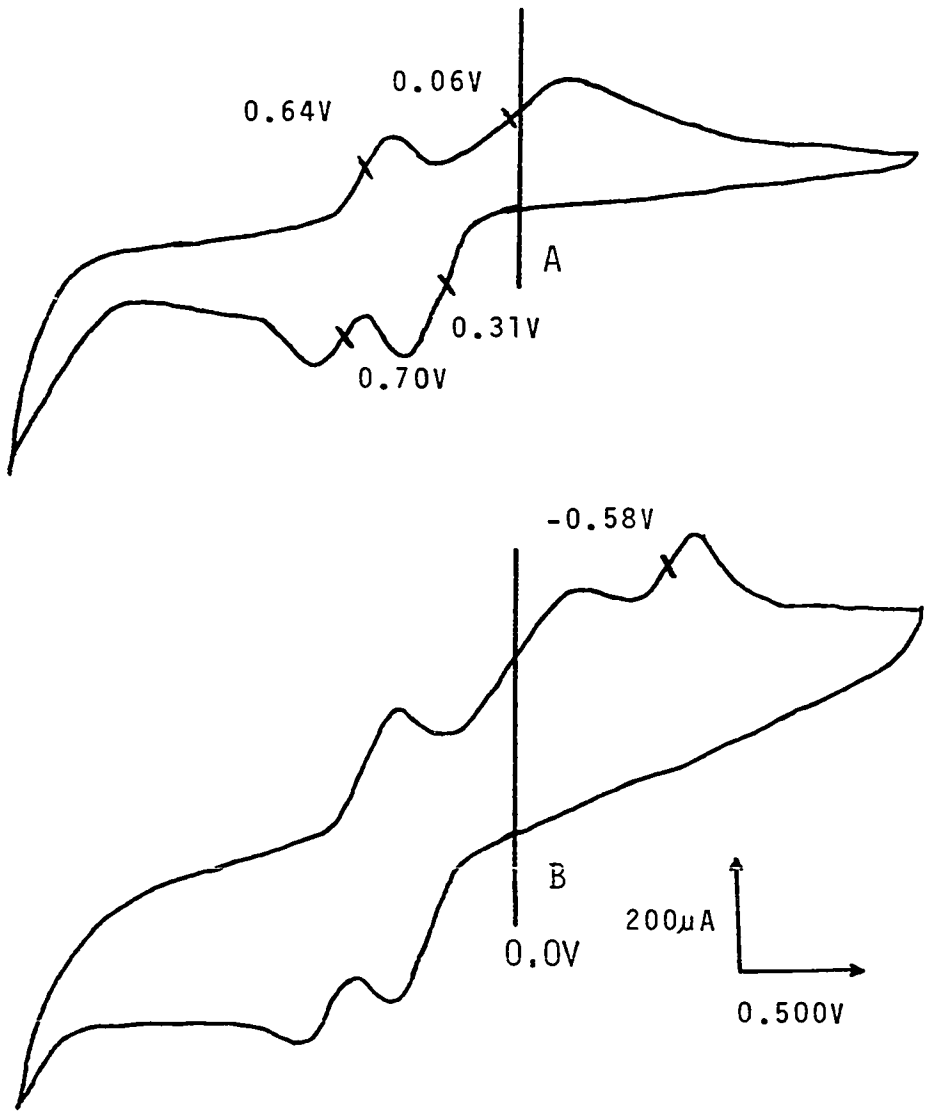

Figure 6. Stationary Pt electrode voltammograms: (A) 1.9 x 10^{-3} M (TBA)I and (B) 5.8 x 10^{-4} M $(TBA)_2Mo_4I_{11}$; scan rate was 1 V/sec

6×10^{-4} M. The effective scanning range of the potential, from +0.10 to -2.00 volts (using a saturated NaCl-calomel reference electrode), was limited by the oxidation of iodide and the reduction of acetonitrile, respectively. There was also a reduction peak observed in the blank at approximately -1.2 volts. The supporting electrolyte, $(TBA)BF_4$, concentration was held constant at 2×10^{-2} M.

The stationary electrode voltammogram of $(TBA)_2Mo_4I_{11}$ contains one new peak; a reduction peak at -0.58 volts compared to (TBA)I as shown in Fig. 6. The redox of iodide in solution and adsorbed onto the electrode result in the two oxidation and two reduction peaks observed in both voltammograms, A and B [35]. The reduction of the $Mo_4I_{11}^{2-}$ anion appears to be an irreversible reaction under these conditions. A rapid conversion to an electrochemically nonoxidizable form is inferred, and subsequent studies with "$Mo_4I_{10}^{2-}$" suggested the following equilibrium exists in solution.

$$Mo_4I_{11}^{3-} \rightleftarrows Mo_4I_{10}^{2-} + I^- \qquad (2)$$

Under low I^- concentrations, the equilibrium lies to the right.

In the absence of a corresponding reoxidation wave, the number of electrons involved in the reduction of $Mo_4I_{11}^{2-}$ can be estimated using Eq. (3) (where n = number of electrons).

$$0.059/n = E_{2/3} - E_{1/3} \qquad (3)$$

$$= 0.638 - 0.579 = 0.059$$

Solving for n, we find the reaction is a one-electron reduction. This confirms earlier results found for the zinc reduction of $Mo_4I_{11}^{2-}$ where the $Mo_4I_{11}^{3-}$ anion was generated. Another important observation from this work was that there were no oxidation waves for $Mo_4I_{11}^{2-}$. Later attempts to oxidize the $Mo_4I_{11}^{2-}$ anion with elemental iodine verified this observation.

Magnetic Properties

$Mo_4I_{11}^{2-}$ is an odd-electron anion and because of its low symmetry there should be one unpaired electron in the ground state. The magnetic behavior of $(TBA)_2Mo_4I_{11}$ was examined over a range of temperatures from 118 K to 333 K. Twelve temperatures were chosen such that their 1/T values decreased in approximately equal increments. The forces were measured at five field strengths and were plotted χ versus 1/H to obtain a field independent value (at the intercept) for each temperature. Next, the apparent molar susceptibility (χ_m) was calculated by first subtracting the diamagnetic contribution of the Teflon sample container, then by dividing the number of grams of sample and multiplying by the molecular weight of $(TBA)_2Mo_4I_{11}$, 2264.62 g/mol. The plot of χ_m versus 1/T was linear as shown in Fig. 7. This indicated simple Curie behavior as given by Eq. 4, where C is the Curie constant, χ_d is the diamagnetic

$$\chi_m = C/T + \chi_d + \chi_{TIP} \qquad (4)$$

contribution from the spin-paired electrons in the compound, and the χ_{TIP} is the temperature independent paramagnetic contribution. A least-squares fit of the twelve data points provided the numerical values for

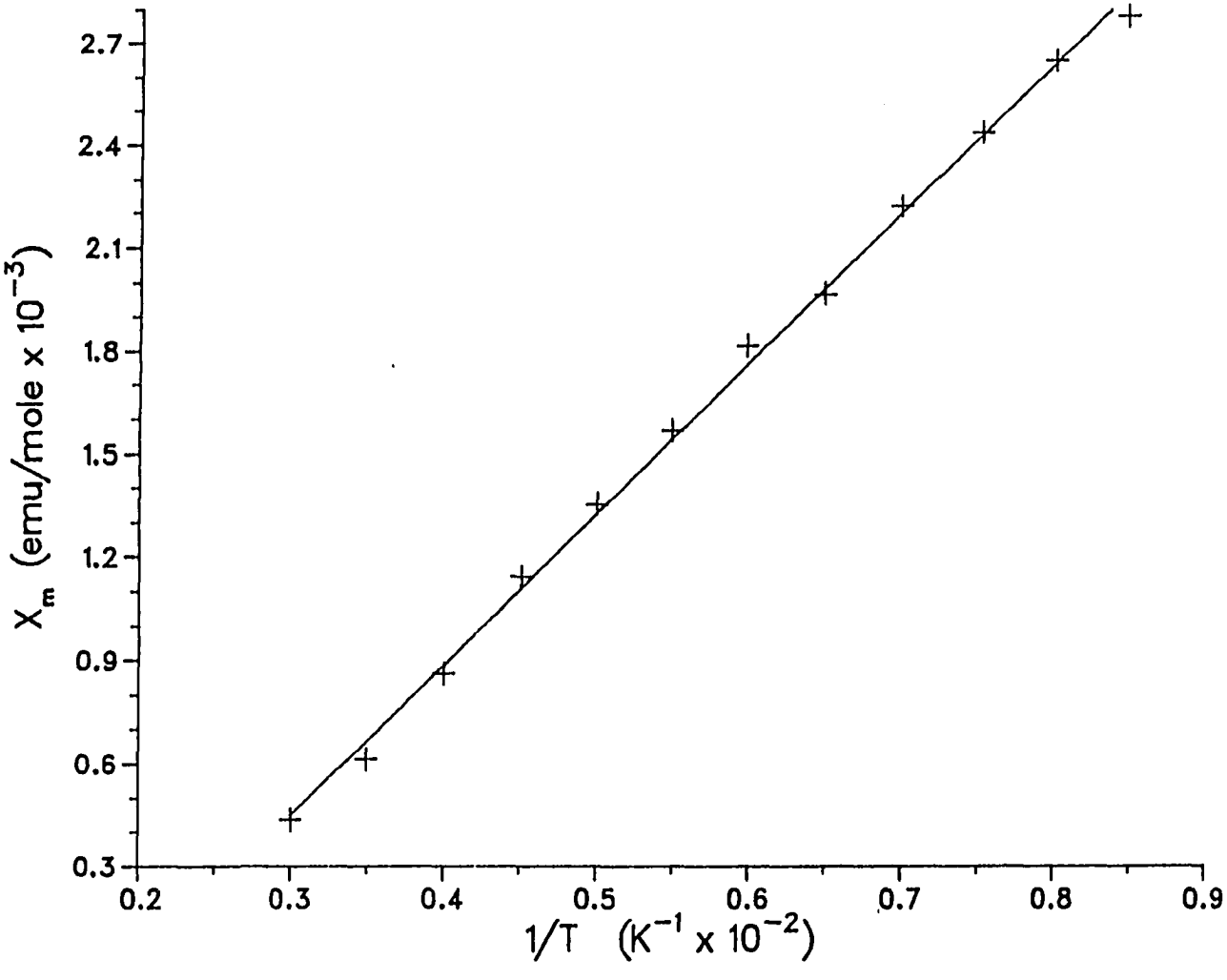

Figure 7. χ_m vs. 1/T plot for $(TBA)_2Mo_4I_{11}$

the slope and the intercept as shown in Eq. (5). The magnetic moment

$$\chi_m = 0.4388 \frac{\text{Kemu}}{\text{mol}} (1/T) - 867 \times 10^{-6} \text{ emu/mol} \quad (5)$$

(μ) was calculated from the slope (C) by Eq. (6). The value of the

$$\mu = 2.828 (C)^{1/2} = 1.87 \mu_\beta \quad (6)$$

magnetic moment, 1.87 μ_β, agreed with the assignment of one unpaired electron in the ground state, but differed significantly from the theoretical spin-only value of 1.73 μ_β. The difference is probably caused by spin-orbital coupling effects which connect the ground state function with a lower energy orbital. χ_{TIP} was found by subtracting the sum of the χ_d's from the intercept: $\chi_{TIP} = (-867 + 968) \times 10^{-6}$ emu/mol = 101 x 10^{-6} emu/mol. Values for χ_d of each atom in the compound were taken from the CRC Handbook of Chemistry and Physics [36].

Work on subsequent compounds required the electron paramagnetic resonance (EPR) spectrum of $(TBA)_2Mo_4I_{11}$ as a reference. (All the EPR work was done at room temperature.) The spectroscopic splitting factor (g) was determined using diphenylpicrylhydrazyl (DPPH) as the standard, g = 2.0037. As seen in Fig. 8, the EPR spectrum can be resolved into parallel ($g_\parallel$) and perpendicular ($g_\perp$) components with $g_\parallel$ = 2.098 and $g_\perp$ = 2.037, $\bar{g}$ = 2.057 (see Table 6). The magnetic moment calculated from the average g-factor was 1.78 μ_β and did not agree well with the value obtained by magnetic susceptibility measurements, 1.87 μ_β. The

$$\mu = g[s(s + 1)]^{1/2} = 2.057[1/2(3/2)]^{1/2} = 1.78 \mu_\beta \quad (7)$$

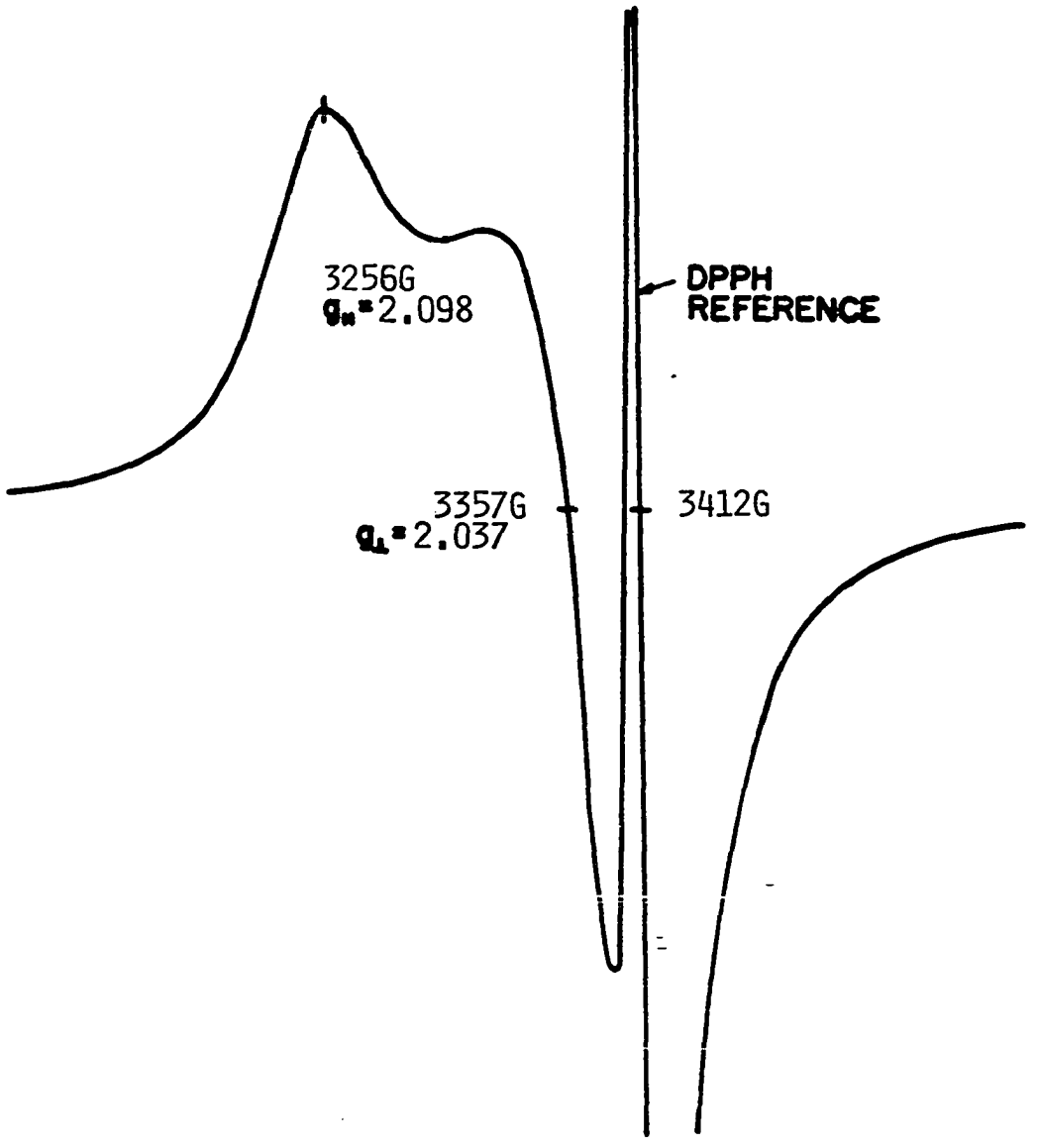

Figure 8. EPR spectrum of $(TBA)_2Mo_4I_{11}$

EPR spectrum of $(TPA)_2Mo_4I_{11}$ was similar to that of the (TBA) salt in both the average g-factor (2.045) and the shape of the resonance absorption.

Table 6. EPR spectra for $(TBA)_2Mo_4I_{11}$ and $(TPA)_2Mo_4I_{11}$

	$\bar{g}$	$g_{\parallel}$	$g_{\perp}$
$(TBA)_2Mo_4I_{11}$	2.057	2.098	2.037
$(TPA)_2Mo_4I_{11}$	2.045	2.088	2.024

Photoelectron Spectroscopy (PES)

The PES spectrum of $(TBA)_2Mo_4I_{11}$ was studied with the intent of using the derived I $3d_{3/2,5/2}$ binding energies to aid in identifying the types of iodide ligands in other compounds. From the crystal structure, the types of iodide ligands present in $(TBA)_2Mo_4I_{11}$ can be designated as triply bridging, doubly bridging and terminal, and are present in a 2:5:4 ratio (from high to low binding energies). The I $3d_{3/2,5/2}$ PES spectrum of $(TBA)_2Mo_4I_{11}$ can be deconvoluted using either two or three independent components using the computer program discussed earlier [27].

The best fit for the two component case, allowing both component height and energy to vary, gave a component area ratio of 6.3:4.7. (Best and Walton deconvoluted the $Mo_4I_{11}^{2-}$ spectrum mechanically and obtained a 7:4 solution [37].) The component of relative area 6.3 is at higher binding energy and was assigned to the bridging iodide ligands. The component of lesser energy was assigned to terminal iodide ligands. When the computer option of fixing the component area ratio was used,

neither the 7:4 nor the 6:5 choices fit the data well. If the triply bridging and doubly bridging iodide ligands were nearly equivalent in binding energy, the 7:4 case would be expected to give the best fit.

To justify the use of three independent peaks, it is necessary to show there is sufficient energy difference to resolve individual components from the triply and doubly bridging iodide ligands. The component areas were thus held in a fixed ratio to guarantee a solution corresponding to the known structure. The new component, found at the highest binding energy, was assigned to the triply bridging iodide ligands. A binding energy difference of 0.6 eV between the triply and doubly bridging ligands was determined, and the difference between the doubly bridging and terminal iodide ligands was found to be 1.1 eV. The three component solution constituted the best fit of the data and agreed with the crystal structure. (The PES spectra of $(TBA)_2Mo_4I_{11}$ normally exhibited an anomalous area on the low binding energy side of the peak. An example of the anomalous area is shown in Fig. 9, centered at 617.8 eV. If the component ratios were not fixed, one of the three components would compensate for this area.)

PES was the physical method which proved most beneficial in determining that the structure of the $Mo_4I_{11}^{2-}$ anion is the same for both (TBA) and (TPA) salts (see Table 7). The spectrum of the (TPA) salt was measured using monochromatic radiation (see Figs. 9 and 10). Using the same procedure as on the (TBA) salt, the data were first fitted with two independent components. The ratio of their component areas was 6.3:4.7 for eleven iodide ligands. Next, resolution of the spectrum with three

Table 7. PES results for (TBA) and (TPA) salts of $Mo_4I_{11}^{2-}$

Salt	(TBA)	(TBA)[a]	(TPA)	(TPA)[a]
Mo, $3d_{5/2}$	229.3	--	229.0	--
FWHM, $3d_{5/2}$	1.4	--	1.5	--
I, $3d_{3/2}$-$3d_{5/2}$	11.6	11.6	11.6	11.6
FWHM, $3d_{3/2}$	2.8	2.3	2.5	2.6
FWHM, $3d_{5/2}$	2.7	2.4	2.6	2.6
2-Components:				
I1, $3d_{5/2}$	620.5	620.6	620.4	620.7
I2, $3d_{5/2}$	619.3	619.4	619.0	619.4
I1:I2[a]	6.3:4.7	6.3:4.7	6.3:4.7	6.3:4.7
3-Components:				
I1, $3d_{5/2}$	620.9	620.8	620.8	621.2
I2, $3d_{5/2}$	620.3	620.4	620.1	620.4
I3, $3d_{5/2}$	619.2	619.3	618.9	619.1
I1:I2:I3[b]	2:5:4[c]	2:5:4[c]	2:5:4[c]	1.9:5.0:4.1

[a]Monochromatic radiation was used.

[b]Based on a total of eleven iodide ligands.

[c]Iodide component area ratio fixed at 2:5:4.

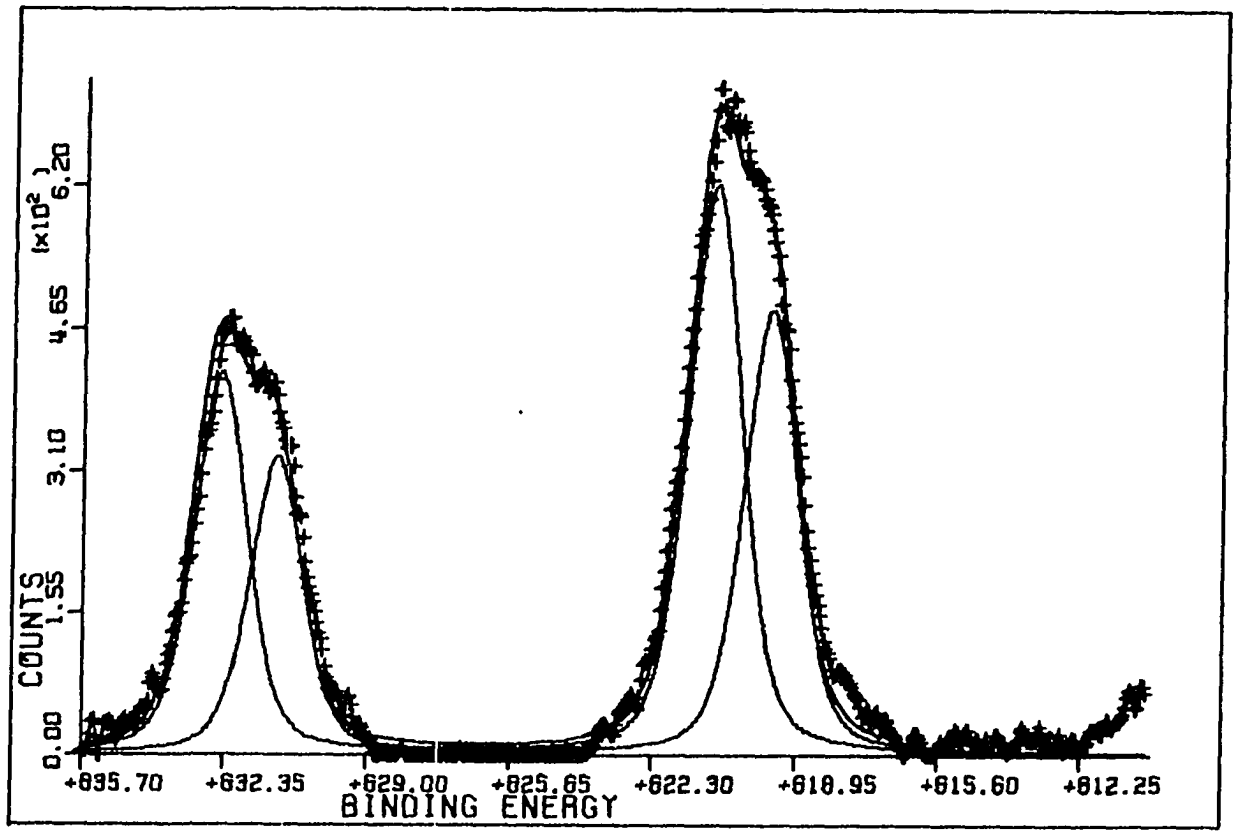

Figure 9. Calculated iodine spectrum of $(TPA)_2Mo_4I_{11}$, two components

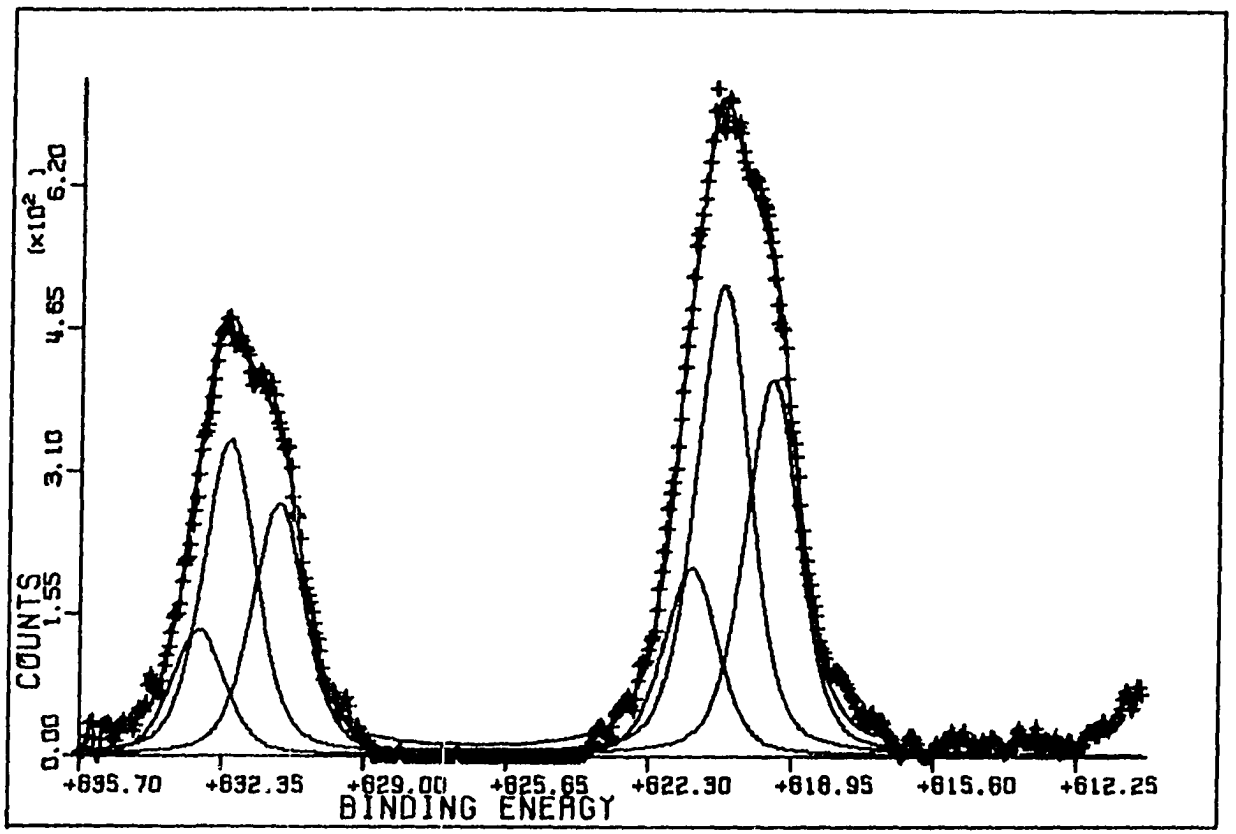

Figure 10. Calculated iodine spectrum of $(TPA)_2Mo_4I_{11}$, three components

independent components was tried. When the component area ratio was fixed at 2:5:4, an improved fit was obtained. (The ratio is for triply bridging:doubly bridging:terminal iodide ligands.) Because of the quality of the monochromatic data, the data were then fitted with three independent peaks for which the component area ratio was not fixed. The component area ratio remained at 1.9:5.0:4.1, and the binding energy difference between the triply and doubly bridging iodides was 0.7 eV and between the doubly bridging and terminal iodide ligands was 1.2 eV. These results match those for the (TBA) salt in energy and component area ratio. This is a clear indication that the anion has the same structure in both salts.

X-Ray Crystal Structure Determination

Since the remainder of this project is based on $(TBA)_2Mo_4I_{11}$, it is vital to first discuss its molecular crystal structure and then its bonding. The I/Mo ratio of 2.75 indicated the anion may have a new structure, different from the previously known tetrahedral chalcogen cubane structure. Suitable crystals were obtained by slowly cooling a saturated acetonitrile solution. They were given to Dr. R. A. Jacobson, who with his co-workers determined the compound's x-ray crystal structure. As mentioned previously, the solution was obtained with some difficulty. From data taken at -75°, the final cell parameters were: $a = 19.99(3)$, $b = 12.49(3)$, $c = 23.67(2)$ Å, $\alpha = 89.89(6)$, $\beta = 105.80(5)$, $\gamma = 90.27(8)°$, $Z = 2$, $C\bar{1}$. The structure was refined with positional and anisotropic thermal parameters for all nonhydrogen atoms using a full matrix least squares procedure [38]. Using 6791 reflections with

$I_o > 3\sigma_I$, the final conventional discrepancy factors were minimized at $R = 0.090$ and $R\omega = 0.122$. The scattering factors used [39] were modified for the real and imaginary parts of anomalous dispersion [40]. The final positional and thermal parameters are listed in Table 16 (in the Appendix), along with the standard deviations as calculated from the inverse matrix of the final least squares cycle.

The severely distorted tetrahedral structure of the $Mo_4I_{11}^{2-}$ anion is illustrated in Fig. 11. In compounds that have a regular tetrahedral cluster unit, there are six equivalent metal-metal bonds. In contrast, the $Mo_4I_{11}^{2-}$ anion has only four of the six molybdenum-molybdenum bonds equivalent. The anion also has two face-bridging, five edge-bridging, and four terminal iodide ligands. The anion bond distances are listed in Table 8.

The only symmetry in the crystal is inversion, CT; and the anion by virtue of its location is not required to possess any symmetry element. However, the anion does contain a pseudo-C_2 axis which passes through I(1) and bisects the Mo(1)-Mo(2) and Mo(3)-Mo(4) bonds. I(1) is interesting for two reasons: it is the only atom that lies on the pseudo-C_2 axis and it occupies the position midway between the two vacant "iodide cube" corners. (The iodide cube will be discussed later.) Also, the two metal-metal bonds bisected by the axis are the longest of those in the cluster. For a more detailed description of the $Mo_4I_{11}^{2-}$ anion structure, we will start with the metal frame.

The metal frame of the $Mo_4I_{11}^{2-}$ anion is a closed polyhedron which appears to be formed from two isosceles triangles sharing a common base.

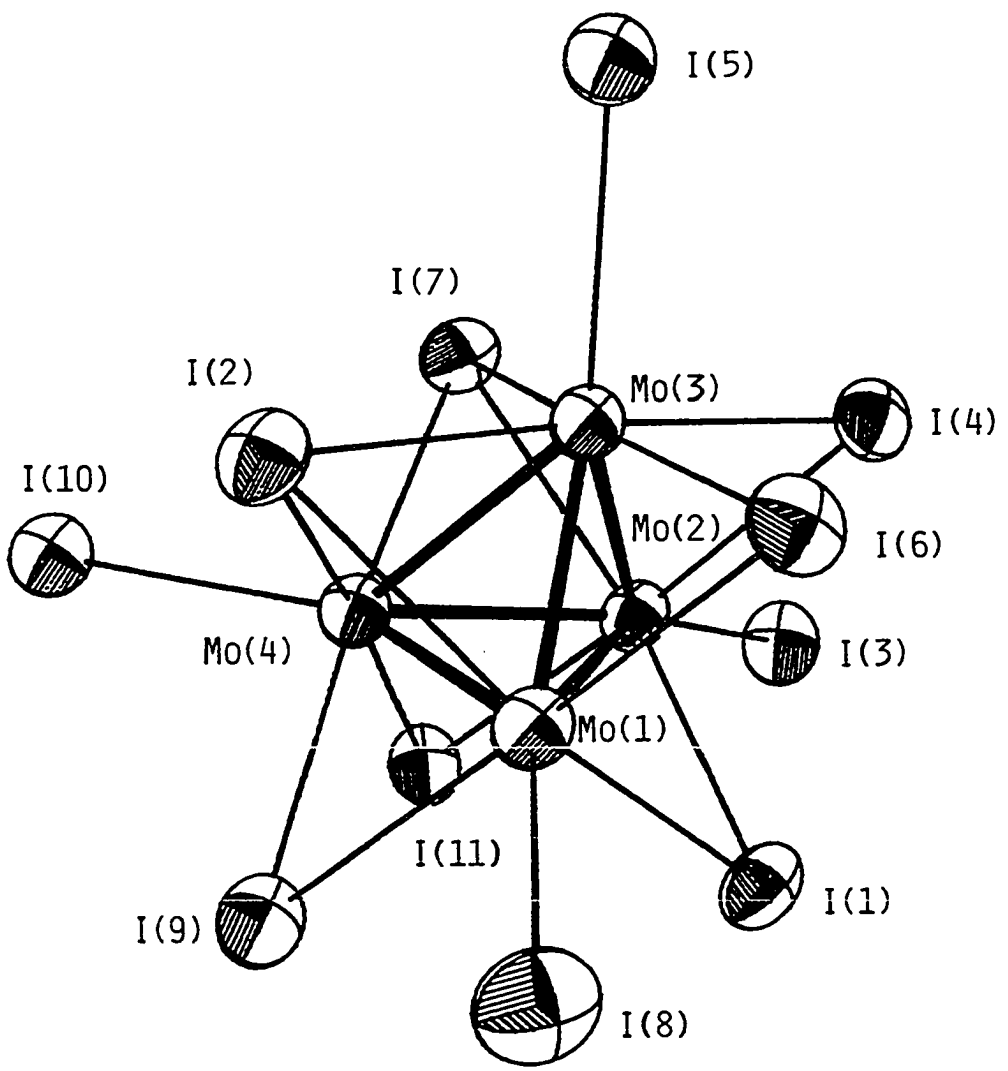

Figure 11. ORTEP view of the $(Mo_4I_7)I_4^{2-}$ anion

Table 8. Bond distances in $Mo_4I_{11}^{2-}$ (Å)

Mo(1) - Mo(2)	3.035 (5)	
Mo(1) - Mo(3)	2.549 (4)	
Mo(1) - Mo(4)	2.552 (5)	
Mo(2) - Mo(3)	2.536 (6)	
Mo(2) - Mo(4)	2.532 (5)	
Mo(3) - Mo(4)	2.669 (5)	
		Average Mo-Mo = 2.645 Å
Mo(1) - I(8)	2.854 (5)	
Mo(2) - I(3)	2.840 (5)	
Mo(3) - I(5)	2.844 (5)	
Mo(4) - I(10)	2.853 (5)	
		Average $Mo\text{-}I_{terminal}$ = 2.848 Å
Mo(1) - I(1)	2.746 (6)	
Mo(1) - I(6)	2.767 (4)	
Mo(1) - I(9)	2.753 (3)	
Mo(2) - I(1)	2.765 (6)	
Mo(2) - I(4)	2.758 (3)	
Mo(2) - I(11)	2.765 (4)	
Mo(3) - I(4)	2.750 (5)	
Mo(3) - I(6)	2.764 (6)	
Mo(4) - I(9)	2.761 (4)	
Mo(4) - I(11)	2.748 (6)	
		Average $Mo\text{-}I_{doubly\ bridging}$ = 2.758 Å
Mo(1) - I(2)	2.837 (6)	
Mo(2) - I(7)	2.852 (6)	
Mo(3) - I(2)	2.808 (4)	
Mo(3) - I(7)	2.830 (5)	
Mo(4) - I(2)	2.804 (5)	
Mo(4) - I(7)	2.823 (4)	
		Average $Mo\text{-}I_{triply\ bridging}$ = 2.826 Å

The polyhedron appears to be closed by a long metal-metal bond between Mo(1) and Mo(2). The common base is formed by the bond joining Mo(3) and Mo(4), 2.669(5) Å. The four equivalent sides of the triangles formed by the bonds between Mo(1)-Mo(3), Mo(1)-Mo(4), Mo(2)-Mo(3), and Mo(2)-Mo(4) all vary from their average bond distance of 2.542 Å by 0.010 Å or less. The atoms at the outer tips of the triangles, Mo(1) and Mo(2), are farther apart at 3.035(5) Å, but still within the limits of a Mo-Mo bond. The dihedral angle between the two triangles is 88.9°. This value falls approximately midway between the dihedral angles between the faces in a regular tetrahedron, 70.5°, and in a regular octahedron, 109.5°.

The bridging iodine atoms in the $Mo_4I_{11}^{2-}$ anion form a pseudo-cube as previously mentioned. I(2), I(4), I(6), I(7), I(9), and I(11) occupy corners of the cube while I(1) occupies the midpoint of a cube edge. Four of the cube faces are occupied by molybdenum atoms; the remaining two unoccupied cube faces are adjacent to each other and I(1) is at the midpoint of their common edge. I(3), I(5), I(8), and I(10) are terminal ligands; one bonded to each molybdenum atom. The average molybdenum-iodine distances are $d(Mo\text{-}I_{tb})$ = 2.826(5), $d(Mo\text{-}I_{db})$ = 2.785(5), and $d(Mo\text{-}I_{t})$ = 2.848(5) Å (where tb = triply bridging, db = doubly bridging and t = terminal). There is no unusual strain within the cluster due to I-I interactions as seen from their nonbonding distances, listed in Table 17 in the Appendix.

In discussing the bridging iodide ligands as a pseudo-cube, another way of visualizing the anion has been alluded to, as a tetranuclear fragment of the well-known $(Mo_6X_8)X_6^{2-}$ octahedral cluster anion. This

comparison becomes obvious when the structures of the following cluster anions are viewed as being formed by the stepwise degradation of the $(Mo_6X_8)X_6^{2-}$ structure: $(Mo_5X_8)X_5^{2-}$, $(Mo_4X_8)Y_4$, $(Mo_4X_7)X_4^{2-}$, and $(Mo_3X_4)X_{6/2}X_{3/3}^{4-}$. Their idealized structures are shown in Fig. 12.

The description of the $(Mo_4I_7)X_5^{2-}$ anion as a tetranuclear fragment of the $(Mo_6X_8)X_6^{2-}$ structure, instead of a distorted tetrahedron, has better enabled us to rationalize the ligand arrangement in the anion.

The frame for the basic unit is a cube of ligand atoms. In the center of each face of the cube lies a metal atom which is also bonded to a terminal ligand. The removal of any metal atom (and its terminal ligand) yields the $(Mo_5Cl_8)Cl_5^{2-}$ structure with the ligand cube still intact. In this cluster anion, not all the metal atoms are equivalent. The apex atom is nine-coordinate while the four basal metal atoms are eight-coordinate. The removal of the remaining apex metal leads to a square metal frame with each metal-metal bond doubly bridged [13]. The removal of a basal metal, a position cis to the vacancy, leads to a butterfly structure. In both cases, the ligand cube remains intact, but they differ significantly in their metal-metal and metal-ligand bonding.

Degradation of the ligand cube is the next step in the process. Two ligand cube corners adjacent to both metal vacancies are now unoccupied; they have been replaced by a single ligand lying on a cube edge halfway between them, forming a pseudo-cube. This yields the idealized structure of the $(Mo_4I_7)I_4^{2-}$ anion. The actual structure is distorted by the formation of a weak bond between the two metal atoms trans to

Figure 12. Structures of fragments generated from $(M_6X_8)X_6^{2-}$: (A) $(Mo_6Cl_8)Cl_6^{2-}$, (B) $(Mo_5Cl_8)Cl_5^{2-}$, (C) $[Mo_4(O\text{-}i\text{-}Pr)_8]Cl_4$, (D) $[Mo_4(O\text{-}i\text{-}Pr)_8]Br_4$, and (E) $(Mo_4I_7)I_4^{2-}$

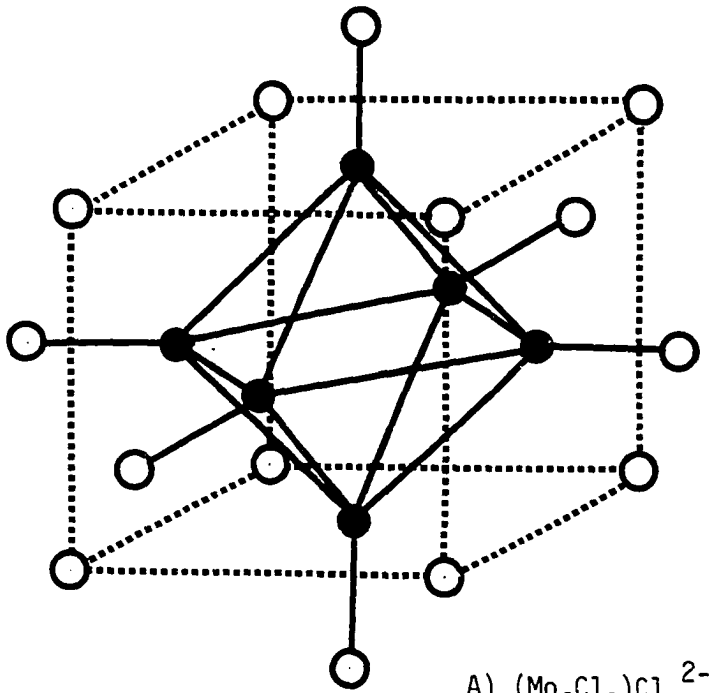

A) $(Mo_6Cl_8)Cl_6^{2-}$

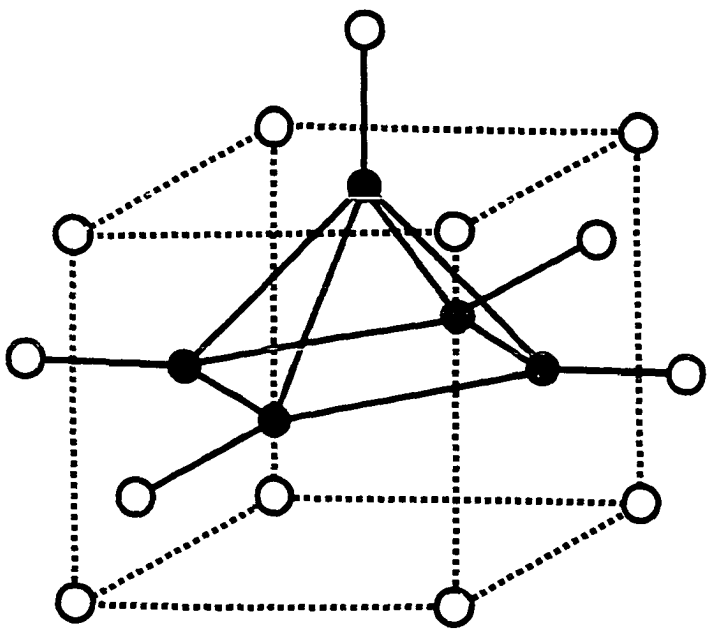

B) $(Mo_5Cl_8)Cl_5^{2-}$

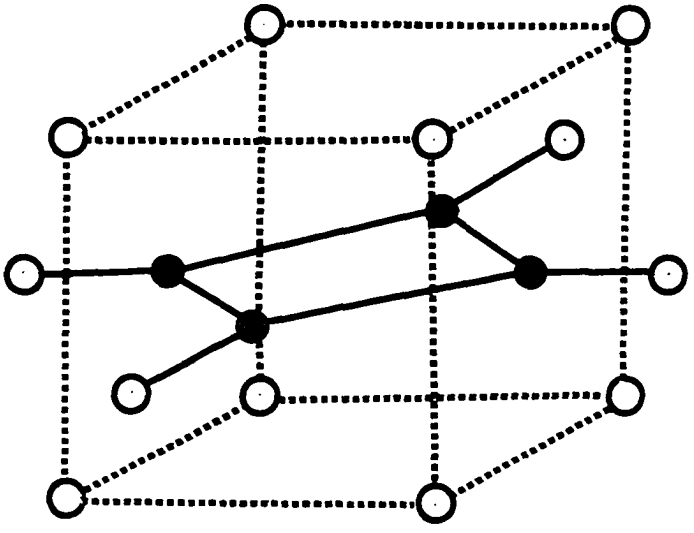

C) $Mo_4(O\text{-}i\text{-}Pr)_8Cl_4$

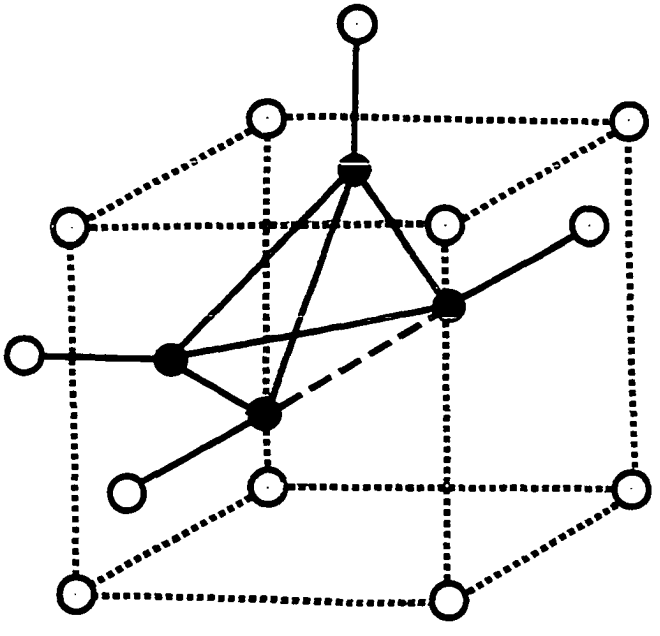

D) $Mo_4(O\text{-}i\text{-}Pr)_8Br_4$

Figure 12. Continued

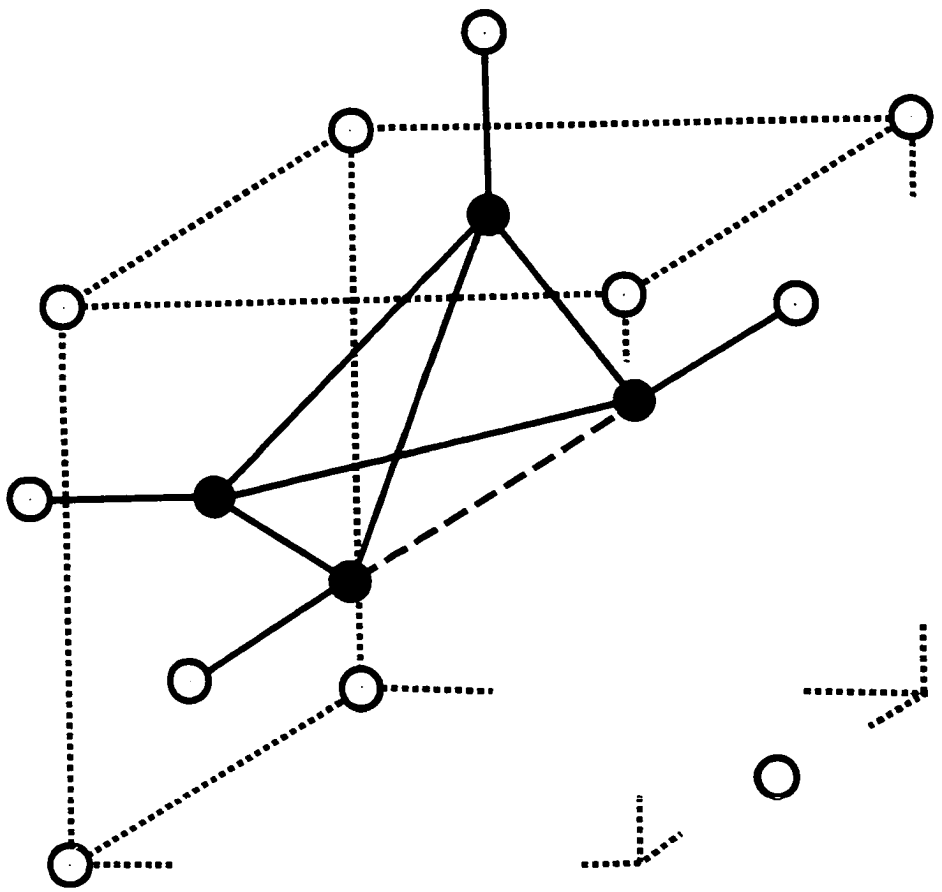

E) $(Mo_4I_7)I_4^{2-}$

Figure 12. Continued

each other. If this exercise is repeated once more, the loss of one of the eight coordinated metal atoms leads to the M_3X_{13} cluster, and only a fragment of the ligand cube remains intact. The utility of this scheme lies in its use as a basis for the possible systematic building up of metal clusters. The addition of more than one kind of metal or ligand to such fragments may provide a means of synthesizing countless analogs. Although the $Mo_4I_{11}^{2-}$ anion may be regarded as a tetranuclear fragment of the $(Mo_6X_8)X_6^{2-}$ structure, there are noteworthy distortions of the idealized $(Mo_4I_7)I_4^{2-}$ structure discussed below.

The Mo-Mo distance between the two trans molybdenum atoms, Mo(1) and Mo(2), is an obvious distortion from the idealized structure. This distance should be equal in length to the edge of the iodine cube. The average cube edge length was calculated to be 3.881 Å, using the six iodide ligands located at the cube corners. The actual Mo-Mo distance of 3.035 Å is 0.846 Å shorter. The shorter Mo(1)-Mo(2) distance is dictated by an optimization of the cluster's Mo-I bonding. As mentioned previously, the dihedral angle between metal planes in an octahedron is 109.5°. In $(Mo_4I_7)I_4^{2-}$, the dihedral angle has a value of 88.9°, midway between that of an octahedron and a tetrahedron (70.5°).

The distortions of the ligand cube can be seen by examining the iodide "pseudo-cube" faces. The cube faces occupied by Mo(3) and Mo(4) are nearly planar. As seen in Table 9, Mo(3) and Mo(4) are both 0.065 Å above their respective iodide cube faces. The dihedral angle between these planes is 89.3°, very close to the 90.0° expected for a cube.

Table 9. Selected least-squares planes and interplane angles for $Mo_4I_{11}^{2-}$

	Atom	Perpendicular Distance from Plane, Å
Plane 1.	4.98 = (0.92x - 4.87) + (0.40y - 1.72) + (-0.03z - 5.64)	
	Mo1	0.09
	I1	-0.39
	I2	-0.43
	I6	0.37
	I9	0.37
Plane 2.	0.88 = (0.92x - 1.92) + (-0.40y - 1.73) + (-0.03z - 5.74)	
	Mo2	0.09
	I1	0.39
	I4	-0.37
	I7	0.43
	I11	-0.37
Plane 3.	4.75 = (0.03x - 3.44) + (-0.71y - 0.40) + (0.70z - 7.05)	
	Mo3	0.05
	I2	-0.01
	I4	-0.01
	I6	-0.02
	I7	-0.02
Plane 4.	3.43 = (0.03x - 3.35) + (0.71y - 0.40) + (0.70 - 4.33)	
	Mo4	-0.05
	I2	0.02
	I7	0.01
	I9	0.01
	I11	0.02
Plane 5.	2.05 = (0.71x - 3.91) + (-0.70y - 0.81) + (-0.03z - 5.67)	
	Mo1	0.00
	Mo3	0.00
	Mo4	0.00
	I6	0.26
	I7	-0.69
	I9	0.30

Table 9. Continued

	Atom	Perpendicular Distance from Plane, Å
Plane 6.	2.49 = (0.72x - 2.89) + (0.70y - 0.82) + (-0.03z - 5.71)	
	Mo2	0.00
	Mo3	0.00
	Mo4	0.00
	I2	0.68
	I4	-0.31
	I11	-0.27

Planes	Dihedral Angles (degrees)
1-2	46.9
1-3	73.8
1-4	73.4
2-3	73.4
2-4	73.7
3-4	89.3
Average	71.8
5-6	88.9

Also, the I-Mo-I bond angles for Mo(3) and Mo(4), listed in Table 10, are consistent with a molybdenum atom lying slightly above an iodine plane. The average I_t-Mo-I_{db} bond angle is 91.4°.

In contrast, the iodine atoms forming the pseudo-cube faces occupied by Mo(1) and Mo(2) are far from coplanar with the metal atoms. This is not unexpected since these faces both contain I(1) which lies on a cube edge instead of a cube corner. While both molybdenum atoms are only 0.1 Å above their respective least-squares planes, their bridging iodide ligands are either well above or well below the least-squares plane. For both planes, I(1) and the triply bridging iodide ligands are about 0.4 Å below the plane while the doubly bridging iodide ligands are about an equal distance above the plane. Now, the I_t-Mo-I_b bond angles for Mo(1) and Mo(2) differ significantly from 90°. The average angle equals 100.2° or 84.4° depending on whether the I_b is below or above the least-squares plane. Also, these two planes are no longer parallel, but have a very acute dihedral angle of 46.9°.

Bonding

The "long bond" between Mo(1) and Mo(2) prompted interest in the bonding of the $Mo_4I_{11}^{2-}$ anion. A qualitative molecular orbital scheme for the metal-metal bonding in the $(Mo_4I_7)I_4^{2-}$ structure was devised. The cluster has 36 metal orbitals, 20 of which are used to form metal-ligand molecular orbitals. The assignment of orbitals was simplified by assuming the anion has C_{2v} symmetry, by constructing a consistent coordinate system - a right-handed orthogonal set of axes on each metal

Table 10. Selected bond angles in $Mo_4I_{11}^{2-}$ (degrees)

Mo(1)-Mo(2)-Mo(3)	53.6(1)	I(1)-Mo(1)-I(6)	94.3(1)
Mo(1)-Mo(2)-Mo(4)	53.6(1)	I(1)-Mo(1)-I(9)	95.5(1)
Mo(1)-Mo(3)-Mo(2)	73.3(1)	I(2)-Mo(1)-I(6)	87.7(2)
Mo(1)-Mo(3)-Mo(4)	58.5(1)	I(2)-Mo(1)-I(9)	86.8(1)
Mo(1)-Mo(4)-Mo(2)	73.1(1)	I(1)-Mo(2)-I(4)	95.5(1)
Mo(1)-Mo(4)-Mo(3)	58.4(1)	I(1)-Mo(2)-I(11)	94.8(1)
Mo(2)-Mo(1)-Mo(3)	53.2(1)	I(7)-Mo(2)-I(4)	86.8(1)
Mo(2)-Mo(1)-Mo(4)	53.3(1)	I(7)-Mo(2)-I(11)	87.0(1)
Mo(2)-Mo(3)-Mo(4)	58.4(1)	I(2)-Mo(3)-I(6)	88.3(1)
Mo(2)-Mo(4)-Mo(3)	58.1(1)	I(2)-Mo(3)-I(7)	99.8(1)
Mo(3)-Mo(1)-Mo(4)	63.1(1)	I(4)-Mo(3)-I(6)	84.4(1)
Mo(3)-Mo(2)-Mo(4)	63.4(1)	I(4)-Mo(3)-I(7)	87.4(1)
Average Mo-Mo-Mo	= 60.0°	I(2)-Mo(4)-I(7)	100.1(1)
		I(2)-Mo(4)-I(9)	87.3(1)
Mo(1)-I(2)-Mo(3)	53.7(1)	I(11)-Mo(4)-I(7)	87.7(1)
Mo(1)-I(2)-Mo(4)	53.8(1)	I(11)-Mo(4)-I(9)	84.6(1)
Mo(3)-I(2)-Mo(4)	56.8(1)	Average (I_b-Mo-I_b)cis	= 90.5°
Mo(2)-I(7)-Mo(3)	53.0(1)		
Mo(2)-I(7)-Mo(4)	53.2(1)	I(1)-Mo(1)-I(2)	159.5(2)
Mo(3)-I(7)-Mo(4)	56.4(1)	I(6)-Mo(1)-I(9)	165.9(1)
Average Mo-I_{tb}-Mo	= 54.5°	I(1)-Mo(2)-I(7)	159.7(1)
		I(4)-Mo(2)-I(11)	165.6(1)
Mo(1)-I(1)-Mo(2)	66.8(1)	I(2)-Mo(3)-I(4)	172.3(1)
Mo(1)-I(6)-Mo(3)	54.9(1)	I(6)-Mo(3)-I(7)	171.3(1)
Mo(1)-I(9)-Mo(4)	55.1(1)	I(2)-Mo(4)-I(11)	171.4(1)
Mo(2)-I(4)-Mo(3)	54.8(1)	I(7)-Mo(4)-I(9)	172.1(1)
Mo(2)-I(11)-Mo(4)	54.9(1)	Average (I_b-Mo-I_b)trans	= 167.2°
Average Mo-I_{db}-Mo	= 57.3°		
		I(3)-Mo(2)-Mo(1)	153.6(1)
I(3)-Mo(2)-I(1)	97.3(2)	I(3)-Mo(2)-Mo(3)	143.1(1)
I(3)-Mo(2)-I(4)	83.8(1)	I(3)-Mo(2)-Mo(4)	143.7(1)
I(3)-Mo(2)-I(7)	103.0(1)	I(5)-Mo(3)-Mo(1)	142.8(1)
I(3)-Mo(2)-I(11)	84.9(1)	I(5)-Mo(3)-Mo(2)	143.6(1)
I(5)-Mo(3)-I(2)	91.1(2)	I(5)-Mo(3)-Mo(4)	134.4(1)
I(5)-Mo(3)-I(4)	91.6(2)	I(8)-Mo(1)-Mo(2)	153.7(1)
I(5)-Mo(3)-I(6)	91.5(2)	I(8)-Mo(1)-Mo(3)	144.0(1)
I(5)-Mo(3)-I(7)	91.4(2)	I(8)-Mo(1)-Mo(4)	143.3(1)
I(8)-Mo(1)-I(1)	96.8(2)	I(10)-Mo(4)-Mo(1)	143.6(1)
I(8)-Mo(1)-I(2)	103.7(2)	I(10)-Mo(4)-Mo(2)	142.9(1)
I(8)-Mo(1)-I(6)	85.0(1)	I(10)-Mo(4)-Mo(3)	134.8(1)
I(8)-Mo(1)-I(9)	83.8(2)	Average I_t-Mo-Mo	= 143.6°
I(10)-Mo(4)-I(2)	91.9(2)		
I(10)-Mo(4)-I(7)	90.8(1)	I_t = terminal	
I(10)-Mo(4)-I(9)	91.7(1)	I_b = bridging	
I(10)-Mo(4)-I(11)	91.1(2)	I_{db} = doubly bridging	
Average I_t-Mo-I_b	= 91.4°	I_{bb} = triply bridging	

atom with their z-axes pointed to the center and by properly grouping the atomic orbitals (see Fig. 13). Assuming the s, px, py and pz orbitals on each molybdenum atom, the dx^2-y^2 orbitals on Mo(1) and Mo(2), and the dxy orbitals on Mo(3) and Mo(4) are used to form the metal-ligand bonds, the remaining metal orbitals are available for metal-metal bonding. A set of linear combinations of atomic orbitals (lcao's) were obtained for the metal-metal bonding (see Table 18 in the Appendix). By inspection, these symmetry combinations predict the cluster has six bonding ($3a_1 + a_2 + b_1 + b_2$), two nonbonding ($a_2 + b_1$), and eight antibonding ($2a_1 + a_2 + 3b_1 + 2b_2$) metal-metal orbitals. The nonbonding orbitals are localized on the eight-coordinated Mo(1) and Mo(2) atoms. As mentioned previously, the cluster has fifteen electrons available for metal-metal bonding. The first twelve electrons should fill the bonding orbitals and the remaining three electrons are then located in the two nonbonding orbitals. Such an arrangement would dictate one unpaired electron, and this prediction was confirmed by the temperature independent magnetic moment of 1.87 μ_β. This qualitative molecular orbital description was verified by the $Mo_4Br_4[OCH(CH_3)_2]_8$ molecule which has the same metal frame and has only twelve electrons available for metal-metal bonding [13].

Ideally, the six metal-metal bonding MOs are distributed in the following manner. The a_1^b orbital formed from the Γyz 3,4 lcao is localized at the Mo(3)-Mo(4) bond. The remaining five metal-metal bonding orbitals are delocalized. The set of MOs, $a_1^b + a_2^b + b_1^b + b_2^b$, are delocalized evenly over the Mo(1)-Mo(3), Mo(1)-Mo(4), Mo(2)-

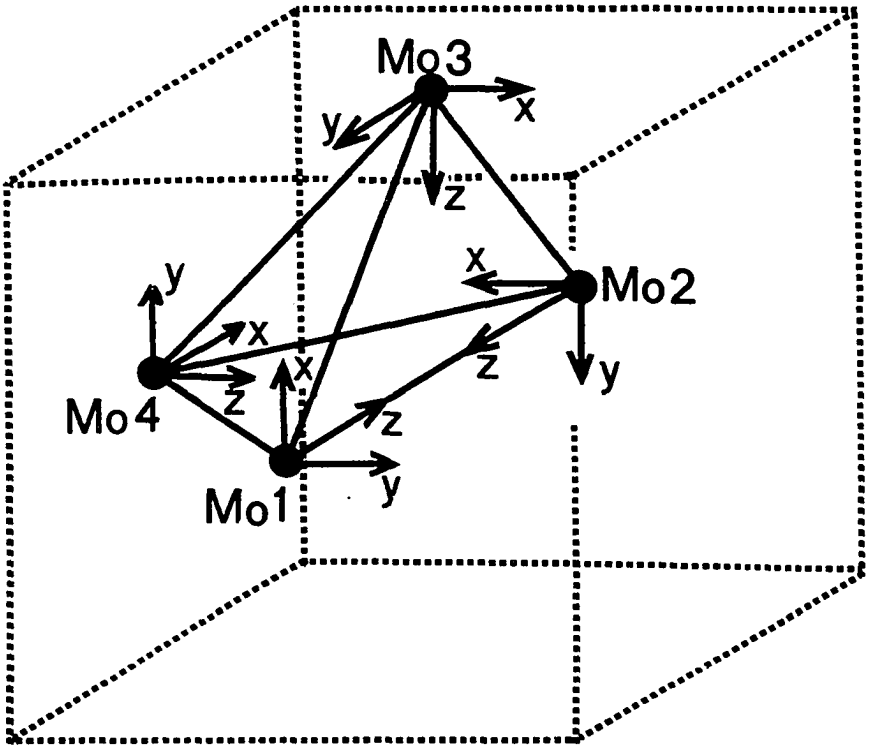

Figure 13. The atomic orbital coordinate system at each metal atom

Mo(3), and Mo(2)-Mo(4) bonds while the a_1^b MO formed from the $rz^2_{1,2,3,4}$ lcao is delocalized over the whole metal frame. And in the ideal case, the sixth metal-metal distance is nonbonding. This arrangement would result in five metal-metal bonds, each with a bond order of approximately 1.2. The metal-metal bonding in $Mo_4Br_4[OCH(CH_3)_2]_8$ fits this model quite well. An examination of the metal-metal distances shows four nearly equivalent bonds ($\bar{d}$ = 2.515 Å), a fifth slightly shorter bond (d = 2.481 Å), and a sixth weakly bonding or nonbonding distance (d = 3.287 Å).

The bonding in $Mo_4I_{11}^{2-}$ differs considerably from the ideal case. The most obvious difference is the shortened Mo(1)-Mo(2) distance. The qualitative MO scheme cannot explain this change. It does not take into account the relative energies of the orbitals or their interactions with metal-ligand orbitals in the cluster. EHMO calculations, performed by Miessner and Korolkov, have now provided a more complete description of the bonding in the $Mo_4I_{11}^{2-}$ anion [41]. The EHMO results are similar to those of the qualitative MO scheme discussed earlier (see Fig. 14). (Note: The coordinate system used by Miessner and Korolkov does not match the system used in determining the qualitative MO analysis. The resulting effect is that the a_1 and a_2 MOs are the same, but the subscripts for the b orbitals, b_1 and b_2, are interchanged. In Figure 14, the EHMO disignations are used.)

The strong covalent character of the metal-ligand bonds has important consequences for the electronic structure of $Mo_4I_{11}^{2-}$. Significant sharing of I_{5p}-AOs with the M-M bonds is one result. This interaction manifests itself in the appearance of two b_1 M-M bonding orbitals, with

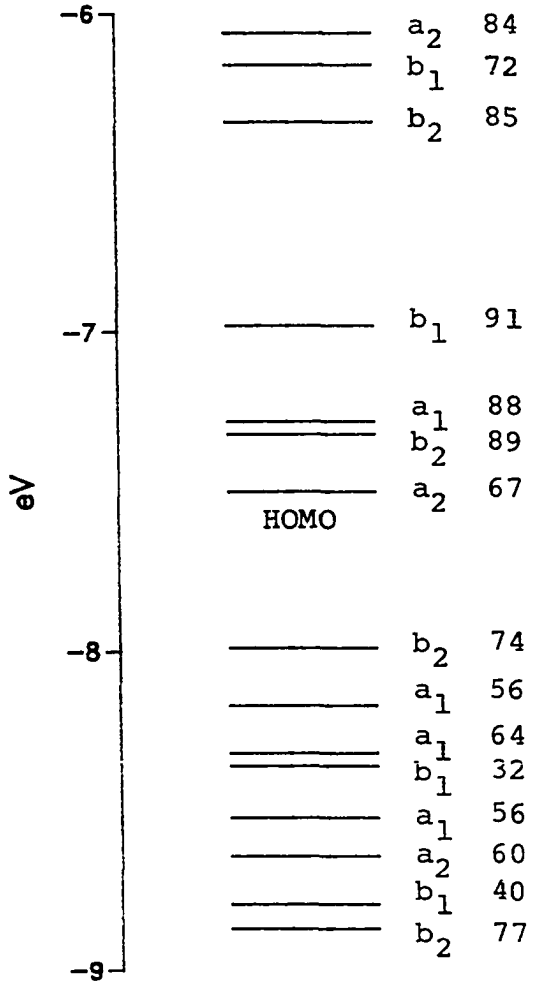

Figure 14. The "metallic" MO diagram of the $Mo_4I_{11}^{2-}$ anion. (The numbers give the percentage Mo character of each MO.)

considerable I_{5p}-AO character, in place of one b_1 M-M bonding orbital as predicted by the qualitative scheme. Also, several orbitals with principally I character are raised in energy and now coincide with MOs with predominately Mo character. (These I orbitals were omitted for clarity.)

The question of the relatively short Mo(1)-Mo(2) distance was also investigated by Miessner and Korolkov. The approach of the Mo(1) and Mo(2) atoms could be viewed as evidence for the formation of a M-M bond, but Miessner and Korolkov's determination of bond orders in the cluster showed no bonding. However, on closer examination, a significant dependence of the electronic structure on the change of the dihedral angle between Mo(1)-Mo(3)-Mo(4) plane and the Mo(2)-Mo(3)-Mo(4) plane was determined. Figure 15 shows a dependence of both the total cluster MO energy (E_{tot}) and the total metal MO energy (E_{met}) on the variation of the dihedral angle. While the dihedral angle is a function of the Mo(1)-Mo(2) distance, a careful examination of both curves shows this dependence is due to changes in E_{tot} and not to any M-M bonding. In $Mo_4(O\text{-}i\text{-}Pr)_8Br_4$, the dihedral angle for a minimum in E_{met} and E_{tot} are expected to coincide since there is no bonding interaction between the tip metal atoms, and the M-X bonding should be well separated in energy from the M-M bonding. Here the dihedral angle is 96.6°, close to the angle calculated for a minimum in E_{met} for $Mo_4I_{11}^{2-}$. In contrast, the actual dihedral angle in $Mo_4I_{11}^{2-}$ is 88.9° and agrees closely with its calculated angle for a minimum in E_{tot}. The fact that the dihedral angles for a minimum in E_{met} and E_{tot} do not coincide is taken as evidence

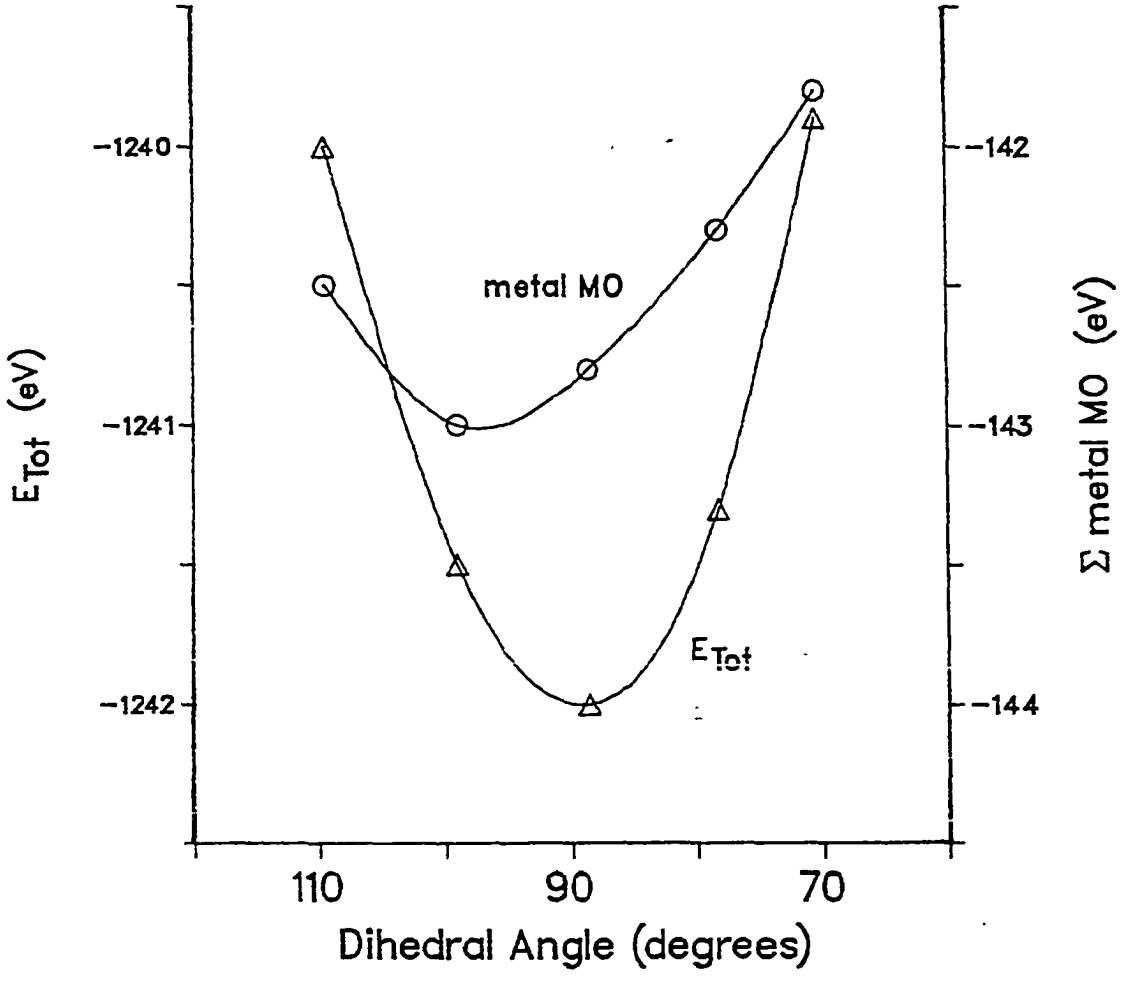

Figure 15. The total cluster MO energy (E_{tot}) and metal MO energy as a function of dihedral angle

that changes in the covalent Mo-I bonding have a more significant effect than changes in the M-M bonding to the total stability of the $Mo_4I_{11}^{2-}$ cluster. Therefore, the dihedral angle and not M-M bonding is the governing factor for the short Mo(1)-Mo(2) distance.

These calculations were repeated by Miessner and Korolkov with different sets of parameters to insure that the conclusions were not dependent on parameterizing or calculation variants. In all cases, no qualitative differences were observed [41].

The Mo-I-Mo bond angles and the Mo-I bond distances also indicate strong cluster bonding. In the $M_2X_9^{n-}$ cluster anion system, one indicator of metal-metal bonding is the M-X-M bond angles [42]. Angles of 70.5° or less verify that a metal-metal bond rather than the bridging ligand is holding the metal atoms in close proximity. If an analogy can be made between the $(Mo_4I_7)I_4^{2-}$ anion and the $M_2X_9^{n-}$ anions, it is that the metal-metal bonding in $(Mo_4I_7)I_4^{2-}$ is quite strong. The $Mo\text{-}I_{db}\text{-}Mo$ angles average 57.3° while the $Mo\text{-}I_{tb}\text{-}Mo$ angles are even more acute, averaging 54.5°. Because of these acute bond angles, one could expect the $Mo\text{-}I_b$ bond distances to lengthen to relieve potential steric strain in the cluster. This is not the case; rather the average $Mo\text{-}I_t$ bond distance is longer than the average $Mo\text{-}I_{db}$ or $Mo\text{-}I_{tb}$ bond distances, 2.848 versus 2.758 and 2.826 Å, respectively. The Mo-Mo and the Mo-I bond distances and the Mo-I-Mo bond angles collectively show $(Mo_4I_7)I_4^{2-}$ to be an unusually strongly bonded cluster anion.

RESULTS FOR RELATED COMPOUNDS

After characterizing $(TBA)_2Mo_4I_{11}$, work was next conducted on the syntheses of either smaller or larger clusters by the thermolysis of $(TBA)Mo(CO)_4I_3$. The reaction conditions of several known molybdenum chloride clusters were considered, and a trend of cluster size increasing with the reaction temperature was observed. For example, $Mo_2Cl_9^{3-}$ is made by a reaction between $MoCl_6^{2-}$ and $Mo(CO)_4Cl_3^-$ at room temperature [1] while a mixture of $Mo_5Cl_{13}^{2-}$ and $Mo_6Cl_{14}^{2-}$ is made by the conversion of "$MoCl_2$" in a $KCl\text{-}AlCl_3\text{-}BiCl_3$ melt at 306°C [18]. (The "$MoCl_2$" is made by the thermolysis of $Mo(CO)_4Cl_2$.) Based on this trend, reactions at lower and higher temperatures than refluxing chlorobenzene (132°C) were investigated.

Syntheses of $Mo_4I_{11}^{2.5-}$ and "$Mo_4I_{10}^{2-}$" Salts

The thermolysis of $(TBA)Mo(CO)_4I_3$ was first studied in chlorobenzene at 80°C, in a dynamic vacuum at 80°C, and in refluxing benzene (80°C). The reaction in chlorobenzene at 80°C yielded an ill-defined product. The infrared spectrum of the product showed the presence of carbon monoxide. Therefore, it was concluded that the refluxing of the solvent is an important factor which guarantees that any free carbon monoxide is quickly flushed out of the system.

The thermolysis of $(TBA)Mo(CO)_4I_3$ in either a dynamic vacuum at 80°C or in refluxing benzene produced the same result, a black solid (see the Reactions E and F in the Experimental chapter). The infrared spectra of the products contained only bands for the cation, verifying

the complete evolution of carbon monoxide. Analytical data for the solids indicated the net composition $(TBA)MoI_3$. After extracting each black solid with chlorobenzene, a pyrophoric black powder was obtained. The initial analyses of these powders provided an I/Mo ratio of 2.75, and their infrared spectra again contained only bands for the cation. After subtracting the percentage Mo and I, the remaining composition was assumed to consist only of the cation. Their (TBA)/Mo ratios were both approximately 5:8, which yields the formula $(TBA)_5Mo_8I_{22}$. An explanation for this is that the reactions generate a mixture of $Mo_4I_{11}^{2-}$ and $Mo_4I_{11}^{3-}$ salts.

In the absence of an oxidizing agent, one would expect the thermolysis of $Mo(CO)_4I_3^-$ to produce $Mo_4I_{11}^{3-}$.

$$4\ Mo(CO)_4I_3^- \longrightarrow Mo_4I_{11}^{3-} + I^- + 16\ CO \qquad (8)$$

As described in Reactions B, C, and D, elemental iodine was used as the oxidizing agent to produce $Mo_4I_{11}^{2-}$. In Reactions E and F, there are no obvious oxidizing agents. So why is a portion of the product oxidized from $Mo_4I_{11}^{3-}$ to $Mo_4I_{11}^{2-}$? Evidence for the answer was found later when the thermolysis of $(TBA)Mo(CO)_4I_3$ was conducted in refluxing o-dichlorobenzene (see Reaction G). In addition to the main product, which was $(TBA)_2Mo_4I_{11}$, a small quantity of $Mo(CO)_6$ sublimed up to the reaction vessel's condenser. While no particular mechanism has been proposed for this reaction, a balanced equation can be written that has $Mo(CO)_6$ as a

$$2\ Mo_4I_{11}^{3-} + Mo(CO)_4I_3^- + 2\ CO \longrightarrow 2\ Mo_4I_{11}^{2-} + 3\ I^- + Mo(CO)_6 \qquad (9)$$

product. The $Mo_4I_{11}^{3-}$ anion is very reactive and would easily serve as a reducing agent for $Mo(CO)_4I_3^-$. Next, chemical and electrochemical reactions were undertaken to isolate the reduced $Mo_4I_{11}^{3-}$ anion.

Assuming that $[(n\text{-}C_4H_9)_4N]_{2.5}Mo_4I_{11}$ was a mixture of $Mo_4I_{11}^{2-}$ and "$Mo_4I_{11}^{3-}$" salts, the synthesis of the "3-" salt was attempted by reducing the 2- salt with zinc in acetonitrile (Reaction H). Problems such as the difficulty in attaining complete reaction, incomplete separation of products, and the pyrophoric nature of the "3-" salt prevented isolation of the pure "$(TBA)_3Mo_4I_{11}$". The actual range of $(TBA)/Mo_4I_{11}$ values found in subsequent reactions were from 2.3 to 2.6.

In an attempt to force the reduction reaction to completion, the same reactants were refluxed in acetonitrile for about eighteen hours (see Reaction I). This afforded a material whose composition was in agreement with the formula "$(TBA)_2Mo_4I_{10}$". A compound of this same composition was also obtained as a product of the thermolysis of $(TBA)Mo(CO)_4I_3$ in refluxing chlorobenzene maintained under a continuous purge of hydrogen gas (see Reaction J). The initial product was soluble in chlorobenzene, so the final product was isolated by first stripping off the solvent, and then breaking the resulting tar with a minimal volume of acetonitrile. Generally, the product is recovered in about 20% yield by this method. A careful examination of the infrared spectra was done in the hope of identifying Mo-H bands, but only bands for the (TBA) cation were observed. Repeating the reaction with deuterium gas gave the same analytical and infrared results. The x-ray

powder patterns of the "$(TBA)_2Mo_4I_{10}$" synthesized by either method were the same, and they differed only slightly from the powder pattern of $(TBA)_2Mo_4I_{11}$.

A single crystal, x-ray structure determination was attempted to identify the new anion's structure. Material made by the hydrogen reaction was recrystallized from acetonitrile. Careful analytical data verified the crystalline material to be "$(TBA)_2Mo_4I_{10}$". Of the several crystals examined, all but one was twinned. And that crystal later proved to be $(TBA)_2Mo_4I_{11}$. No partial occupancy of any iodine positions was observed for the crystal, and further work was discontinued.

The role solubility plays in the synthesis of these metal cluster compounds was also examined by changing the cation. Tetraethylammonium (TEA) and tetrapropylammonium (TPA) iodide salts were used because they are readily available.

The (TEA) and (TPA) salts of the $Mo(CO)_4I_3^-$ are both made by the same procedure as for $(TBA)Mo(CO)_4I_3$ (see Reaction A). The thermolysis of $(TEA)Mo(CO)_4I_3$ in refluxing chlorobenzene yields a brown solid which was found to have a net composition close to $(TEA)MoI_3$. This composition corresponds to a recovery of the starting material minus the evolved carbon monoxide. Attempts to separate pure products from the solid by extracting with acetonitrile were unsuccessful, but changes in the iodine to molybdenum and cation to molybdenum ratios for the two extraction fractions imply the solid was a mixture. The solid obtained when hydrogen gas was bubbled through the refluxing solution appeared to be different, but again no pure products were isolated.

The thermolysis of $(TPA)Mo(CO)_4I_3$ in refluxing chlorobenzene is a more interesting reaction. Even with prolonged reflux times, in excess of twenty-four hours, small amounts of carbon monoxide were still present in the solid products. The presence of carbon monoxide ligands was confirmed by the infrared spectrum of this solid. The problem of incomplete carbon monoxide evolution was subsequently alleviated by bubbling nitrogen gas through the refluxing chlorobenzene solution.

By following the latter procedure, two products were recovered; one remained in solution and the other was obtained as a precipitate. The residue recovered from the solution afforded a material of variable stoichiometry which approximates $(TPA)_4Mo_2I_8$. The formation of this material appears to be related to the product formed in the reaction between $(TBA)_2Mo_4I_{11}$ and excess (TBA)I in chlorobenzene. Attempts to recrystallize this material by slow extraction with acetonitrile did not lead to a crystalline product. Analytical data indicated that the insoluble product was "$(TPA)_2Mo_4I_{10}$". Both products of this reaction appear to contain Mo(II) species and together the sum of their constituents is again $(TPA)MoI_3$.

The same results are not obtained if hydrogen gas is bubbled through the solution during thermolysis, for then "$(TPA)_2Mo_4I_{10}$" is produced nearly quantitatively. Clearly, the hydrogen served as a driving force to the reaction. As with "$(TBA)_2Mo_4I_{10}$", an examination of the infrared spectra showed only bands for the (TPA) cation.

In the characterization of the "$Mo_4I_{10}^{2-}$" salt, it became obvious that the anion was not simply $Mo_4I_{10}^{2-}$. The original formula assignment

was based on the assumption that the products from the zinc reduction of $(TBA)_2Mo_4I_{11}$ at room temperature and at refluxing acetonitrile (80°C) would be similar. Also, independent of synthesis procedure used, the composition for "$Mo_4I_{10}^{2-}$" was always the same: I/Mo = 2.5 and cation/Mo = 0.5. In subsequent work, questions about the true composition of "$Mo_4I_{10}^{2-}$" arose.

Characterization of the "$Mo_4I_{10}^{2-}$" anion has been a difficult problem. After initially analyzing the data, no conclusion was reached. Evidence from chemical analyses and spectra appeared to conflict. All the spectra measured showed salts of "$Mo_4I_{10}^{2-}$" to be similar to those of $Mo_4I_{11}^{2-}$, even to being paramagnetic, but the analyses were clearly different. Especially troubling was the magnetic data (EPR). It was expected from the MO scheme that "$Mo_4I_{10}^{2-}$" should be diamagnetic since it would be an even electron species with an orbital singlet ground state. Assuming that the signal in the EPR spectra might be caused by trace impurities, the magnetic susceptibility of $(TPA)_2Mo_4I_{10}$ was measured. Not only did the magnetic susceptibility results verify that the material was paramagnetic, they also indicated that this salt has one unpaired electron per two $Mo_4I_{10}^{2-}$ units. Based on this new information, the data were re-evaluated. An outline of the new conclusions is presented below.

While not conclusive, the classification of "$Mo_4I_{10}^{2-}$" as a $Mo_4I_{10}^{2-}$, $Mo_4I_{10}H^{2-}$ mixed salt is consistent with all the data. Electrochemical as well as magnetic data indicated "$Mo_4I_{10}^{2-}$" is a mixture with a paramagnetic and a diamagnetic component. The electrochemical data

further showed that a solution of "$(TBA)_2Mo_4I_{10}$" containing excess iodide behaved as if it were a mixture of $Mo_4I_{11}^{3-}$ and $Mo_4I_{11}^{2-}$ salts, and that an equilibrium exists between $Mo_4I_{11}^{3-}$ and $Mo_4I_{10}^{2-}$. These data along with Reactions G and H, and the analytical data suggest that "$Mo_4I_{10}^{2-}$" is really a $Mo_4I_{10}^{2-}$, $Mo_4I_{10}X^{2-}$ mixed salt.

Since metal-hydride bands were never identified in any "$Mo_4I_{10}^{2-}$" infrared spectra, the assignment of $Mo_4I_{10}X^{2-}$ as $Mo_4I_{10}H^{2-}$ is based on indirect evidence. It is assumed that the metal-hydride infrared bands (if they exist) are either hidden under cation bands or too broad and weak to be identified [43]. Two reactions provided possible evidence. First, $CDCl_3$ reacted with "$(TPA)_2Mo_4I_{10}$" to form a small quantity of $CDHCl_2$. Only a reaction with a metal-hydride would be expected to produce the $CDHCl_2$. The other reaction was the thermolysis of $(TPA)Mo(CO)_4I_3$. The yield of "$(TPA)_2Mo_4I_{10}$" depended on the gas used to flush the reaction. When hydrogen gas was used, a near quantitative yield was obtained, whereas only a 65% yield is obtained when nitrogen gas is used.

Related Reactions

Simultaneously with the attempts to synthesize smaller molybdenum iodide clusters, work was started on synthesizing clusters larger than the $Mo_4I_{11}^{2-}$ anion. By the addition of metal atoms to $Mo_4I_{11}^{2-}$, one could envision the formation of the $Mo_5I_{13}^{2-}$ and $Mo_6I_{14}^{2-}$ anions. The chloride analogs ($Mo_5Cl_{13}^{2-}$ and $Mo_6Cl_{14}^{2-}$) have been synthesized by reduction of molybdenum chlorides in a $KCl\text{-}AlCl_3$ melt at 306°C [18].

1,2-Dichlorobenzene was chosen as the solvent for these studies. In addition to having solvent properties similar to chlorobenzene, 1,2-dichlorobenzene refluxes at a much higher temperature, 177°C. Its choice is consistent with the assumption that at higher reaction temperatures, larger molybdenum iodide clusters will be formed (as seen, for example, in melt reactions).

Initially, it was shown that the thermolysis of $(TBA)Mo(CO)_4I_3$ in refluxing dichlorobenzene produced only $(TBA)_2Mo_4I_{11}$ (see Reaction G). The approach was then changed to a trial reaction between one or more equivalents of $(TBA)Mo(CO)_4I_3$ and $(TBA)_2Mo_4I_{11}$ in hopes of obtaining metal addition to a pre-existing metal cluster. A dilute $(TBA)Mo(CO)_4I_3$-dichlorobenzene solution was slowly titrated into a refluxing $(TBA)_2Mo_4I_{11}$-dichlorobenzene solution. Even though the resulting reaction product was found to have a decreased I/Mo ratio as might be expected if some larger clusters were being formed, work was discontinued when it became clear the results were not reproducible and the reaction products could not be separated into pure components.

Finally, experiments were undertaken to synthesize an oxidized product from $(TBA)_2Mo_4I_{11}$. Using iodine as an oxidizing agent, it was hoped to obtain possibly $(TBA)Mo_4I_{11}$ or some other new cluster that would add to our understanding of the relationship between the geometry and the number of metal core electrons in clusters. Would the new cluster retain the $Mo_4I_{11}^{2-}$ structure with six bonding and two nonbonding metal-based orbitals or would it convert to some new structure such as that of $CsNb_4Cl_{11}$ which has five bonding and two nonbonding orbitals?

This question is still unanswered since the reaction with iodine did not proceed as expected. A new product containing acetonitrile was formed which proved to have a higher ligand to metal ratio, but the same metal oxidation state as in the $Mo_4I_{11}^{2-}$ cluster anion (see Reaction M). In this product, an acetonitrile to molybdenum ratio of 1.0 and an iodide to molybdenum ratio of 2.25 was found. These ratios result in a molecular formula of $Mo_4I_9(CH_3CN)_4$, and suggest that two iodide ligands have been replaced by four acetonitrile ligands. A small portion of the $Mo_4I_{11}^{2-}$ anion was also converted to a more highly oxidized molybdenum iodide salt.

Since $Mo_4I_9(CH_3CN)_4$ appears to be insoluble in acetonitrile, a soluble derivative was sought to verify the compound's structure. Propionitrile, tributylphosphine and triphenylphosphine were tried in ligand exchange reactions. It appears that reactions take place in all three cases, but products were precipitated from only the two phosphine solutions. Infrared spectra and molybdenum and iodide analyses indicated that both products had the approximate formula $Mo_4I_9(PR_3)_2$. Ligand exchange reactions using AgCl resulted in mixed halide clusters of the form $Mo_4I_{11-x}Cl_x^{2-}$. Further work was discontinued when attempts to purify any of these products failed.

The question of how the $Mo_4I_9(CH_3CN)_4$ structure was related to that of $Mo_4I_{11}^{2-}$ was illuminated by showing that $Mo_4I_9(CH_3CN)_4$ could be reconverted to $(TBA)_2Mo_4I_{11}$ (see Reaction N). While the reaction between $Mo_4I_9(CH_3CN)_4$ and (TBA)I in refluxing chlorobenzene to obtain $(TBA)_2Mo_4I_{11}$ does not prove the $(Mo_4I_7)I_4^{2-}$ structure has been retained, this reaction

together with the PES and infrared spectrum of $Mo_4I_9(CH_3CN)_4$, as well as thermogravimetric analysis data, strongly implies retention of the basic framework of the $Mo_4I_{11}^{2-}$ structure.

Magnetic Properties

The magnetic behavior of "$(TPA)_2Mo_4I_{10}$" made under a nitrogen atmosphere (Reaction K) was examined over the range of 93K to 295K. This compound was chosen for this purpose because its preparation was most convenient and its spectroscopic properties were representative of all four "$Mo_4I_{10}^{2-}$" salts. Based on the paramagnetism of $(TBA)_2Mo_4I_{11}$, it was first assumed that the "$Mo_4I_{10}^{2-}$" anion would be diamagnetic. Both magnetic susceptibility data and EPR spectra showed this assumption to be incorrect.

The data were collected and the magnetic susceptibilities calculated by a computer controlled Faraday balance system [26]. The field strength was held constant at 1.8 Tesla and the temperature range from room temperature to near liquid nitrogen temperature was covered. Using 2025.54 g/mol as the molecular weight of "$(TPA)_2Mo_4I_{10}$", the apparent molar susceptibilities were calculated from the gram susceptibilities by the computer. The plot of χ_m vs. 1/T was linear, indicating simple Curie behavior. The numeric values of the slope and the intercept were 0.1940K emu/mol and -615×10^{-6} emu/mol, respectively. The magnetic moment was calculated from the slope by Eq. (6). The value of the

$$\mu = 2.828(C)^{1/2} = 1.25\ \mu_\beta$$

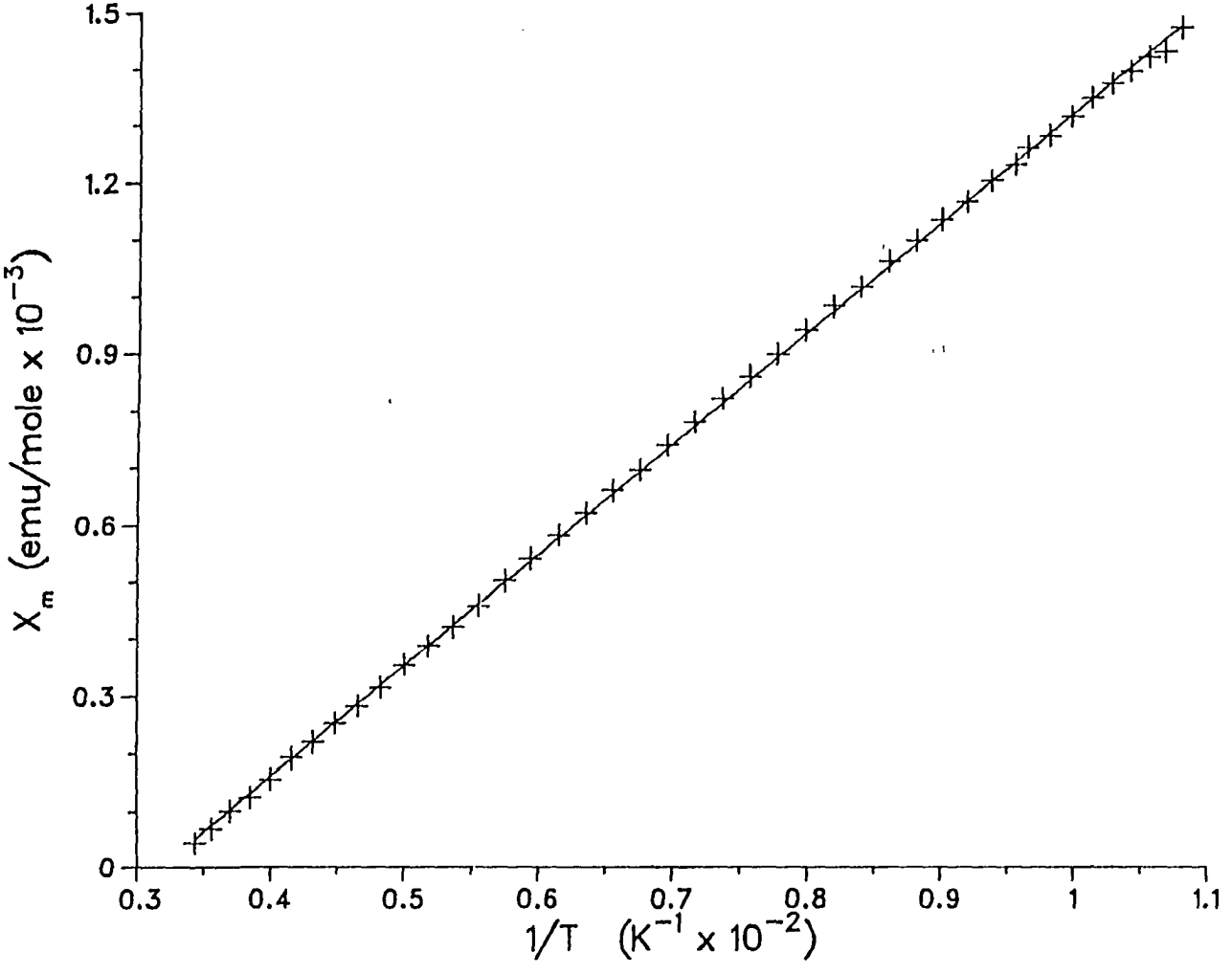

Figure 16. χ_m vs. 1/T plot for $(TPA)_4Mo_8I_{20}X$

magnetic moment, 1.25 μ_β, indicated 0.6 unpaired electrons per molecule. Because of the unusual value of the magnetic moment, other possible molecular formulas were examined. If the molecular weight is doubled to 4051.08 g/mol (for the formula $(TPA)_4Mo_8I_{20}$), the magnetic moment becomes 1.73 μ_β. A plot of the new χ_m vs. 1/T is shown in Fig. 16. The numerical values for the least-squares slope and intercept are now 0.3880K emu/mol and -1232×10^{-6} emu/mol, respectively. The magnetic moment of 1.73 μ_β matches the theoretical spin-only value for one unpaired electron. This is a very interesting result since the formula "$(TPA)_4Mo_8I_{20}$" implies an even electron material. These data agree with the net formula $(TPA)_4Mo_8I_{20}X$, where X is a ligand which dictates an odd electron count in the cluster unit.

The EPR spectra of the "$Mo_4I_{10}^{2-}$" salts are also consistent with the presence of a species with an unpaired electron. Just as with $Mo_4I_9(CH_3CN)_4$, which has fifteen MCE, the EPR spectra of these salts are quite similar to the spectra of the $Mo_4I_{11}^{2-}$ salts (see Table 11 and Fig. 17). These data indicate the "$Mo_4I_{10}^{2-}$" salts are mixtures with a paramagnetic component. The electronic structure of these paramagnetic components appear to be equivalent to that of the $Mo_4I_{11}^{2-}$ anion.

The assignment of "$Mo_4I_{10}^{2-}$" as a $(Mo_4I_{10}^{2-})(Mo_4I_{10}H^{2-})$ mixed salt is consistent with the data. While the presence of a hydrido ligand would have a negligible effect on the chemical analyses of the "$Mo_4I_{10}^{2-}$" salts, it would have a significant effect on the material's magnetic properties. (However, the magnetic data do not rule out C, N, O or Cl as possible X atoms.)

Table 11. EPR spectra of the $Mo_4I_{11}^{2-}$, "$Mo_4I_{10}^{2-}$", and $Mo_4I_9(CH_3CN)_4$ compounds

	g	$g_{\parallel}$	$g_{\perp}$
$(TBA)_2Mo_4I_{11}$	2.057	2.098	2.037
"$(TBA)_2Mo_4I_{10}$"[a]	2.054	2.097	2.032
"$(TBA)_2Mo_4I_{10}$"[b]	2.048	2.086	2.029
$(TPA)_2Mo_4I_{11}$	2.045	2.088	2.024
"$(TPA)_2Mo_4I_{10}$"[c]	2.044	2.081	2.026
"$(TPA)_2Mo_4I_{10}$"[d]	2.043	2.080	2.025
$Mo_4I_9(CH_3CN)_4$	2.057	2.095	2.038

[a]Synthesized using reaction procedure I.

[b]Synthesized using reaction procedure J.

[c]Synthesized using reaction procedure K.

[d]Synthesized using reaction procedure L.

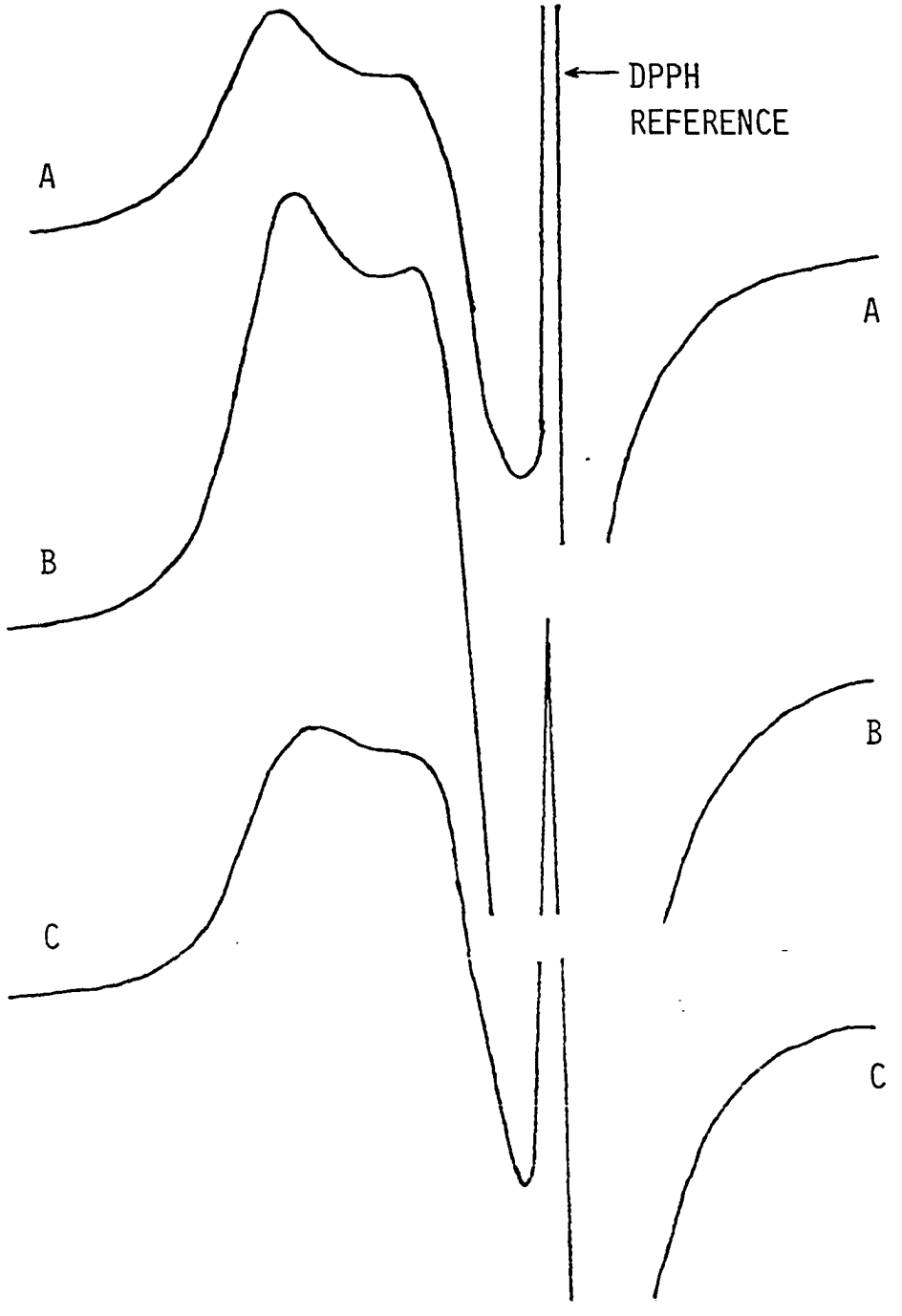

Figure 17. EPR spectra of (TBA) salts: (A) $Mo_4I_{11}^{2-}$, (B) "$Mo_4I_{10}^{2-}$" made by Reaction I, and (C) "$Mo_4I_{10}^{2-}$" made by Reaction J

Cyclic Voltammetry

It had been shown earlier that $(TBA)_2Mo_4I_{11}$ could be reduced by either chemical or electrochemical means. This work was now expanded using cyclic voltammetry to see whether or not the reduction of $(TBA)_2Mo_4I_{11}$ was reversible. Previously, a stationary electrode and a fast scan rate were used. Under these conditions, it was hoped that any reduced species would remain in contact with the electrode long enough to be oxidized back to the starting material. The absence of such a wave implied the transformation of $Mo_4I_{11}^{3-}$ to $Mo_4I_{10}^{2-}$ is very fast. After verifying the previous results, a new approach was tried. "$(TBA)_2Mo_4I_{10}$" was oxidized in the presence of free (TBA)I. The spinning electrode method was used this time. Since this method constantly brings fresh solution to the surface of the electrode, it measures bulk solution properties. (The same results were obtained for "$(TBA)_2Mo_4I_{10}$" made by either Reaction I or J.) Figure 18 shows the results. In Reaction A, the solution contained only $(TBA)_2Mo_4I_{11}$ and the supporting $(TBA)BF_4$ electrolyte, and showed a single reduction wave with an $E_{1/2}$ of -0.50 volts. In Reaction B, a solution 3×10^{-4} M in $(TBA)_2Mo_4I_{10}$ and 6×10^{-4} M in (TBA)I was scanned from +0.25 to -1.80 volts. The voltammogram contained three reduction waves at -0.15, -0.51 and -1.26 volts, and an oxidation wave at -0.57 volts. The reduction waves were assigned to adsorbed iodide on the electrode, $Mo_4I_{11}^{2-}$, and an impurity in the blank, respectively. The assignment of $Mo_4I_{11}^{2-}$ as the species being reduced at -0.51 volts was based on the results of solution A. Since this wave was present prior to any oxidation of the solution, the

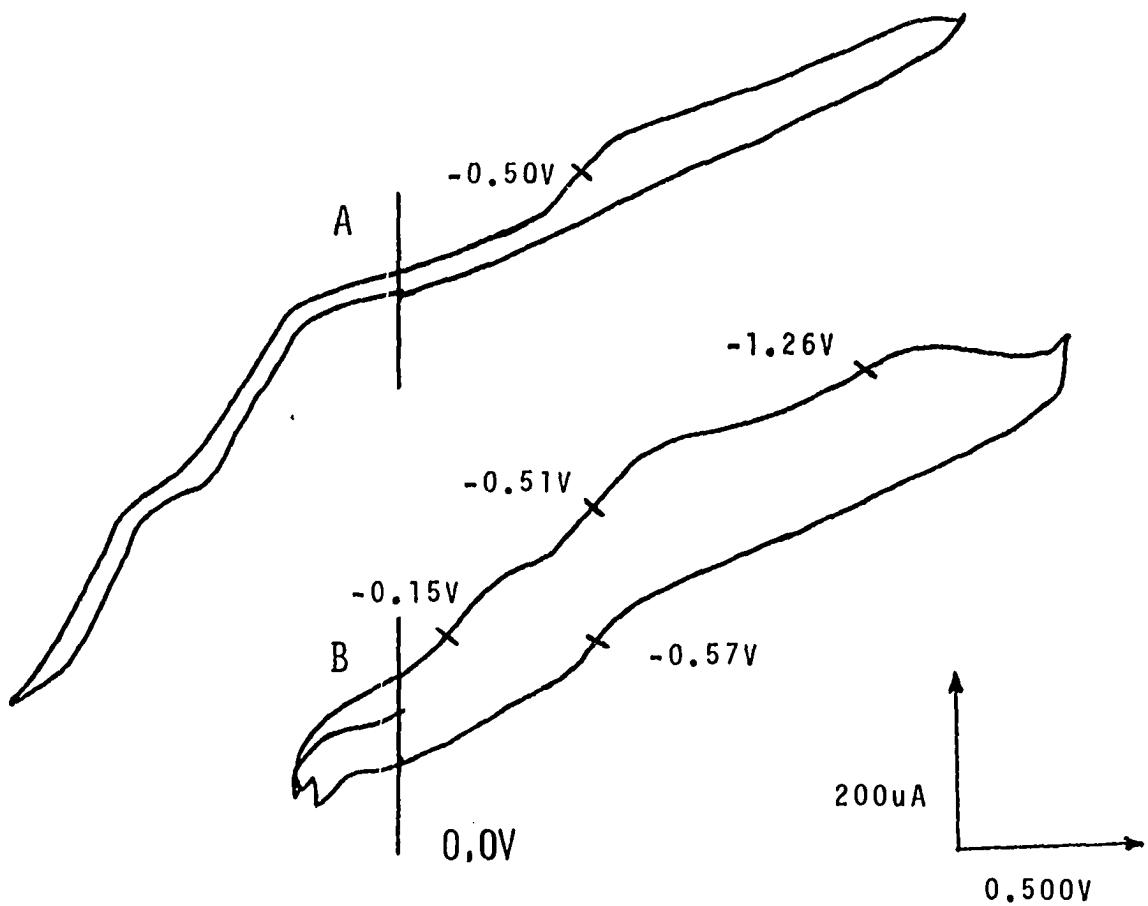

Figure 18. Spinning Pt electrode voltammograms: (A) 6.2 x 10^{-4} M $(TBA)_2Mo_4I_{11}$ and (B) 6.0 x 10^{-4} M "$(TBA)_2Mo_4I_{10}$" and 6.0 x 10^{-4} M (TBA)I; the scan rate was 0.200 V/sec and the electrode reaction rate was 600 RPM

species must have existed in some form in the initial "$Mo_4I_{10}^{2-}$" solution. Also, the amplitudes of this wave and the oxidation wave at -0.57 volts were approximately equal throughout the experiment, implying they had equivalent concentrations from beginning to end. These facts contradict the assumption that "$(TBA)_2Mo_4I_{10}$" in an acetonitrile solution is a single compound. Invoking the existence of a metal hydride species, $Mo_4I_{10}H^{2-}$, would explain the initial reduction wave and the behavior of a $Mo_4I_{11}^{2-}$ like species in solution.

The previously unobserved oxidation wave at -0.57 volts can be assigned to the oxidation of a second species, the $Mo_4I_{10}^{2-}$ anion (or the $Mo_4I_{11}^{3-}$ anion). This oxidation wave and the reduction wave at -0.51 volts are assumed to be a redox pair based on three observations. First, the relative amplitudes of both waves were constant with time. Also, there are no additional oxidation or reduction waves nearby, and the difference in their $E_{1/2}$'s, 0.06 volts, is appropriate for a one electron reaction. The E_o for this redox reaction is -0.54 volts with respect to the SCE reference electrode.

Earlier electrochemical work had shown the reduction of $Mo_4I_{11}^{2-}$ was not reversible. Together with Reactions H and I, the data suggested the following equation:

$$Mo_4I_{11}^{2-} + e^- \longrightarrow Mo_4I_{11}^{3-} \longrightarrow Mo_4I_{10}^{2-} + I^- \quad . \qquad (10)$$

The addition of excess iodide in solution B has enabled the oxidation of $Mo_4I_{10}^{2-}$ to now take place. This dependence on the iodide concentration for reversibility implies an intermediate step prior to oxidation.

$$Mo_4I_{10}^{2-} + I^- \rightleftarrows Mo_4I_{11}^{3-} \qquad (2)$$

If it was possible to oxidize the $Mo_4I_{10}^{2-}$ anion directly, an oxidation wave should have also been observed for solution A.

Spectra of the "$Mo_4I_{10}^{2-}$" Salts and $Mo_4I_9(CH_3CN)_4$

In this section, the similarities and differences of the various compounds will be discussed for each method. $(TBA)_2Mo_4I_{11}$ will frequently be used as a reference in these comparisons.

In all the products of the thermolysis reactions discussed, the spectra verified that the "$Mo_4I_{10}^{2-}$" compounds contained no residual carbon monoxide or coordinated solvent molecules. Careful examination of the spectra failed to show any bands over the region of 2800 to 1500 cm^{-1}, and from 1500 to 700 cm^{-1}, only bands for nujol and the cations, (TBA) or (TPA), were identified. Since metal hydrides are frequently identified on the basis of their infrared spectra, the spectra were re-examined. No metal-hydride bands were observed in the region 1500 to 2500 cm^{-1}. This would preclude the possibility of a terminal hydride ligand in "$Mo_4I_{10}^{2-}$", but not a bridging (M-H-M) hydride ligand. Whereas terminal hydride ligands show M-H stretching and bending modes in the ranges of 2300 to 1600 and 900 to 600 cm^{-1}, respectively; bridging M-H-M modes generally occur in the range of 1700 to 700 cm^{-1} [43]. Also, the bridging modes are generally broad and weak. Therefore, it would be possible for a bridging hydride band to be hidden by the cation bands.

The observed bands in the far infrared over the range of 600 to 80 cm^{-1} are listed in Table 12. Regardless of the associated cation or method of synthesis, the spectra for all four salts of "$Mo_4I_{10}^{2-}$" and those for salts of the $Mo_4I_{11}^{2-}$ anions are nearly identical. Each spectrum exhibits three strong Mo-I stretching bands at approximately 192, 182 and 169 cm^{-1}, and a weaker Mo-I stretching band at 204 cm^{-1}. The spectra also have one or two bands in the 111-100 cm^{-1} region which are unassigned. The close correspondence of spectra is a clear indication that all six anions are structurally similar.

Table 12. Far-infrared spectra of the "$Mo_4I_{10}^{2-}$" salts

Compound	Reaction Procedure	Observed Peaks (cm^{-1})
"$(TBA)_2Mo_4I_{10}$"	I	205(m), 191(s), 182(s), 168(s), 111(w), 103(m)
"$(TBA)_2Mo_4I_{10}$"	J	202(m), 194(s), 183(s), 169(s), 106(m)
"$(TPA)_2Mo_4I_{10}$"	K	205(w), 192(s), 183(s), 169(s), 102(s)
"$(TPA)_2Mo_4I_{10}$"	L	204(m), 194(s), 184(s), 172(s), 108(s)

s = strong
m = medium
w = weak

For $Mo_4I_9(CH_3CN)_4$, the infrared spectrum over the region of 4000 to 600 cm^{-1} shows only bands for acetonitrile. The C-N stretching band arrangement is a strong doublet of doublets at 2308, 2297, 2281 and 2269 cm^{-1}, and a much weaker band at 2246 cm^{-1} (see Fig. 19). The strong bands clearly show that two different kinds of acetonitrile are

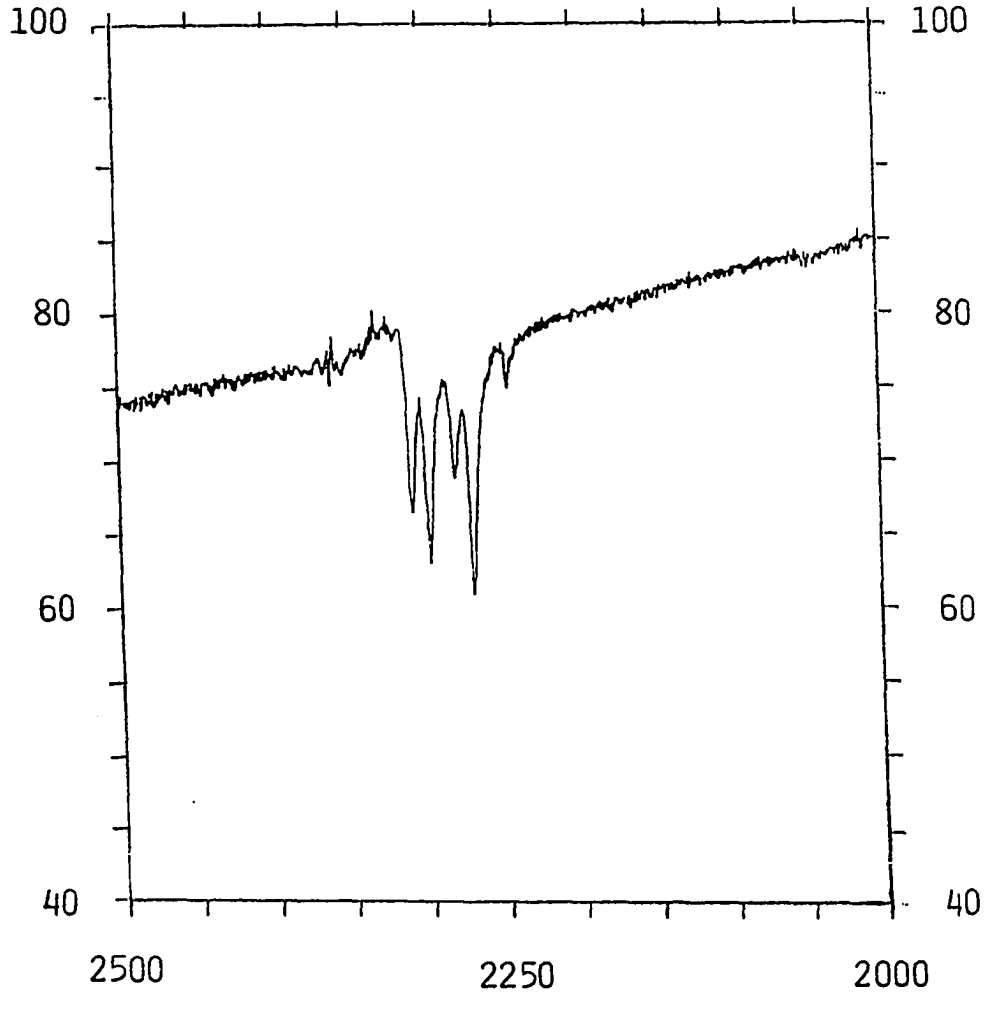

Figure 19. The infrared spectrum of $Mo_4I_9(CH_3CN)_4$ from 2000 to 2500 cm^{-1}

coordinated to the molybdenum cluster. The weaker band, at 2246 cm^{-1}, is free acetonitrile which is slowly lost by the compound

As in the comparisons of the infrared spectra, the electronic spectra of the compounds in this section only reconfirm their similarities to each other and to the $Mo_4I_{11}^{2-}$ anion. The spectra of "$(TBA)_2Mo_4I_{10}$", "$(TPA)_2Mo_4I_{10}$" and $Mo_4I_9(CH_3CN)_4$ were all obtained from nujol mulls. Each spectrum has a band at 490 nm and a shoulder at approximately 640 nm.

X-ray powder patterns were used for comparison of products. The powder patterns of "$(TBA)_2Mo_4I_{10}$" made by either the zinc reduction of $(TBA)_2Mo_4I_{11}$ or the thermolysis of $(TBA)Mo(CO)_4I_3$ under a hydrogen atmosphere, and of $(TBA)_2Mo_4I_{11}$ all closely match each other. The powder patterns of "$(TPA)_2Mo_4I_{10}$" made by the thermolysis of $(TPA)Mo(CO)_4I_3$ under either a nitrogen or a hydrogen atmosphere also match each other (see Table 15 in the Appendix). Again, the results are interpreted to mean that the two (TBA) salts and the two (TPA) salts of the "$Mo_4I_{11}^{2-}$" anions are the same.

Thermogravimetric Analysis

The thermogravimetric analysis of $Mo_4I_9(CH_3CN)_4$ was done by the 3M Central Research Laboratories - Analytical Research Group. The instrument used was a Perkin-Elmer TGS-1. The sample was maintained under a nitrogen atmosphere, and was heated at the rate of 2 1/2°C per minute. Decomposition of the sample started at about 70°C and reached a plateau at about 210°C. At this point, there was a 5.5% weight loss which

corresponds to a loss of 2.3 acetonitrile ligands per $Mo_4I_9(CH_3CN)_4$ molecule. A second stage of decomposition started at 240°C and continued steadily with decrease in rate at about 460°C. At 460°C, there was a 23.4% total weight loss which corresponds to a loss of 4 acetonitrile ligands and 1.8 iodide ligands. (An approximate formula at that point was Mo_4I_7.) These data showed that approximately half the acetonitrile is easily lost and the remainder is strongly bonded to the cluster.

Photoelectron Spectroscopy (PES)

Based on our experiences with the PES spectra of the $Mo_4I_{11}^{2-}$ salts, it was hoped that PES spectra could provide information about the structure of new compounds. This would be of special interest for compounds where single crystals could not be obtained, e.g., $Mo_4I_9(CH_3CN)_4$.

The PES spectrum of $Mo_4I_9(CH_3CN)_4$ was very informative about the arrangement of iodide ligands in the cluster. The iodine $3d_{3/2,5/2}$ spectrum was fitted with two and then with three independent components using the computer program previously discussed. The best fit for the two component case gives a 6.7 to 2.3 peak area ratio for the bridging to terminal iodide ligands. Based on work with the $Mo_4I_{11}^{2-}$ anion, this ratio is consistent with seven bridging and two terminal iodide ligands. Acetonitrile ligands occupy the remaining coordination sites. The trial fitting with three independent components is taken as evidence for the same conclusion. Both the energies and the relative areas of the three independent peaks were allowed to vary. The solution with the lowest χ^2 gives a 1.2:6.4:1.4 peak area ratio from high to low binding energy.

The peak energies and their energies of separation (from each other) are in good agreement with the results found for the $Mo_4I_{11}^{2-}$ anions. Therefore, the components are assigned as rising from triply bridging, doubly bridging, and terminal iodide ligands, respectively (see Table 13).

Keeping in mind the conclusions of the two component solution and the known structure of the $Mo_4I_{11}^{2-}$ starting material, the area ratios indicate that there are equal numbers of triply bridging and terminal iodide ligands, two each. This implies that the original two triply bridging and five doubly bridging iodide ligands of the $Mo_4I_{11}^{2-}$ anion remain intact, and that two terminal iodides have been replaced by acetonitrile. The thermogravimetric analysis and infrared spectra indicate that two nitrile ligands are strongly coordinated. The two more weakly coordinated nitriles are bound in a fashion which cannot be specified. Evidently the coordination number of two Mo atoms in the cluster unit has been increased.

The PES spectra of the "$Mo_4I_{10}^{2-}$" salts are not very informative. The results are similar for both (TBA) and (TPA) salts; their spectra can be only differentiated into bridging and terminal iodide ligands in approximately a three to two ratio. Attempts at three component solutions did not give improved fits to the data and are of doubtful validity. Results such as these could be expected for a mixture of two components with similar, but not equivalent ligand binding energies. However, if the two component solution is valid, these data would suggest that a bridging iodide ligand has been lost or replaced, and the cluster still has four terminal iodide ligands. Therefore, if one of the "$Mo_4I_{10}^{2-}$"

Table 13. PES spectra for $Mo_4I_9(CH_3CN)_4$, and (TBA) and (TPA) salts of "$Mo_4I_{10}^{2-}$"

Compound	$Mo_4I_9(CH_3CN)_4$	"$(TBA)_2Mo_4I_{10}$"[a]	"$(TBA)_2Mo_4I_{10}$"[b]	"$(TPA)_2Mo_4I_{10}$"[c]	"$(TPA)_2Mo_4I_{10}$"[d]
Mo, $3d_{5/2}$	229.3	229.7	229.3	229.1	229.1
FWHM, $3d_{5/2}$	1.2	1.7	1.2	1.4	1.6
I, $3d_{3/2}$-$3d_{5/2}$	11.5	11.6	11.6	11.5	11.7
FWHM, $3d_{3/2}$	1.9	2.6	2.4	2.6	2.5
FWHM, $3d_{5/2}$	1.9	2.8	2.4	2.8	2.6
2-Components:					
I1, $3d_{5/2}$	620.2	620.5	620.3	620.6	620.5
I2, $3d_{5/2}$	619.2	619.1	619.0	619.2	619.3
I1:I2	6.7:2.3[e]	5.5:4.5[f]	5.8:4.2[f]	5.9:4.1[f]	5.9:4.1[f]
3-Components:					
I1, $3d_{5/2}$	620.7	620.9	620.7	620.7	620.7
I2, $3d_{5/2}$	620.0	620.0	619.9	619.8	620.0
I_3, $3d_{5/2}$	618.9	619.0	618.8	619.0	619.1
I1:I2:I3	1.2:6.4:1.4[e]	3.8:4.6:1.8[f]	3.1:4.0:2.9[f]	4.3:2.4:3.3[f]	2.8:4.2:3.0[f]

[a]Synthesized using reaction procedure I.

[b]Synthesized using reaction procedure J.

[c]Synthesized using reaction procedure K.

[d]Synthesized using reaction procedure L.

[e]Based on a total of nine iodide ligands.

[f]Based on a total of ten iodide ligands.

components is a metal hydride cluster, the hydrogen atom is expected to occupy a bridging position.

Mass Spectroscopy

While previous data have implied the presence of a metal hydride fraction in "$Mo_4I_{10}^{2-}$", data had not proved a hydride cluster exists. It was hoped that the M-H cluster would react with $CDCl_3$ to form M-Cl and $CDHCl_2$ (or other products). The $CDHCl_2$ would then be detected by mass spectroscopy. The experiment did show the presence of $CDHCl_2$, but at levels only slightly above experimental error. The measurements were repeated with the same results. Evidence for other products (HD or HCl/DCl) was not found, but there were experimental difficulties with these measurements.

A sample of "$(TPA)_2Mo_4I_{10}$" was loaded into a tube in the dry box. Next, the tube was evacuated on a vacuum line and a 25-fold excess of degassed $CDCl_3$ was vacuum distilled into the tube. The tube was then heated for twelve hours at 60°C. Later, the tube was connected directly to the mass spectrometer and the vapor over the solution was examined.

An initial examination of the region from m/z = 84 to 89 for evidence of $CDHCl_2$ was unsuccessful. Spectra from both the solvent and the reaction were measured and compared, and no differences were observed. Next, the region from m/z = 47 to 52 was measured. The m/z 52/51 ratio was found to be a sensitive indicator for the presence of $CDHCl_2$ in the mixture. The fragmentation of the solvent leads to a $^{12}CD^{37}Cl^{+\cdot}$ ion peak at m/z = 51 and a $^{13}CD^{37}Cl^{+\cdot}$ ion peak at m/z = 52. (Fragments of CCl

interfere with comparisons of the analogous ^{35}Cl ions.) If a small quantity of $CDHCl_2$ is present in the reaction solution, it leads to a $^{12}CDH^{37}Cl^+$ ion peak at m/z = 52. Therefore, increases in the m/z 52/51 ratio are a measure of the $CDHCl_2$ present in the sample. The data are shown in Table 14.

Table 14. Analysis of the percent $CDHCl_2$ in the sample as determined by mass spectroscopy

Trial	m/z	$CDCl_3$ (%)	Sample (counts = %)	ICV (%)[a]	TIC (%)[b]
1	51	100	22500 = 100	100	100
	52	1.40	440 = 1.96	0.56	0.08
2	51	100	34500 = 100	100	100
	52	1.26	500 = 1.45	0.19	0.03

[a]ICV means the isotope corrected value. In this case, ^{13}C isotope contributions have been removed.

[b]TIC means total ion current. Based on library spectra, m/z = 51 is 1.3% of the TIC for $CDCl_3$ and m/z = 52 is 9.3% of the TIC for $CDHCl_2$.

Since there was a 25-fold excess of solvent, a complete reaction would yield $CDHCl_2$ as 4% of the mixture. The measurement of 0.08% $CDHCl_2$ indicates a reaction efficiency of only 2%. If the hydride ligand occupied a bridging position as possibly indicated by infrared and PES data, a low reaction efficiency would not be unreasonable.

SUMMARY

The major product of the thermolysis of $(R_4N)Mo(CO)_4I_3$ (where R = Pr, Bu) depends on the reaction conditions. Solvent is a factor; the use of a noncoordinating solvent yields cluster compounds while the use of coordinating solvents lead to monomeric products. The salt's solubility, the reaction temperature, carbon monoxide concentration in solution are all factors, and their effects are interrelated. It was hoped that a series of molybdenum iodide clusters, from large to small, would be synthesized by changing the reaction conditions, but only tetranuclear cluster anions were obtained.

Using $(TBA)Mo(CO)_4I_3$ under simple reflux in a noncoordinating solvent, the reaction product has a general formula $(TBA)_xMo_4I_{11}$. The values of x vary from 2.5 for refluxing benzene (80°C) to 2.0 for refluxing σ-dichlorobenzene (177°C). The oxidation state of the molybdenum frame increases with increasing reaction temperature. This change is thought to be due to the rate the $Mo_4I_{11}^{3-}$ anion reacts further with the $Mo(CO)_4I_3^-$ anion.

The $Mo_4I_{11}^{2-}$ salts are made by adding iodine to the thermolysis reaction (Reaction B). The $Mo_4I_{11}^{2-}$ anion is very stable, and has been well characterized. Key points of the anion's characterization are its magnetic properties and its structure. The magnetic moment was calculated from temperature independent magnetic susceptibility data and later verified by EPR data. The magnetic moment value of 1.87 μ_B agrees with the assignment of one unpaired electron per anion.

A x-ray crystal structure determination established the exact structure of $(TBA)_2Mo_4I_{11}$. The anion can be viewed as a distorted tetrahedral fragment of the $(Mo_6Cl_8)Cl_6^{2-}$ structure. The metal frame has a closed butterfly arrangement of atoms. There are five strong Mo-Mo bonds, four average 2.542 Å and the fifth is 2.669 Å long. The sixth Mo-Mo distance in the anion, between Mo(1) and Mo(2), is 3.035 Å long. This "long" distance falls between the values expected for a Mo-Mo single bond and a nonbonding distance. A qualitative MO scheme was devised to explain the metal-metal bonding in the cluster. It predicted six metal-metal bonding orbitals and two metal-metal nonbonding orbitals located on Mo(1) and Mo(2), but this scheme could not shed any light on the "long" Mo(1)-Mo(2) distance. Subsequently EHMO calculations were performed on the anion. They indicated the covalent nature of the Mo-I bonds in the anion had significant consequences on the anion's electronic structure. Now there are eight bonding MO with significant Mo AO character. The next MO, about 0.5 eV higher in energy, is the HOMO and is slightly antibonding in character. It also predicts that no bonding exists between Mo(1) and Mo(2). Instead, the "long" Mo(1)-Mo(2) distance is the result of a minimum in total bonding energy, Mo-Mo and Mo-I. The calculations by Miessner and Korolkov showed that the total bonding energy is a function of the dihedral angle between the Mo(1)-Mo(3)-Mo(4) and Mo(2)-Mo(3)-Mo(4) metal planes, and is a minimum at 88.6°.

The iodide ligands form a pseudo-cube around the metal frame. Six ligands occupy corners of the cube, one ligand, I(1), lies approximately midway on the remaining cube edge, and four ligands are bonded terminally

to Mo atoms. This results in the anion having three kinds of iodide ligands (triply bridging, doubly bridging and terminal) in a 2:5:4 ratio. This knowledge proved useful in analyzing the PES spectra of this and other molybdenum iodide clusters. The short Mo-I distances and the acute Mo-I-Mo bond angles are also good indicators of the strong bonding in the cluster.

The stability of the $Mo_4I_7^{2+}$ basic frame was reaffirmed by an unsuccessful attempt to oxidize $(TBA)_2Mo_4I_{11}$ with iodine in acetonitrile. (Attempts to oxidize $(TBA)_2Mo_4I_{11}$ electrochemically also failed.) Instead, a ligand exchange reaction takes place, producing $Mo_4I_9(CH_3CN)_4$. The $Mo_4I_9(CH_3CN)_4$ EPR spectrum matched that of its $(TBA)_2Mo_4I_{11}$ starting material (for both shape and energy). Also, the PES study of the compound showed that the remaining iodide ligands were present in a 2:5:2 triply bridging:doubly bridging:terminal ligand ratio. Therefore, the two iodide ligands lost are from terminal positions. While both EPR and PES data indicate the cluster's $(Mo_4I_7)^{2+}$ basic frame has been left intact, TGA and infrared data show the presence of two kinds of coordinated acetonitrile in the compound. The exact nature of the acetonitrile bonding is not clear.

Based on the characterization of $(TBA)_2Mo_4I_{11}$, $(TBA)_{2.5}Mo_4I_{11}$ is assumed to be an equal mixture of the $Mo_4I_{11}^{2-}$ and $Mo_4I_{11}^{3-}$ salts. This product can be synthesized by the thermolysis of $(TBA)Mo(CO)_4I_3$ (as in Reactions E and F) or by the zinc reduction of $(TBA)_2Mo_4I_{11}$ in acetonitrile (Reaction H). The pyrophoric nature of the mixture implies that

the $Mo_4I_{11}^{3-}$ anion is more labile in its reactivity towards oxidants than the $Mo_4I_{11}^{2-}$ anion.

The thermolysis of $(R_4N)Mo(CO)_4I_3$ with a continuous gas (N_2 or H_2) purge in a noncoordinating solvent gives results different than the simple reflux reactions described earlier. The flushing action of the gas was intended to eliminate any free carbon monoxide from the solution. The product of these reactions (J, K and L) were all analyzed as "$(R_4N)_2Mo_4I_{10}$". The same product is also obtained from the zinc reduction of $(TBA)_2Mo_4I_{11}$ in refluxing acetonitrile (Reaction I). In all cases, the "$Mo_4I_{10}^{2-}$" anion is stable.

Far infrared, UV-visible, and powder pattern spectral studies showed that for each salt, a close relationship exists between the "$Mo_4I_{10}^{2-}$" anion and the $Mo_4I_{11}^{2-}$ anion, and the "$Mo_4I_{10}^{2-}$" anions prepared by either method were the same. At the same time, unexpected results were obtained from magnetic and electrochemical studies. In these studies, "$Mo_4I_{10}^{2-}$" salts behaved as if they were a $Mo_4I_{11}^{2-}\cdot Mo_4I_{11}^{3-}$ mixed salt. This assessment conflicted with the analytical data. After re-examining all the data, it was postulated that the "$Mo_4I_{10}^{2-}$" is really a $Mo_4I_{10}H^{2-}\cdot Mo_4I_{10}^{2-}$ mixed salt. While no direct proof for a hydride has been found, the existence of a $Mo_4I_{10}H^{2-}$ anion is consistent with all the data.

BIBLIOGRAPHY

1. Delphin, W. H.; Wentworth, R. A. D. and Matson, M. S. Inorg. Chem. 1974, 13, 2552.

2. Cotton, F. A. Inorg. Chem. 1964, 3, 1217.

3. McCarley, R. E. In "Mixed-Valence Compounds", Kluewer Boston: Hingham, MA, 1980, p. 337.

4. Bino, A.; Cotton, F. A. and Dori, Z. J. J. Am. Chem. Soc. 1978, 100, 5252.

5. Bino, A.; Cotton, F. A. and Dori, Z. J. Inorg. Chem. Acta 1979, 33, 133.

6. Mattes, R. and Mennemann, K. Z. Anorg. Allg. Chem. 1977, 437, 175.

7. Bino, A.; Cotton, F. A. and Dori, Z. J. J. Am. Chem. Soc. 1981, 103, 243.

8. Bino, A.; Cotton, F. A.; Dori, Z. J.; Koch, S.; Küppers, H.; Millar, M. and Sekutowski, J. C. Inorg. Chem. 1978, 17, 3245.

9. Ardon, M.; Cotton, F. A.; Dori, Z. J.; Fang, A.; Kapon, M.; Reisner, G. M. and Shaia, M. J. Am. Chem. Soc. 1982, 104, 5394.

10. Chisholm, M. H.; Folting, K.; Huffman, J. C. and Kirkpatrick, C. C. J. Am. Chem. Soc. 1981, 103, 5967.

11. Perrin, C.; Chevrel, R. and Sergent, M. C. R. Acad. Sci. Paris 1975, 280C, 949.

12. Perrin, C.; Chevrel, R. and Sergent, M. C. R. Acad. Sci. Paris 1975, 281C, 23.

13. Chisholm, M. H.; Errington, R. J.; Folting, K. and Huffman, J. C. J. Am. Chem. Soc. 1982, 104, 2025.

14. Stensvad, S.; Helland, B. J.; Babich, M. W.; Jacobson, R. A. and McCarley, R. E. J. Am. Chem. Soc. 1978, 100, 6257.

15. McCarley, R. E.; Ryan, T. R. and Torardi, C. C. ACS Symp. Ser. 1981, 155, 41.

16. Chisholm, M. H.; Huffman, J. C. and Leonelli, J. J. Chem. Soc., Chem. Comm. 1981, 270.

17. McGinnis, R. N.; Ryan, T. R. and McCarley, R. E. J. Am. Chem. Soc. 1978, 100, 7900.

18. Jodden, K.; von Schnering, H. G. and Schafer, H. Angew. Chem. 1975, 87, 594.

19. Schafer, H.; von Schnering, H. G.; Tillack, J.; Kuhner F.; Wohrle, H. and Bauman, H. Z. Anorg. Allg. Chem. 1967, 353, 281.

20. Cotton, F. A. and Haas, T. E. Inorg. Chem. 1964, 3, 10.

21. Schafer, H. Angew. Chem. Internat. Edn. 1967, 6, 637.

22. Chevrel, R.; Sergent, M. and Prigent, J. Mat. Res. Bull. 1974, 9, 1487.

23. Marezio, M.; Dernier, P. D.; Remeika, J. P.; Corenzuit, E. and Matthias, B. T. Mat. Res. Bull. 1973, 8, 657.

24. Siepmann, R. and von Schnering, H. G. Z. Anorg. Allg. Chem. 1968, 357, 289.

25. Converse, J. G. Ph.D. Thesis, Iowa State University, Ames, Iowa, 1968.

26. Stierman, R. J. Ph.D. Thesis, Iowa State University, Ames, Iowa, 1982.

27. Luly, M. H. "APES--A Fortran Program to Analyze Photoelectron Spectra", U.S. Department of Energy Report IS-4694, Ames Laboratory, Iowa State University, Ames, Iowa, 1979.

28. Rohrbaugh, N. J. and Jacobson, R. A. Inorg. Chem. 1974, 13, 2535.

29. Jacobson, R. A. J. Appl. Cryst. 1976, 9, 115.

30. De Meulenaer, J. and Tompa, H. Acta Cryst. 1965, 19, 1014.

31a. Lawton, S. L. and Jacobson, R. A. Inorg. Chem. 1968, 7, 2124.

31b. King, R. B. Inorg. Chem. 1964, 3, 1039.

32. Delphin, W. H. and Wentworth, R. A. D. J. Am. Chem. Soc. 1973, 95, 7920.

33. McCarley, R. E.; Templeton, J. L.; Colburn, T. J.; Katovic, V. and Hoxmeier, R. J. Adv. Chem. Ser. 1976, No. 150, 318.

34. Glickman, H. P. and Walton, R. A. Inorg. Chem. 1978, 19, 3197.

35. Johnson, D. C. J. Electrochem. Soc. 1972, 119, 331.

36. Weast, R. C., Ed. "CRC-Handbook of Chemistry and Physics", 53rd ed. The Chemical Rubber Co.: Cleveland, Ohio, 1971-72, p. E109.

37. Best, S. A. and Walton, R. A. Inorg. Chem. 1979, 18, 484.

38. Busing, W. R.; Martin, K. O. and Levy, H. A. "ORFLS, A Fortran Crystallographic Least Squares Program", U.S. Atomic Energy Commission Report ORNL-TM-305, Oak Ridge National Laboratory, Oak Ridge, TN, 1962.

39. Hanson, H. P.; Herman, F.; Lea, J. D. and Skillman, S. Acta Cryst. 1960, 17, 1040.

40. Templeton, D. H. "International Tables for X-ray Crystallography", The Knoch Press: Birmingham, England, 1962, Vol. III, Table 3.3.2c, p. 215.

41. Miessner, H. and Korolkov, D. V. Z. Anorg. Allg. Chem. 1983, 496, 175.

42. Cotton, F. A. and Ucko, D. A. Inorg. Chim. Acta 1972, 6, 161.

43. Cooper, C. B.; Shriver, D. F.; and Onaka, S. Adv. Chem. Ser. 1978, 167, 232.

APPENDIX

Table 15. X-ray powder pattern d-spacings and relative intensities

$(TBA)_2Mo_4I_{11}$	$(TBA)_2Mo_4I_{10}$[a]	$(TBA)_2Mo_4I_{10}$[b]	$(TPA)_2Mo_4I_{10}$[c]	$(TPA)_2Mo_4I_{10}$[d]
11.17 s	11.25 s	11.27 s	10.68 vs	10.71 vs
10.12 vs	10.27 vs	10.27 vs	9.68 w	9.58 w
8.98 w	9.11 w	9.11 w	7.62 m	7.58 m
8.31 w	8.39 w	8.39 w	7.15 m	
7.21 w	7.28 w	7.08 w	4.35 m	4.38 m
6.56 w	6.67 w	6.65 w	4.13 m	
6.00 w	6.03 w	6.11 w	3.57 s	3.57 s
5.30 w	5.32 w	5.33 w	3.37 w	
	4.43 w	4.37 w	3.09 w	3.09 w
4.08 w	4.08 w	4.12 w	2.98 m	2.97 m
3.93 w	3.94 w	3.98 w	2.77 w	2.77 w
3.77 w	3.80 w		2.68 w	2.68 w
3.66 w	3.70 w	3.71 w	2.60 w	2.60 w
3.53 w	3.56 w	3.55 w	2.52 w	2.53 w
3.40 w	3.43 w		2.46 w	2.46 w
3.33 w	3.31 w	3.33 w	2.40 w	
3.21 w	3.17 w	3.20 w	2.33 w	
3.06 w	3.09 w	3.10 w	2.19 w	2.19 w
	3.00 w	2.99 w	2.14 m	2.15 m
2.95 w	2.95 w		2.06 w	2.06 w
2.82 w	2.85 w	2.82 w	1.86 m	1.87 m
2.69 w	2.66 w		1.76 w	

w = weak
m = medium
s = strong
vs - very strong

[a]Prepared by reaction I, Zn reduction of $(TBA)_2Mo_4I_{11}$ in refluxing acetonitrile.

[b]Prepared by reaction J, thermolysis of $(TBA)Mo(CO)_4I_3$ under H_2 in refluxing chlorobenzene.

[c]Prepared by reaction K, thermolysis of $(TPA)Mo(CO)_4I_3$ under N_2 in refluxing chlorobenzene.

[d]Prepared by reaction L, thermolysis of $(TPA)Mo(CO)_4I_3$ under H_2 in refluxing chlorobenzene.

Table 16. Final atomic positional and isotropic thermal parameters for $(TBA)_2Mo_4I_{11}$[a]

Atom	Fractional Coordinates[b]			Isotropic Thermal Factor[c]
	x	y	z	$\bar{B}$
Mo(1)	3261(1)	1471(1)	2471(1)	2.90(11)
Mo(2)	1761(1)	1482(1)	2524(1)	3.02(11)
Mo(3)	2721(1)	236(1)	3083(1)	2.79(11)
Mo(4)	2292(1)	239(1)	1912(1)	2.70(11)
I(1)	2520(1)	3318(1)	2500(1)	3.78(11)
I(2)	3566(1)	-748(1)	2461(1)	3.48(11)
I(3)	506(1)	2502(1)	2575(1)	4.80(11)
I(4)	2026(1)	1409(1)	3730(1)	3.85(11)
I(5)	3046(1)	-1394(1)	3958(1)	3.66(11)
I(6)	3859(1)	1426(1)	3672(1)	3.66(11)
I(7)	1433(1)	-737(1)	2532(1)	3.45(11)
I(8)	4522(1)	2474(1)	2418(1)	4.43(11)
I(9)	2995(1)	1412(1)	1268(1)	3.63(11)
I(10)	1956(1)	-1381(1)	1033(1)	3.64(11)
I(11)	1160(1)	1441(1)	1325(1)	3.66(11)
N(1)	3628(9)	5455(15)	1024(11)	4.5(9)
C(1)	1914(14)	4047(27)	290(13)	5.7(17)
C(2)	4843(13)	3522(23)	455(12)	4.9(14)
C(3)	5002(17)	2278(24)	508(19)	8.0(18)
C(4)	2541(12)	4710(23)	298(12)	5.0(14)
C(5)	4262(16)	3792(22)	727(13)	5.0(15)
C(6)	1447(14)	4491(27)	671(14)	6.3(18)
C(7)	4137(11)	4994(18)	651(12)	4.0(11)
C(8)	3496(12)	6650(18)	820(12)	4.3(11)
C(9)	2986(14)	4796(25)	977(11)	6.5(15)
C(10)	4146(11)	7391(20)	942(13)	4.6(12)
C(11)	3915(18)	8570(20)	807(16)	6.6(15)
C(12)	4520(17)	9293(21)	935(14)	6.0(15)
C(13)	4092(14)	5391(19)	1684(11)	4.6(12)
C(14)	3708(17)	5937(24)	2078(13)	6.0(16)
C(15)	4065(22)	5588(23)	2712(13)	9.1(19)
C(16)	3641(36)	6206(27)	3111(23)	15.3(30)

[a]In this and succeeding tables, estimates of standard deviations are given in parentheses for the least significant figures.

[b]The positional parameters are in fractional unit cell coordinates ($\times 10^4$).

[c]The $\bar{B}$ equals $1/3(B_{11} + B_{22} + B_{33})$.

Table 16. Continued

Atom	Fractional Coordinates[b]			Isotropic Thermal Factor[c]
	x	y	z	$\bar{B}$
NB	1353(10)	5478(18)	4004(10)	5.1(11)
CB(1)	1291(23)	6163(26)	1863(16)	8.5(20)
CB(2)	1051(20)	5571(27)	2320(13)	7.4(20)
CB(3)	1324(18)	5962(23)	2910(16)	7.8(16)
CB(4)	958(14)	5394(21)	3313(12)	4.7(13)
CB(5)	2059(14)	4789(24)	4086(12)	5.3(15)
CB(6)	883(12)	7400(19)	4040(11)	4.1(12)
CB(7)	469(17)	9294(24)	4060(17)	7.4(17)
CB(8)	1061(15)	8555(22)	4187(14)	5.4(14)
CB(9)	1518(15)	6662(20)	4206(14)	6.6(14)
CB(10)	767(16)	3818(21)	4268(14)	6.0(14)
CB(11)	887(12)	4998(21)	4348(13)	5.0(13)
CB(12)	2429(17)	4661(32)	4652(16)	8.7(22)
CB(13)	163(13)	3505(21)	4541(13)	5.3(13)
CB(14)	64(16)	2288(24)	4514(16)	7.1(16)
CB(15)	3614(13)	4478(28)	4359(13)	6.3(17)
CB(16)	3107(12)	4019(29)	4725(13)	5.2(14)

Table 17. Selected I-I nonbonding distances in the $Mo_4I_{11}^{2-}$ anion

Atom 1	Atom 2	Distance, Å
I(2)	I(6)	3.877(6)
I(2)	I(7)	4.313(7)
I(2)	I(9)	3.847(6)
I(4)	I(6)	3.704(6)
I(4)	I(7)	3.847(6)
I(7)	I(11)	3.872(6)
I(9)	I(11)	3.708(6)
	Average d(I-I) on cube edges = 3.881 Å	
I(1)	I(4)	4.081(5)
I(1)	I(6)	4.054(5)
I(1)	I(9)	4.078(5)
I(1)	I(11)	4.058(5)
	Average d(I-I) on pseudo-cube edges = 4.068 Å	
I(3)	I(1)	4.199(7)
I(3)	I(4)	3.751(5)
I(3)	I(7)	4.471(9)
I(3)	I(11)	3.789(5)
I(5)	I(2)	4.034(5)
I(5)	I(4)	4.021(8)
I(5)	I(6)	4.005(8)
I(5)	I(7)	4.068(5)
I(8)	I(1)	4.199(7)
I(8)	I(2)	4.460(9)
I(8)	I(6)	3.794(5)
I(8)	I(9)	3.733(5)
I(10)	I(2)	4.058(5)
I(10)	I(7)	4.046(5)
I(10)	I(9)	4.013(8)
I(10)	I(11)	4.012(8)
	Average d(I-I) from terminal to cube atoms = 4.041 Å	

Table 18. A qualitative molecular orbital scheme for $Mo_4I_{11}^{2-}$ [a]

Γz^2:	$2a_1 + b_1 + b_2$	
	a_1^b	$(z_1^2 + z_2^2) + (z_3^2 + z_4^2)$
	a_1^*	$(z_1^2 + z_2^2) - (z_3^2 + z_4^2)$
	b_1^*	$z_3^2 - z_4^2$
	b_2^*	$z_1^2 - z_2^2$
$\Gamma xz_{1,2}, yz_{1,2}, xz_{3,4}, x^2 - y^2{}_{3,4}$:	$2a_1 + 2a_2 + 2b_1 + 2b_2$	
	a_1^b	$(xz_1 + yz_2) + [x^2 - y^2)_3 + (x^2 - y^2)_4]$
	a_1^*	$(xz_1 + yz_2) - [x^2 - y^2)_3 + (x^2 - y^2)_4]$
	a_2^b	$(yz_1 - xz_2) + (xz_3 + xz_4)$
	a_2^*	$(yz_1 - xz_2) - (xz_3 + xz_4)$
	b_1^b	$(yz_1 + xz_2) + [(x^2 - y^2)_3 - (x^2 - y^2)_4]$
	b_1^*	$(yz_1 + xz_2) - [(x^2 - y^2)_3 - (x^2 - y^2)_4]$
	b_2^b	$(xz_1 - yz_2) + (xz_3 - xz_4)$
	b_2^*	$(xz_1 - yz_2) - (xz_3 - xz_4)$
$\Gamma yz_{3,4}$:	$a_1 + b_1$	
	a_1^b	$yz_3 + yz_4$
	b_1^*	$yz_3 - yz_4$
$\Gamma xz_{1,2}$:	$a_2 + b_1$	
	a_2^n	$xy_1 + xy_2$
	b_1^n	$xy_1 - xy_2$

[a]The symmetry combinations predict the cluster has 6 bonding ($3a_1 + a_2 + b_1 + b_2$), 2 nonbonding ($a_2 + b_1$), and 8 antibonding ($2a_1 + a_1 + 3b_1 + 2b_2$) M-M orbitals.

Table 19. Bond distances in the $(TBA)_2Mo_4I_{11}$ cations

Atoms	Distance, Å	
N(1)-C(7)	1.63(3)	
N(1)-C(8)	1.57(3)	
N(1)-C(9)	1.50(3)	
N(1)-C(13)	1.52(3)	
NB(1)-CB(4)	1.61(3)	
NB(1)-CB(5)	1.62(3)	
NB(1)-CB(9)	1.56(3)	
NB(1)-CB(11)	1.52(3)	
		Average N-C = 1.57
C(1)-C(4)	1.50(4)	
C(1)-C(6)	1.57(4)	
C(2)-C(3)	1.58(4)	
C(2)-C(5)	1.51(4)	
C(4)-C(9)	1.61(4)	
C(5)-C(7)	1.52(4)	
C(8)-C(10)	1.55(3)	
C(10)-C(11)	1.55(4)	
C(11)-C(12)	1.47(4)	
C(13)-C(14)	1.59(4)	
C(14)-C(15)	1.54(4)	
C(15)-C(16)	1.63(7)	
CB(1)-CB(2)	1.49(5)	
CB(2)-CB(3)	1.44(5)	
CB(3)-CB(4)	1.52(4)	
CB(5)-CB(12)	1.35(5)	
CB(6)-CB(8)	1.50(4)	
CB(6)-CB(9)	1.53(4)	
CB(7)-CB(8)	1.47(4)	
CB(10)-CB(11)	1.50(4)	
CB(10)-CB(13)	1.57(4)	
CB(12)-CB(16)	1.55(4)	
CB(13)-CB(14)	1.53(4)	
CB(15)-CB(16)	1.60(4)	
		Average C-C = 1.53

Table 20. Selected Bond Angles in the $(TBA)_2Mo_4I_{11}$ cations

Atoms	Bond Angle, in Degrees	
C(7)-N(1)-C(8)	104.6(18)	
C(7)-N(1)-C(9)	114.5(19)	
C(7)-N(1)-C(13)	101.7(17)	
C(8)-N(1)-C(9)	115.3(18)	
C(8)-N(1)-C(13)	111.0(18)	
C(9)-N(1)-C(13)	109.1(20)	
CB(4)-NB(1)-CB(5)	104.9(18)	
CB(4)-NB(1)-CB(9)	112.1(20)	
CB(4)-NB(1)-CB(11)	108.5(18)	
CB(5)-NB(1)-CB(9)	111.4(19)	
CB(5)-NB(1)-CB(11)	111.6(19)	
CB(9)-NB(1)-CB(11)	108.4(20)	
		Average C-N-C = 109.3°
C(4)-C(1)-C(6)	115.1(26)	
C(3)-C(2)-C(5)	110.5(24)	
C(1)-C(4)-C(9)	106.4(22)	
C(2)-C(5)-C(7)	107.1(22)	
C(8)-C(10)-C(11)	109.7(20)	
C(8)-C(11)-C(12)	110.8(25)	
C(13)-C(14)-C(15)	109.0(25)	
C(14)-C(15)-C(16)	104.7(31)	
CB(1)-CB(2)-CB(3)	115.1(30)	
CB(2)-CB(3)-CB(4)	109.3(27)	
CB(8)-CB(6)-CB(9)	113.1(21)	
CB(6)-CB(8)-CB(7)	115.6(24)	
CB(11)-CB(10)-CB(13)	107.7(23)	
CB(5)-CB(12)-CB(16)	113.5(29)	
CB(10)-CB(13)-CB(14)	109.4(22)	
CB(12)-CB(16)-CB(15)	114.7(26)	
		Average C-C-C = 110.7°
N(1)-C(7)-C(5)	113.3(20)	
N(1)-C(8)-C(10)	116.4(18)	
N(1)-C(9)-C(4)	109.8(21)	
N(1)-C(13)-C(14)	109.1(21)	
NB(1)-CB(4)-CB(3)	114.7(22)	
NB(1)-CB(5)-CB(12)	113.9(25)	
NB(1)-CB(9)-CB(6)	113.7(21)	
NB(1)-CB(11)-CB(10)	114.7(23)	
		Average N-C-C = 113.2°

Table 21. Atomic temperature factors for $(TBA)_2Mo_4I_{11}$

Atom	B_{11}	B_{22}	B_{33}	B_{12}	B_{13}	B_{23}
Mo(1)	3.0(1)	2.6(1)	3.1(2)	-0.4(1)	0.4(2)	-0.1(1)
Mo(2)	3.1(1)	2.9(1)	3.1(2)	-0.1(1)	0.7(2)	0.1(1)
Mo(3)	2.8(1)	2.9(1)	2.7(2)	-0.4(1)	2.4(2)	0.1(1)
Mo(4)	2.7(1)	2.8(1)	2.7(2)	-0.1(1)	0.4(2)	-0.1(1)
I(1)	4.3(1)	2.7(1)	4.4(2)	-0.3(1)	1.1(2)	0.1(1)
I(2)	3.3(1)	3.2(1)	3.9(2)	0.3(1)	0.7(2)	0.1(1)
I(3)	4.1(1)	5.0(1)	5.2(2)	1.0(1)	1.1(2)	-0.1(1)
I(4)	4.3(1)	3.9(1)	3.3(2)	-0.5(1)	0.4(2)	-0.3(1)
I(5)	3.3(1)	4.0(1)	3.7(2)	-0.3(1)	0.4(2)	0.9(1)
I(6)	3.6(1)	4.3(1)	3.1(2)	-1.1(1)	-0.2(2)	-0.1(1)
I(7)	3.1(1)	3.3(1)	3.9(2)	-0.9(1)	0.7(2)	-0.3(1)
I(8)	3.7(1)	4.8(1)	4.8(2)	-1.2(1)	1.4(2)	0.1(1)
I(9)	3.8(1)	3.9(1)	3.1(2)	-0.5(1)	0.7(2)	0.1(1)
I(10)	3.3(1)	3.9(1)	3.7(2)	-0.4(1)	0.7(2)	-0.9(1)
I(11)	3.1(1)	4.6(1)	3.3(2)	0.5(1)	0.2(2)	0.2(1)
N(1)	1.8(7)	4.0(9)	7.9(12)	-0.2(7)	1.2(7)	1.1(9)
C(1)	4.1(13)	8.1(19)	5.0(14)	2.0(12)	-1.2(11)	0.7(13)
C(2)	2.8(10)	6.4(16)	5.6(14)	0.4(10)	0.5(9)	-0.7(11)
C(3)	6.5(18)	4.1(14)	13.3(29)	-1.7(12)	2.3(17)	-4.5(16)
C(4)	1.8(9)	7.1(16)	6.2(14)	-1.9(10)	1.1(9)	-0.6(11)
C(5)	7.6(18)	4.7(13)	6.2(14)	-2.6(12)	3.9(14)	-2.7(11)
C(6)	3.0(12)	8.4(19)	7.7(19)	0.2(11)	2.6(12)	-0.2(15)
C(7)	1.2(9)	3.6(11)	7.3(14)	0.3(8)	0.2(9)	1.0(10)
C(8)	2.8(10)	2.9(10)	7.1(14)	1.0(8)	0.7(11)	0.9(10)
C(9)	4.7(13)	7.9(17)	3.9(12)	-2.3(12)	2.6(11)	-0.3(11)
C(10)	1.8(9)	4.3(12)	7.7(17)	-0.8(9)	1.2(9)	-0.7(11)
C(11)	7.8(19)	2.3(11)	9.7(23)	-0.1(11)	-0.5(17)	1.1(13)
C(12)	7.0(18)	3.5(12)	7.5(19)	-0.9(11)	0.7(14)	-0.5(11)
C(13)	6.5(15)	3.7(11)	3.7(10)	-1.2(11)	2.3(11)	0.6(9)
C(14)	7.4(18)	5.7(16)	4.8(14)	1.6(13)	-0.9(12)	-2.3(11)
C(15)	16.4(31)	4.9(14)	5.8(14)	-2.1(17)	8.9(19)	-0.7(11)
C(16)	28.1(62)	3.0(14)	14.7(37)	-2.4(24)	14.7(42)	-0.9(18)
NB(1)	2.5(9)	5.6(12)	7.3(12)	0.9(8)	1.2(9)	0.3(10)
CB(1)	12.6(30)	4.5(15)	8.1(22)	-1.7(17)	3.2(19)	0.8(14)
CB(2)	11.4(27)	6.6(19)	4.4(12)	-0.3(17)	2.6(14)	-0.3(12)
CB(3)	9.0(19)	4.7(14)	9.5(21)	0.5(13)	4.7(17)	2.4(14)
CB(4)	5.2(15)	4.1(12)	4.8(12)	0.4(10)	0.7(11)	-0.6(10)
CB(5)	5.0(13)	6.0(16)	5.0(14)	-0.4(12)	-0.5(11)	-1.1(11)
CB(6)	3.6(12)	3.7(11)	5.2(12)	1.2(9)	2.1(14)	0.8(9)
CB(7)	7.0(19)	4.2(14)	11.0(23)	-1.2(14)	3.7(17)	3.3(14)
CB(8)	4.7(13)	3.9(12)	7.5(17)	-1.3(11)	1.2(12)	-0.5(11)
CB(9)	6.7(15)	2.4(11)	8.9(19)	-2.2(11)	2.6(12)	0.1(10)
CB(10)	6.4(16)	3.7(12)	7.9(17)	-0.6(11)	2.8(12)	1.0(11)

Table 21. Continued

Atom	B_{11}	B_{22}	B_{33}	B_{12}	B_{13}	B_{23}
CB(11)	2.7(10)	4.6(13)	7.7(17)	0.5(9)	1.4(11)	1.0(11)
CB(12)	5.6(18)	11.6(24)	8.7(22)	0.4(16)	2.3(16)	5.1(18)
CB(13)	3.7(12)	5.0(12)	7.3(17)	-1.8(9)	2.3(11)	-2.1(11)
CB(14)	4.9(16)	4.7(14)	11.8(23)	-1.3(12)	2.5(16)	3.3(15)
CB(15)	3.6(10)	9.2(21)	6.2(14)	-1.2(12)	2.6(11)	0.2(14)
CB(16)	2.7(10)	7.2(16)	5.6(14)	0.3(11)	0.2(11)	0.8(11)